UNIVERSITY OF PISA
DEPARTMENT OF BIOLOGY

MASTER OF SCIENCE IN MOLECULAR AND CELLULAR BIOLOGY

Master of Science thesis

Accademic year 2013-2014

Developing new tools for symbiotic calcium analysis: cloning and testing a new calcium sensor to study calcium spiking in *Medicago truncatula* root hair cells

Student

Annalisa Bellandi

Supervisors

Monica Ruffini Castiglione

Giles E. D. Oldroyd

TABLE OF CONTENTS

Alla mia famiglia

Chapter 1

General introduction

1. VERSATILITY OF CALCIUM SIGNALLING

Calcium is a universal intracellular messenger and plays a key role in an incredible variety of processes. In animals, for example, during the fertilization the mammalian eggs generate regular calcium (Ca^{2+}) spikes that last for about two hours and lead to the cycling B activation and to the completion of meiosis [1][2]. Later in the development, calcium signalling controls specification process responsible for pattern formation and cell differentiation [1]. There are evidences that a gradient of Ca^{2+} plays a role during the development of the dorsoventral axis in *Xenopus laevis* [3][4], *Danio rerio* [5] and *Drosophila melanogaster* [6]. Neuronal differentiation is influenced by calcium transients, Ca^{2+} spikes promote normal neurotransmitters expression and channel maturation while calcium waves in the growth cones control neurite extension and its ability to locate its target [7][8]. Calcium has also a central role in leading the cell toward the proliferation or the death [1]. In fact calcium can interact with proliferation signalling pathways such as those regulated through MAPK (mitogen activated protein kinase) and PI3K (phosphatidylinositol-3-OH kinase), but at the same time is also part of both the intrinsic and extrinsic apoptosis pathways. For example, Ca^{2+} in the intrinsic pathway leads to the activation of transcription factors that trigger the production of components such as FasR (first apoptotic signal receptor) and FasL (Fas ligand). While in the intrinsic pathway an excessive increase of the cytosolic calcium concentration ($[Ca^{2+}]_{cyt}$) stimulates an elevation in the uptake of this ion in the mitochondria which can

induce formation of MPTP (mitochondrial permeability transition pore). Moreover calcium-dependent cysteine proteases mediate the cleavage of members of Bcl-2 (B-cell lymphoma 2) protein family inducing MOMP (mitochondrial outer membrane permeabilisation) and the subsequent release of proapoptotic protein from the mitochondria into the cytosol [9]. More than 20 years ago has been reported that also in plants calcium is linked to apoptosis: a sustained calcium influx was ad example observed during bacterial induction of hypersensitive cell death in tobacco [10] and soybean [11]. Nowadays we know that the plant cells sensing pathogenic microorganisms evoke an innate immune reaction that can include triggering of basal defence response and programmed cell death (hypersensitive response, HR). Both of this pathways involve an elevation of $[Ca^{2+}]_{cyt}$ due to phosphorylation events, G-protein signalling and/or an increase of cyclic nucleotides. The events that trigger the cascade is the pathogen recognition via the perception of pathtogen-associated molecular pattern (PAMP) molecules or via the interaction between the pathogen virulence gene products and the corresponding plant resistance gene products [12].

As we can see in Table 1.1, in plants several other answer to biotic and abiotic stimuli, as well as physiological processes, are controlled by variations of the intracellular calcium concentration. For example, in *Papaver rhoeas* (the field poppy), has been observed that increases of $[Ca^{2+}]$ in the shank and decreases of $[Ca^{2+}]$ in the tip of incompatible pollen tubes are involved in the SI (self-incompatibility) signalling pathway [13]. Cold shock, heat shock, salinity, hypo-osmotic stress and mechanical stimulation all induce a response through changes in the $[Ca^{2+}]_{cyt}$.

Developmental process or environmental change	**Caracteristic $[Ca^{2+}]_{cyt}$ perturbation**	**Store releasing Ca^{2+} to cytosol**
Pollen tube elongations	Oscillation of the high apical $[Ca^{2+}]_{cyt}$	Apoplast and internal
Pollent tube self-incompatibility response	Intracellular $[Ca^{2+}]_{cyt}$ wave in shank	Apoplast and internal (IP_3-dependent)

Cell polarity after fertilization	Intracellular $[Ca^{2+}]_{cyt}$ wave from sperm fusion site leading to sustained $[Ca^{2+}]_{cyt}$ elevation	Apoplast
Cell division	Elevated $[Ca^{2+}]_{cyt}$	
Seed germination	Slow rise in $[Ca^{2+}]_{cyt}$	
Apoptosis	Slow sustained $[Ca^{2+}]_{cyt}$ elevation	
Red light	Elevated $[Ca^{2+}]_{cyt}$	Apoplast
Blue light	Brief spike in $[Ca^{2+}]_{cyt}$	Apoplast
Circadian rhythms	Circadian oscillation in $[Ca^{2+}]_{cyt}$	
Stomatal closure	Elevated $[Ca^{2+}]_{cyt}$ at cell periphery, elevated around vacuole, oscillation in $[Ca^{2+}]_{cyt}$	Apoplast, vacuole, apoplast
Increasing apoplastic Ca^{2+}	Oscillation in $[Ca^{2+}]_{cyt}$ of guard cells	Apoplast
Auxin responses	Slow prolonged increase in $[Ca^{2+}]_{cyt}$, oscillations in $[Ca^{2+}]_{cyt}$	
Root cell elongation	Sustained $[Ca^{2+}]_{cyt}$ elevation	Apoplast
Root hair elongation	Sustained high apical $[Ca^{2+}]_{cyt}$	Apoplast
Nodulation	Initial rise and then oscillations in $[Ca^{2+}]_{cyt}$	Apoplast
Senescence	Sustained $[Ca^{2+}]_{cyt}$ elevation	

UV-B	Slow rise of $[Ca^{2+}]_{cyt}$, elevated $[Ca^{2+}]_{cyt}$ sustained for several minutes	Apoplast
Heat-shock	Elevated $[Ca^{2+}]_{cyt}$ sustained for 15-30 min	Apoplast and internal (IP_3-dependent)
Cold-shock	Single brief $[Ca^{2+}]_{cyt}$ calcium spike, oscillation in $[Ca^{2+}]_{cyt}$	Apoplast
Slow cooling	Brief $[Ca^{2+}]_{cyt}$ spike, slow $[Ca^{2+}]_{cyt}$ elevation	Apoplast, Apoplast and internal (IP_3-dependent)
Oxidative stress	Brief $[Ca^{2+}]_{cyt}$ spike, sustained $[Ca^{2+}]_{cyt}$ elevation, oscillation in $[Ca^{2+}]_{cyt}$	Apoplast, Apoplast and internal (IP_3-dependent)
Anoxia	Slow spike, sustained $[Ca^{2+}]_{cyt}$ elevation	Apoplast, internal (including mitochondria)
Drought/hyper-osmotic stress	Slow spike, sustained $[Ca^{2+}]_{cyt}$ elevation	Apoplast and vacuole
Salinity	Slow $[Ca^{2+}]_{cyt}$ spike (minutes), sustained $[Ca^{2+}]_{cyt}$ elevation (hours), reduced $[Ca^{2+}]_{cyt}$ (days)	Apoplast and internal (IP_3-dependent)
Hypo-osmotic stress	Small and then big $[Ca^{2+}]_{cyt}$ elevation	Apoplast, Apoplast and internal (IP_3-dependent)
Mechanical stimulation	Single brief $[Ca^{2+}]_{cyt}$ spike, tissue $[Ca^{2+}]_{cyt}$ wave	Internal
Aluminium stress	Elevated $[Ca^{2+}]_{cyt}$	

Pathogens	Slow $[Ca^{2+}]_{cyt}$ spike (minutes), sustained $[Ca^{2+}]_{cyt}$ elevation (hours), oscillation in $[Ca^{2+}]_{cyt}$	Apoplast, Apoplast and internal (IP_3-dependent)

Table 1.1: examples of developmental processes and responses to biotic and abiotic stresses initiated by perturbations in cytoplasmic calcium concentration [14].

Although the cases presented so far are just some examples of the versatility and universality of calcium as an intracellular messenger, the question that may rise up at this point is: how can a single ion be responsible of such a variety of signalling processes? Each individual calcium response is characterised by frequency, amplitude, spatio-temporal location and dynamics, varying these characteristics we can obtain a particular calcium signature that can be decoded and then evoke a specific developmental process or response. Calcium channels, ATPases and transporters, as well as the possibility to release calcium from different stores, are shaping the calcium signatures [15]. This means that, as a result of the variation and regulation of these factors, we can obtain $[Ca^{2+}]$ fluctuations which can be either monophasic (spikes), oscillatory, sustained, combined or wave-shaped and show different amplitude, frequency and location. The cellular and developmental contest is also responsible of the variety and the availability, as well as the regulation, of the decoding process components. These are calcium-binding proteins and the activation of specific of them in consequence of a particular calcium signal constitutes the decoding of the signature.

2. Calcium and calcium signalling in plants

Calcium is an element present and required in relatively high quantity in plants as it carries out several functions: beside the classical role as an important intracellular messenger, it has a structural role in the cell wall and membranes and works as a counter-cation for anions in the vacuole [16]. Calcium, hence classified as a macronutrient, is absorbed from the soil solution in its ionic form, with an uptake rate that is higher in the apical than in the distal root zone [16]. This is due to the fact that calcium is delivered to the shoot via the xylem but its mobility is low in the phloem, so

the apical cells of the root have to provide the calcium to the shoot but also meet their own calcium demand by direct uptake from the external solution [16]. Calcium may reach the xylem through the symplastic way or through an apoplastic way. Voltage dependent (activated by depolarization and hyperpolarization) calcium channels on the plasma membrane allow calcium to enter into the cytoplasm of the cell of the roots following its electrochemical gradient [17]. The negative charges of the pectins carboxylic groups in the cell wall do not constitute an obstacle for the access of calcium to the apoplast, in fact they can bind the cation forming a calcium store [16]. At the root tip were the endodermal cell are still immature and unsuberised, or in basal root zones where lateral root emerge from the pericycle disrupting the integrity of the Casparian band, calcium can reach the xylem following the apoplastic way [16]. Where the Casparian band blocks the apoplastic path, calcium can reach the stele through the symplastic pathway, once here Ca^{2+}-ATPase catalyse the efflux of the cation from the symplast to the xylem [16]. Since calcium is cytotoxic, as it can interfere with the phosphate metabolism causing the formation of insoluble salt and it can compete with Mg^{2+} in the interaction with ATP, a strategy conserved throughout the evolution from bacteria to eukaryotes is to maintain the $[Ca^{2+}]_{cyt}$ low and creating stores of this cation [18][19].

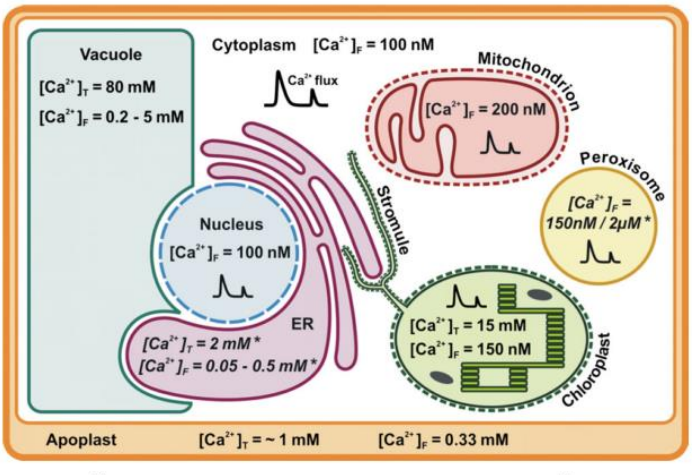

Fig. 1.1: Summary of organelles calcium concentration in plant cells. $[Ca^{2+}]_F$ = concentration of free calcium; $[Ca^{2+}]_T$ = total amount of calcium, considering also the calcium permanently or transiently bound to chelating agents and proteins. The star (*) indicates values taken from the animal field [18].

The main calcium storage compartments in plants are the vacuole, the endoplasmic reticulum (ER) and the apoplast. But recently became clear that also mitochondria, chloroplasts and peroxisome can influence the calcium signalling pathway in the cytoplasm and in the entire cell [18]. Speaking about the calcium concentrations in living systems, we must point out that this element is present in part in solution as a free ion and in part bound to chelating agents such as malate, citrate and isocitrate and proteins [18]. This second fraction of calcium is not immediately available for calcium signalling, but calcium binding storage proteins such as calreticulin in the ER and RVCaB (radish vacuolar calcium-binding protein) are useful as they can improve the calcium storage capacity of the organelles [20][18]. The figure 1.1 summarize the [Ca^{2+}] in different compartments of plant cells, the concentration of free calcium in the cytoplasm is around 100 nM while in ER and in vacuole we reach the mM order. This difference enables the generation of calcium signals in the cytoplasm [18].

2.1. Shaping cytosolic calcium signature

2.1.1. Channels

As we mentioned before, we can say that the calcium signatures are shaped by channels, pumps and transporters that manage the movement of calcium from a compartment to another.

Three types of nonselective cation channels (NSCCs) have been characterised electrophysiologically in the plasma membrane of plant cell: mechanosensitive Ca^{2+} channels (MCC), depolarisation-activated Ca^{2+} channels (DACC) and hyperpolarisation-activated Ca^{2+} channels (HACC) [15]. While there are evidences of the participation of the MCCs and HACCs in shaping the calcium signatures (see for example the proved role of the former in generating calcium influx during pollen tube germination and elongation [21] and of the latter in shaping calcium signatures in guard cells and root hair cells [15]), there are no direct proofs linking the DACCs activity to cytosolic calcium signalling events. However, the fact that the plasma membrane depolarization is an early response to many environmental stresses that stimulate increase of $[Ca^{2+}]_{cyt}$ suggests that DACCs may be involved in this process [15]. In addition to that,

two ion channel homologous genes are good candidates for plasma membrane Ca^{2+}-permeable channels in plants: the cyclic nucleotide gated channel (CNGC, [22]) gene and the glutamate receptors-like (GLR, [23]) gene. Both of these channels are NSCCs. Studies of knockout, overexpression and mutation reported evidences of the putative CNGCs being implicated in Ca^{2+} signalling during pathogen-induced cell death [24] and pollen tube growth [25][26]. In a similar way the putative GLR channel resulted linked for example to cell division, programmed cell death [27] and resistance to pathogen attack [28].

In the tonoplast there are at least four type of Ca^{2+}-permeable channels that may contribute to stimulus-induced increases of cytosolic Ca^{2+}: the inositol(1,4,5)-triphosphate ($InsP_3$)-gated channels, the cyclic ADP-ribose (cADPR)-gated channels (activated respectively by $InsP_3$ and cADPR), the vacuolar voltage-gated Ca^{2+} channels (VVCa, activated by hyperpolarization of the membrane and by $[Ca^{2+}]_{vacuole}$) and the slow-activating vacuole channels (SV, activated by depolarization of the membrane and by $[Ca^{2+}]_{cyt}$ [19][29]. The opposite characteristics of the VVCa and SV channels and their identical distribution, conductance and ions affinity lead to the suggestion that they actually are the same channel just inserted in the membrane in a reverse orientation [29].

Remains to be established whether the $InsP_3$-gated channels and the cADPR-gated channels are also present in the ER membrane, although calcium release from ER vesicles has been reported in response to these two ligands [29][30]. However, Ca^{2+} release from the ER has been reported in response to various ligands such as inositol hexakiphosphate ($InsP_6$) [32] and nicotinic acid adenine dinucleotide phosphate (NAADP) [33], suggesting the potential of ligand-gated endomembranes channels in shaping the cytosolic calcium signatures [15]. Voltage-gated NSCCs has been electrophysiologically characterized in ER vescicles of *Bryonia dioica* (BCC1 [34]) and *Lepidum sativum* (LCC1 [35]). The channel BBC1 resulted controlled both by the voltage of the ER membrane and the $[Ca^{2+}]_{ER}$. An increase in the $Ca^{2+}{}_{ER}$ activity would stimulate the opening of the channel, while the depolarization of the membrane caused by the cations efflux would close the channel. This double control system, eventually cyclic, could

generate $[Ca^{2+}]_{cyt}$ transient increases that could be modulated in their amplitude and frequency through the regulation of the channel activity [17].

2.1.2. Transporters

While all these channels permit the influx of Ca^{2+} in the cytoplasm from the stores following its electrochemical gradient, calcium efflux from the cytoplasm requires transporters. Two main types of calcium transporters are present in plants: high-affinity Ca^{2+}-ATPases and low-affinity Ca^{2+}-exchangers. Isoforms of two P-type ATPases belonging to the first group (ER-type Ca^{2+}-ATPase (ECA) and autoinhibited Ca^{2+}-ATPase (ACA)) have been observed in ER membrane [32][33], plasma membrane [38] and tonoplast [39]. These plant ACAs present a N-terminal autoinhibitory domain which is released when bound to the Ca^{2+}-calmodulin (CaM) complex, an increase of the $[Ca^{2+}]_{cyt}$ would lead in this way to an activation of the pump [40]. The variability in the N-terminal domains and the presence of various isoforms of CaM in plants suggest the potential versatility of the system. Although there is evidence of ECAs being stimulated by CaM [41], in some other cases CaM regulation or presence of CaM binding domain were not noticed [42]. Even though more proofs are required to unequivocally demonstrate the implication of ECAs in shaping the calcium signatures, the fact that they undergo transcriptional regulation during some stress response [35][36] may suggest their implication. However further experiments are required to actually prove the direct role of ACAs and ECAs in shaping the calcium signatures.

The Ca^{2+}-exchangers have a lower affinity for calcium but a higher capacity compared to the pumps [15]. Plants possess H^+/Ca^{2+} exchangers encoded by the family of genes called *CAX* (calcium exchangers) [45]. H^+/Ca^{2+} exchange activity has been reported in the plasma membrane [46], while H^+/Ca^{2+} exchangers have been identified in the tonoplast of different plants species [47]–[49]. Several evidences demonstrate the potential for differential regulation of these exchangers and suggest that they may be involved in restoring the basal $[Ca^{2+}]_{cyt}$ after stress induced elevations [15].

2.2. Shaping the non-cytosolic calcium signatures

Although so far we considered almost only the calcium signals generated in the cytoplasm, shaped variation and oscillation in the [Ca^{2+}] with particular signalling roles also occur in non-cytosolic locations.

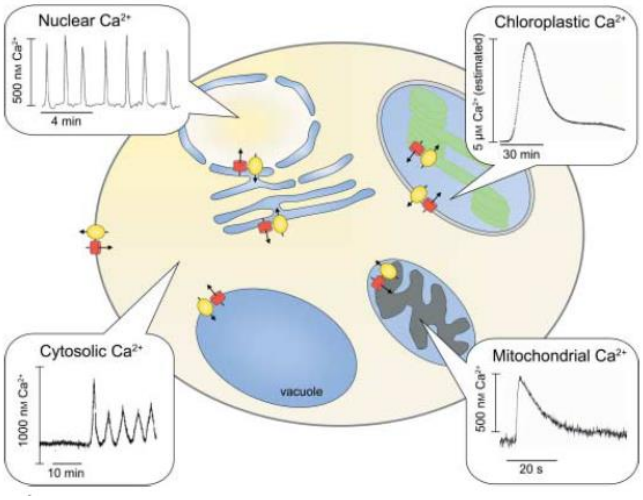

Fig 1.2: examples of cytosolic and non-cytosolic calcium signatures in plants [15]

2.2.1. Chloroplast

Circadian oscillation of [Ca^{2+}] have been reported targeting reporters to the stroma and might be that these oscillations have a role in switching off the photosynthetic process at night [50]. Is not well understood how the calcium flux in the stroma is generated but in the inner envelope of pea a pH gradient-dependent (or membrane voltage-dependent) Ca^{2+} uniport is present. In addition to that calcium could arrive in the stroma also from the thylakoid. Although we only know an H^+/Ca^{2+} exchanger that load the calcium in the thylakoids [51] and NSCC activated at membrane potentials that promote cation influx into the intrathylakoid space [52] while the export pathway is not well understood. Chloroplast may be important also in participating to calcium-signalling events in the cytoplasm. In fact, a lower elevation in the $[Ca^{2+}]_{cyt}$ and an higher $[Ca^{2+}]_{chl}$ combined with an inhibition of the programmed cell death ad a slowing down of the flowering process have been noticed overexpressing the pea chloroplast protein PPF1 (a putative Ca^{2+} channel) [52][53]. Moreover, the

deletion of *CAS*, which is encoding for a calcium-binding protein specifically present at the thylakoids membrane, cause loss of the stomatal closure in response to the increase in the $[Ca^{2+}]_{ext}$ [55].

2.2.2. Mitochondria

Increase of the calcium concentration in the mitochondria has been reported in response to physiological and environmental stimuli. In the case of cold and osmotic shocks the signatures of the cytosolic and mitochondrial calcium were very similar, although the $[Ca^{2+}]_{mit}$ peak was about one-half of the $[Ca^{2+}]_{cyt}$ peak. While, mechanical and oxidative stresses evoked a calcium response in the mitochondria quite distinct from the cytosolic one. These results indicates that $[Ca^{2+}]_{mit}$ and $[Ca^{2+}]_{cyt}$ are differentially regulated and that mitochondrial specific calcium signals exist in plants [56].

2.2.3. Nucleus

Although has been debated, it is now accepted that the nucleus of the plant cells can generate calcium signals on its own [57] and that these responses have a distinct biological role from the cytosolic ones. In fact, several experiences, reporting differences in the timing and in the shape between the nuclear and cytoplasmic calcium signatures, demonstrated that the variations in the nucleoplasmic calcium concentration ($[Ca^{2+}]_n$) are not mirroring for diffusion the variations in the cytosol. For example, in tobacco cell suspension cultures where the osmolarity of the medium was lowered, the $[Ca^{2+}]_{cyt}$ increased in a bimodal manner while the $[Ca^{2+}]_n$ showed a monophasic rapid increase. Subsequently, when the $[Ca^{2+}]_{cyt}$ started decreasing, the $[Ca^{2+}]_n$ was maintained at more than 1/3 of its maximal value. Following an increase of the growth medium osmolarity, instead, rise in the $[Ca^{2+}]_{cyt}$ and no changes in the $[Ca^{2+}]_n$ were reported [58]. Moreover, upon treatment with cryptogein (a polypeptidic elicitor), cytoplasmic calcium signature was bimodal and constituted by an early big peak followed by a sustained $[Ca^{2+}]_{cyt}$ elevation of at least 2 hours while in the nucleus a different calcium dynamic was reported: a weak early transient

was followed by an intense peak that lasted for at least 1 hour. The cytosolic peak occurs around 5 minutes post treatment while the main nuclear peak about 20 minutes later [59].

In addition to that, have been shown that the jasmonic-acid-isoleucine conjugated (JA-Ile) induces a clear and strong bimodal calcium response in the nucleus but did not modify the $[Ca^{2+}]_{cyt}$ (fig 1.3) [60].

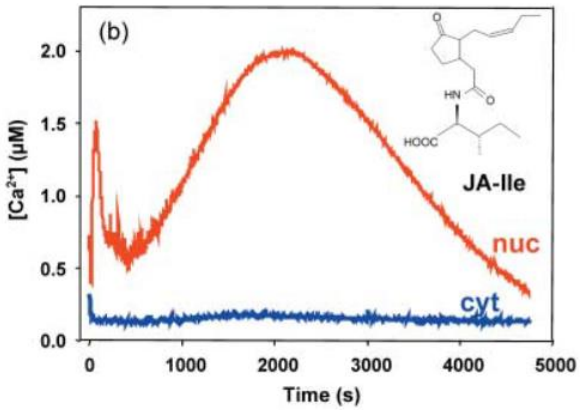

Fig. 1.3: JA-Ile elicites changes in the nuclear calcium concentration but not in the cytoplasmic calcium concentration [60].

The fact that isolated nuclei resulted able to sense some stimuli (such as mechanical stimulation, cold or acidity) and convert them in intranuclear calcium signals [61], demonstrate that the nuclei have a calcium-mobilizing machinery as well as an independent calcium reservoir. Nevertheless, other evidences pointed out that, whether the nucleus showed independence at least in some cases, the cytosol can participate to the nuclear calcium homeostasis. For example, long-chain base sphingoid (LCBS) derivatives, which are involved the calcium signalling pathway that regulate the stomatal closure in response to abscissic acid [62], elicited variations in the $[Ca^{2+}]_n$ in both isolated and not isolated nuclei but the kinetic and the amplitude of the signals in the two situations were different [63].

In addition to the influence of the cytosol in controlling nuclear calcium response, it is possible also that the nucleus influences the cytosolic calcium signalling. That has been suggested by the result of the heterologous expression

in yeast of DMI1 (doesn't make infection 1), which is a ion channel located in the nuclear envelope of plant cell nuclei. Peiter *et al.* showed that DMI1 yeast decreases the release of calcium from ER and may be a regulator of cytosolic calcium [64].

However, whether autonomous or regulated by the cytosol, nuclear calcium signals are fundamental in plant cells, for example they are required for wind-induced calmodulin expression [65] and for sphingolipid-induced cell death [66].

Among the models for the study of nuclear calcium signalling in plant we can find the oscillation of the [Ca^{2+}] in the nuclei of epidermal cells that occur during both bacterial and mycorrhizal symbiotic signalling [67][68][69]. The present work is focused on the study of calcium spiking occurring in the nuclei of *Medicago truncatula* Gaertn. root hair cells during the establishment of nitrogen-fixing symbiosis. In reason of that, we will carry out a deeper examination of the machinery required for shaping the nuclear symbiotic calcium signature in the paragraph 3.4 of this chapter. More in general not so much is known about biochemical activities in the nuclear envelope directly linked to the nuclear calcium homeostasis. A voltage dependent NSCC, regulated also by micromolar concentrations of calcium on the inner side of the membrane, was identified with the patch-clamp technique on excised patches of nuclear envelope [70]. But we still do not know the location and the vectorial arrangement of this channel. While we are aware of the presence of Ca^{2+}-ATPases on the outer nuclear membrane that pump calcium in the nuclear envelope lumen [71][72].

2.3. Decoding the calcium signatures

The components of the calcium signatures decoding system are calcium binding protein. Upon the binding of calcium, some of these proteins can directly convert the signal in a phosphorylation activity or in a transcriptional activity. Other proteins, such as calmodulin (CaM), undergo conformational changes subsequently to the binding of calcium but play their role in the transduction of the signal only indirectly, i.e. by interacting with other target proteins [73]. Calcium is bound by

these calcium sensors through conserved motifs such as EF-hand motif, or through annexin fold and C2 domain [74]. CaM, CaM-like (CML), Ca^{2+}-dependent protein kinases (CPKs) and calcineurin B-like (CBL) proteins are three well characterized families of proteins containing EF-hand motifs in plants. CaM has two pairs of EF-hand motifs and, once bound the calcium, undergo to a conformational change that lead to the exposure of a hydrophobic region. The target Ca^{2+}/CaM-interacting proteins, can recognise this region [19]. The CaM binding transcription activators (CAMTAs) are activated upon the binding of the Ca^{2+}/CaM complex. Their role is to bind promoters of genes to induce the gene expression and they have been for example associated with plant defence [75] and cold tolerance [76]. The complex Ca^{2+}/CBL proteins transduces the calcium signal by interacting and activating the CBL-interacting protein kinases (CIPKs) [77]. The CIPKs can also directly convert the calcium signal in a phosphorylation activity of their target, as they present both the kinase domain and EF-hand motif [78]. The CBLs/CIPKs work is linked to biotic and abiotic stress responses [79][80][81]. For example target of CIPKs are implicated in mediating stomatal closure [82] and in defence response via ROS production [83].

Another example of this double regulation system, direct by calcium and indirect by the Ca^{2+}/CaM complex, is CCaMK (Ca^{2+} and Ca^{2+}/CaM-dependent kinase). A nuclear localized CCaMK decodes the nuclear calcium signature during symbiosis calcium signalling [84]. We will speak more about CCaMK in the paragraph 3.5 of this chapter.

3. NUCLEAR CALCIUM SIGNALLING IN PLANT-RHIZOBIA ENDOSYMBIOSIS

3.1. Plant-microbes endosymbiosis, a general overview

Heinrich Anton de Bary coined the term “symbiosis” in 1879 to describe a “long-term relationship formed between unlike organisms”. Although in the beginning this definition was including interactions from mutualism to parasitism, today usually refers to mutually beneficial relations.

Among the plant-microbes root endosymbiosis, we can find the mycorrhizal symbiosis and the nitrogen-fixing symbiosis. Mychorrhizal fungi can institute this

type of relationship with over the 90% of all plant species. While the fungus obtain an additional source of carbon, by participating in this symbiosis, the plant derives increased level of micro and macronutrient from the soil. The nitrogen-fixing symbiosis group encompasses many different plant and bacteria species but only bacteria belonging to the genus *Frankia* and *Rhizobium* can institute endosymbiosis with plants through the formation of root nodules. Plants that entertain symbiotic interaction with *Frankia,* which are named actinorhizal, belong to the Fagales, Cucurbitales and Rosales clades [85][86]. Only legumes (*Fabaceae*) and *Parasponia* (*Cannabaceae*) form the rhizobial association [87].

One of the first molecular communication events between the plant and these microbes, which introduce to the symbiotic intracellular signalling pathway, happen through microbial compounds that bind receptors present on the plant cell plasma membrane. Mychorrhizal fungi produce compounds called Myc factors (mychorrhization factors) and rhizobial bacteria produce Nod factors (nodulation factors), both of these molecules are lipochitooligosaccharides (LCOs) and present a variety of modifications depending on the producing organism [88][89]. While the composition of the *Frankia* exudates is still unknown. Despite the many differences present between these three types of plant-microbe symbiosis, that lie for example in the microbial factors structure and the plant receptors type as well as in the different infections strategies, all these symbiotic signalling pathways have in common the triggering of nuclear calcium signatures.

The classical plant model *Arabidopsis thaliana* is not able to support mychorrhizal association but legumes are a good system to study symbiotic signalling as they can form symbioses with both fungi and rhizobia. In this work, we focused on the study of the nuclear calcium oscillations triggered by Nod factor perceptions in *M. truncatula* root hair cells.

3.1.1. Plant-rhizobia endosymbiosis

Two main infection strategies have been reported in plant-rhizobia endosymbiosis. The first one, which takes place in *Sesbania rostrata*, is the lateral root base infection or crack entry mechanism. In fact the bacteria enter

the root through a crack in the epidermal cell layer, typically at the base of a lateral root, and initiate an intercellular infection [90]. In the second strategy, used in most legumes and in *M. truncatula*, the infection starts from the root hair cells in a so called “intracellular way”. Despite of the name, the bacteria never get in contact with the cytoplasm but proceed through the cells in a channel created by the invagination of the plasma membrane. Both mechanisms are dependent on Nod factor signalling [91].

The first molecular event necessary for the instauration of the symbiosis is the production of flavonoids by the plant roots. Flavonoids are ubiquitous in plants and are involved in process such as defence response and lignin and anthocyanin production [92]. In the symbiotic contest, these polyaromatic compounds are responsible of activating a chemotaxis response of rhizobia as well as of triggering the synthesis of Nod factors. The flavonoids signal is transduced in the rhizobia through NodD transcriptional regulators [93] which trigger the transcription of bacteria nodulation genes (*nod*) directly binding their promoter [94][95]. These genes encode proteins responsible of the Nod factors synthesis [94]. In this first phase of the symbiotic interaction lies the mechanism that guarantees the specificity of the interaction. Although many different forms of flavonoids and Nod factors exist, each particular plant host produces the flavonoid that is specific for the bacterial partner and *vice versa*. For example, positive chemotaxis of *Sinorhizobium melitoti* was observed only in response of the flavone luteolin which is produced by its plant host *Medicago sativa* and not in response of similar flavonoids [96]. At the same time, a positive feedback loop enhancing the production of flavonoids happens only in presence of compatible rhizobial species and is dependent on Nod factor structure [97]. Moreover the DNA bending induced by the binding of the NodDs on the *nod* promoter, and required for the RNA polymerase binding, resulted more efficient upon appropriate flavonoid treatment [95].

As said before, Nod factors are LCOs. This means that they have a chitin backbone constituted by 3 to 5 β-1,4-liknked *N*-acetylglucosamine residues where additional substituents and decorations are added. These modifications include binding of fatty acid chain, glycosylation, sulfation, acetylation, N and O-

methylation [98]. These decorations, the length of the backbone chain and the saturation degree of the N-acyl groups vary between Nod factors of different rhizobial species and this is important for the specificity of the symbiotic interaction [99], [100].

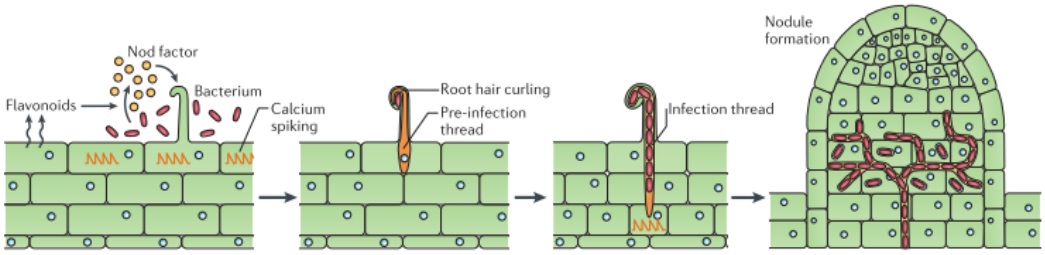

Fig. 1.4: schematic representation of the main steps of the rhizobium-legume endosymbiosis instauration through the intracellular infection strategy [101].

The positive chemotaxis response evoked in the bacteria by the flavonoids is important as to start the infection process the bacteria have to be attached to the root hair cell surface [102]. After this first phase of diffusible signals exchange and the attachment of the rhizobia, the root hair starts curling and doing so it entraps a single bacterial cell in a “shepherd’s crook” curl. The entrapped cell proliferates and forms a microcolony. A reorganization of the cytoskeleton generate a cytoplasmic channel that constitute the pre-infection tread, then a tubular structure called infection tread is formed by hydrolysis of the plant cell wall and invagination of the plasma membrane [103][104]. In the meanwhile, in the root cortex below the infection site, a nodule meristem is initiated. The infection tread will grow toward the emerging nodule and will ramify in the nodule tissue. Here the bacteria can leave the infection tread and be released in membrane-bound compartments in the plant cells where they will differentiate in a nitrogen fixing state [101]. Nuclear calcium oscillations during the establishment of these symbioses occur in both epidermal cells and cortical cells. In epidermal cells this phenomenon is triggered by Nod factors perception, while calcium oscillation in cortical cells appear in the target cell and in the neighbouring ones during the infection process before the colonization of the cell by the microbes. The frequency of the oscillation in the neighbouring

cells is initially low but it increases when the symbionts become near to the target cell [105]. In this last period the calcium signature of the cortical cells result more similar to the ones observed in epidermal cells in response to Nod factors [67].

3.2. Calcium responses in root hair cells upon Nod factor signals

In root hair cells exposed to Nod factors two different calcium response have been observed: a calcium flux in the cytosol and calcium spiking in the nuclear region.

3.2.1. Calcium influx

A rapid calcium influx in the cytosol was observed within one minute of adding Nod factors [106] and resulted followed by efflux of Cl^-, K^+ and alkalinisation of the cytoplasm. This explained the membrane depolarization and pH changes that were reported as an early response to Nod factors 10^{-10}-10^{-7} [107]. This early calcium flux was observed in the tip region of root hair cells treated with Nod factors in *Vicia sativa* [108], *Phaseolus vulgaris* [109] and in *M. sativa* [110]. This increase of the cytosolic calcium concentration near the tip of the root hair could be associated with root hair deformation, while the increase in the cytoplasmatic calcium level reported behind the root tip might be associated with the amplification of the Nod signal and the induction of downstream events [110]. Microinjection of *M. truncatula* root hair cells with calcium sensitive dye revealed that the flux was located in the tip region of the cell [111].

3.2.2. Calcium spiking

A calcium spiking activity was reported in the nuclear region of *M. sativa* upon Nod factors treatment in 1996 [67]. In the same work was noticed that these regular oscillations had a mean period of 60 s, started around ten minutes after the exposure to the Nod factors and lasted up to three hours. Moreover they showed a rapid rising phase (1-4 s) followed by slower decreasing phase (around 30 s). Later, this response has been investigated in several legumes.

Miwa et al. reported in 2006 that the average frequency of the spikes is 60-100 s and depends on the position of the root hair cell along the root and also proposed that the number of spikes (although in conjunction with other factors) was required for the induction of early nodulation gene expression. In particular, they observed that 36 consecutive spikes were sufficient and that an equivalent number of spikes was required even when the period between each spike was extended [68]. Using nuclear targeted calcium sensors also intranuclear calcium spiking in *M. truncatula* root hair cells in response to Nod factors was demonstrated [112].

3.3. Linking the Nod factor perception to the activation of nuclear calcium release

Through mutant screens has been proven that the perception of the Nod factors signals involves plasma membrane receptor-like kinases with extracellular Lysine motifs (LysM) domains [113]. These motifs are present in bacteria and eukaryotic protein and bind oligosaccharides, which are chemically similar to the nod factor backbone. The identified receptors are the Nod factor receptor 1 (NFR1) of *Lotus japonicus* which correspond to the LysM kinase 3 (LYK3) of *M. truncatula,* and the NFR5 of *L. japonicus* corresponding to the NFP (Nod factors receptor) of *M. truncatula* [114]. [115]. Evidence suggest that NFR1 and NFR5 work in heterodimers or heterocomplexes [101]. Although the direct interaction *in vivo* of these receptors and Nod factors has not be proven, the fact that the expression of NFR5 and NFR1 in *M. truncatula* alter the host specificity of this species [116] suggest that they are directly involved in the specificity recognition. Another gene, encoding for a leucine-rich-repeat (LRR)-containing receptor-like kinase (known as *SYMRK,* symbiosis receptor-like kinase, in *L. japonicus* and as *DMI2,* doesn't make infection 2, in *M. truncatula*), resulted required for Nod factor signalling [117][118]. Although the exact function of *SYMRK*/*DMI2* is it not yet known, it could work in complex with the Nod factor receptor [119] and be associated with the production of a secondary messenger. The identity and the nature of this secondary messenger that would link the signal recognition occurred at the plasma membrane with the

calcium changes in the nucleus remain unknown. However, some observation could suggest possible candidates. *SYMRK*/*DMI2* can interact with e-hydroxy-3-methylglutaryl-CoA reductase (HMGR) [120] which is involved in mevalonate production and mevalonate can resulted able to evoke calcium oscillation in *M. truncatula* [101]. *SYMRK*/*DMI2* can also associate to MAPKK [121]. The HMGR could be involved in the generation of the secondary messenger while the MAPKK could trigger a phosphorylation cascade; both of these events could be, directly or indirectly, linked to the regulation or activation of the calcium channels involved in shaping the nuclear calcium spiking.

3.4. The nuclear machinery required for symbiotic calcium response

In *L. japonicus* two cation channels located in the nuclear membranes, CASTOR and POLLUX, have been identified as essential for perinuclear calcium spiking [122]. Similarly, in *M. truncatula* the ion channel DMI1 (POLLUX ortholog) and the Ca^{2+}-ATPase MCA8 resulted essential for the nucleoplasmic calcium oscillations. MCA8 is located in the nuclear envelope while DMI1 preferentially localises in the inner nuclear membrane [123][124][125]. Probably DMI1 exercises the roles of both POLLUX and CASTOR, rendering the ortholog of CASTOR redundant in *M. truncatula* [125]. Using the information on the location of MCA8 and DMI1 and the observation that calcium oscillations occur predominantly a the periphery of the nucleus [112][123] in mathematical modelling analysis [126], we could build a model where three components are required to shape the intranuclear calcium spiking: a channel that allow the influx of calcium into the nucleoplasm, a pump or a symporter that can push the calcium back into the nuclear envelope and a ion channel that works to balance the membrane depolarization induced by the calcium movements [101]. DMI1 permeates potassium and seems unlikely that could permeates calcium too [122][125]; it may act instead as regulator of a putative calcium channel through the modulation of the membrane potential [64] [127]. First a K^+ influx through DMI1 would partially activate a calcium channel, allowing an initial calcium influx. A calcium-binding pocket in DMI1 [128] would sense this calcium increase and this would lead to the full activation of DMI1. The

following K^+ influx would hyperpolarize the membrane and subsequently the voltage gated calcium channel would be open allowing the massive calcium influx. Then the pump would pump the calcium back in the store [129].

Other proteins resulted fundamental for symbiotic nuclear calcium oscillation are NUP85, NUP133 and NENA [130]–[132]. All of them are nucleoporins and are all part of the nucleopore scaffold [133]. The observation that in yeast nucleoporins of the nucleopore scaffold are required to transport protein in the inner nuclear membrane (INM) [134][135], lead to the hypothesis that the nucleopore scaffold could be fundamental to translocate in the INM proteins required for the generation of the calcium oscillation in the nucleoplasm. Another possibility is that the nucleopore allows the diffusion of the symbiotic signals from the cytoplasm to the nucleoplasm [127].

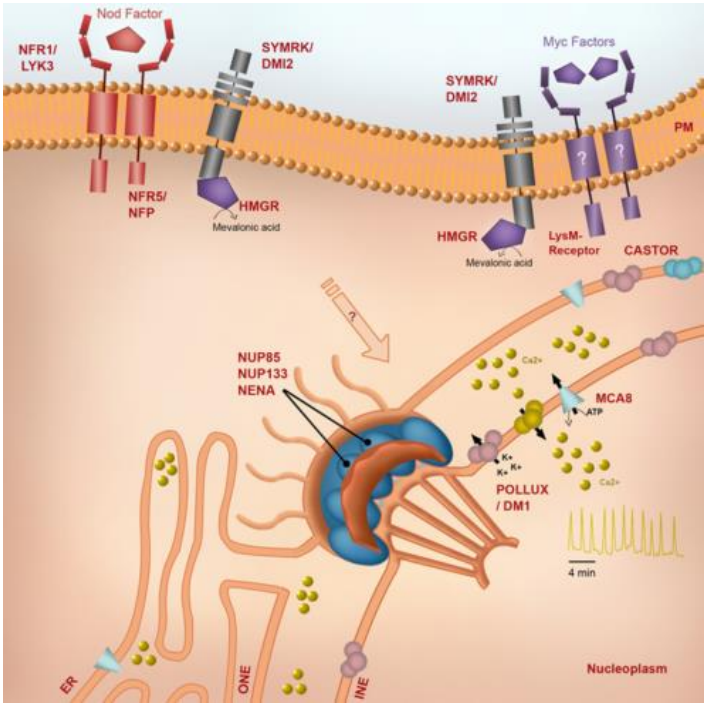

Fig 1.5: schematic representation of the machineries required for the perception of nod factors and the generation of nuclear calcium spiking [127].

3.5. Decoding the nuclear symbiotic calcium signals: CCaMK

CCaMK seems to be the key to decode the nuclear calcium spikes and trigger the downstream symbiotic signalling events. Gain of function of CCaMK is sufficient to

induce spontaneous nodule formation in absence of rhizobia [136][137] and promotion of structure involved in mycorrhizal colonization [138]. CCaMK is a Ser/Thr protein kinase and present three EF-hands motif at the C-terminus and a CaM-binding domain near the kinase domain [136][137]. Calcium binding to the EF-hands lead to autophosphorylation which stabilises the inactive form of CCaMK, while the Ca^{2+}/CaM complex binding overrides the effect of the autophosphorylation and activates the protein. Since the EF-domain and the CaM-binding domain have different affinities for their ligands, the hypothesis is that at basal level of calcium CCaMK is maintained in an inactive state, while it is activated during the spiking [139]. CCaMK can interact and phosphorylate CYCLOPS (or IPD3 in *M. truncatula*) [140]. CYCLOPS/IPD3 resulted fundamental for rhizobial and mycorrhizal colonisation [141][142] but its specific role remain to be determined. It may regulate CCaMK or directly coordinate the transcriptional downstream events working together with the GRAS family transcriptional regulators [143].

4. CALCIUM INDICATORS USED IN PLANT CELLS

4.1. Dyes

The first tools used for calcium imaging in living systems have been the dyes, organic compounds that are able to bind calcium and change optical proprieties upon this process. In the beginning murexide, azo dyes and chlorotetracycline were used but they showed low sensitivity, cellular toxicity or low accuracy. In 1980, BAPTA was created and this opened the door to the creation of various polycarboxylate dyes [144][145]. Single wavelength and double wavelength dyes have been developed during the years and some of the problems presented by the first dyes, such as low sensitivities or low accuracies, have been solved. However, two main disadvantages are shared by all these reporters. First, since dyes present heavily charged groups they are almost membrane impermeable and loading them in plant cell result a challenging task. To overcome this problem a variety of approach have been applied but all of them require time and additional work. The

second common disadvantage of the dyes is the risk of compartmentalization in the organelles and so of an uneven distribution throughout the cell [146].

4.2. Protein-based calcium indicators

The main advantage shared among all the protein-based indicators is that they can be addressed to different cellular compartments simply by introducing in their nucleotidic sequence the nucleotides that encode for the appropriate aminoacidic localisation signals. Moreover, tissue-specific promoters or inducible promoters can be used opening to more choices and experimental opportunities.

4.2.1. Aequorin

Aequorin (AEQ) is a calcium sensitive photoprotein identified in the jelly fish *Aequorea Victoria*. The protein has a prosthetic group, the coelenterazine, and three EF-hand motifs. In presence of molecular oxygen the apoprotein assembles spontaneously with its prosthetic group to form the holoprotein. When calcium is bound by the EF-hand motifs the protein acts as an oxygenase on the coelenterazine and releases excited coelenteramide and carbon dioxide. When the coelenteramide goes back to the ground state, it emits blue light (469 nm) which can be detected with a luminometer and correlates with the [Ca^{2+}] (event though there are overestimation problems). The disadvantage of the Aequorin is that the signal from a single cell is too low to permit good studies on single cell calcium dynamics [145][146].

4.2.2. Green fluorescent protein-based calcium indicators

The calcium indicators based on GFP (or on GFP variants) can be divided in two groups: the ones FRET (Föster resonance energy transfer) based and the ones constituted by a single fluorescent protein. Three main type of these calcium sensors are in use currently: the cameleons [147] (FRET-based), the camgaroos [148] and the pericams [149] (single fluorescent protein-based). In 1997 the first two GFP-based calcium indicators were developed [147][150] and the one built

by Tsien group was the cameleon, the most widely used GFP-based calcium sensor in plants at present.

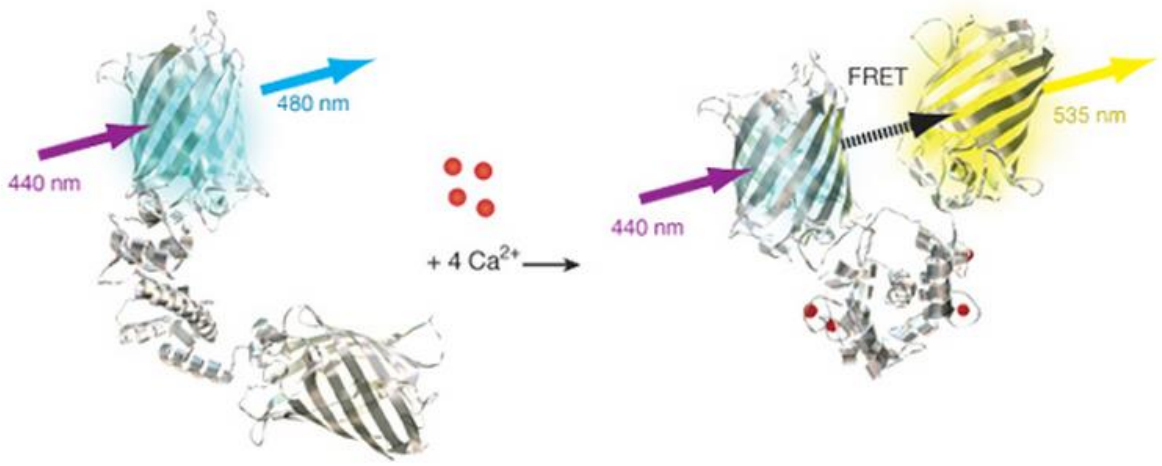

Fig 1.6: schematic representation and working principle of the cameleons [151].

The yellow cameleon (YC), the most used, is made of a cyan fluorescent protein (CFP, a mutated GFP with a shifted absorption and emission) and a yellow fluorescent protein (YFP, another GFP variant) linked together through a CaM and the M13 fragment of the myosin light chain (M13). Exciting the specimen with a 440 nm light, in absence (or with low levels) of calcium we obtain emission of light at 480 nm due to the fluorescence of the CFP. When the calmodulin binds calcium, it changes conformation and this allows the interaction with the M13. This interaction will lead to approach the two fluorescent proteins and so the FRET will increase. FRET is a physicochemical process characterised by the transfer of energy from an excited donor chromophore to an acceptor chromophore without associate radiation release. FRET is proportional to the 6^{th} power of the distance so, because this phenomenon may occur, we need the two chromophores to be really near (2-7 nm) as well as we need that the emission spectrum of the first chromophore overlap the excitation spectrum of the second one. In the yellow cameleon that is binding calcium, the light emitted from the CFP excites the YFP, so upon the same excitation wavelength of 440 nm, in presence of calcium, we will obtain an emission of light with a wavelength of 535 nm [145]. Therefore the calcium

levels will be evaluated in terms of ratio between the level of emission at 535 nm (emission of the YFP, coming from the molecules of sensor binding calcium) and the level of emission at 480 nm (emission of the CFP, coming from the molecules of sensor that are not binding calcium). Various modifications have been done since the first cameleon to reach the YC3.6 which have an apparent dissociation constant of 250 nM and a Hill constant of 1.7 [152]. Although the cameloens permitted a series of exciting observations, they present the typical disadvantages of the FRET-based reporters. Two above all are that they are limited in the colour variants and they limit the possibility to combine different fluorescent sensor in the same cell at the same time.

5. PURPOSE OF THE WORK: THE GECO AS NEW TOOLS TO STUDY NUCLEAR SYMBIOTIC CALCIUM SIGNALLING

The mentioned problems of the cameleons could be overcome by using single GFP-based reporters.

The GECOs (genetically encoded calcium sensors for optical imaging) are the evolution of the G-CaMP. These reported, developed in 2001, are constituted by a circularly permutated enhanced GFP (cpEGFP) which is fused at its N-terminus with the M13 fragment of the myosin light chain and at its C-terminus with the CaM [153].

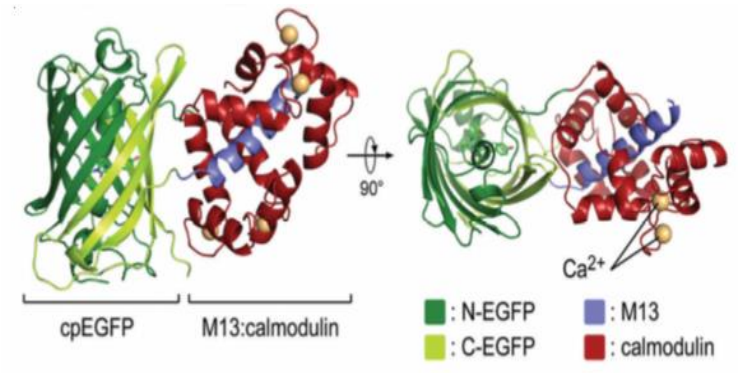

Fig. 1.7: schematic representation of the GECO [154].

The circular permutation destabilizes the deprotonated form of the fluorophore so, when the sensor is not binding calcium, we have only a low level of fluorescence due to

the protonated form of the fluorophore. But when the CaM binds calcium it becomes able to interact with the M13, with the external residues of the fluorescent protein barrel and with residues that interact with the fluorophores, these interactions stabilise the deprotonated form of the fluorophore and this lead to a change in the absorbance and to a big increase in the emission intensity [154].

A) B)

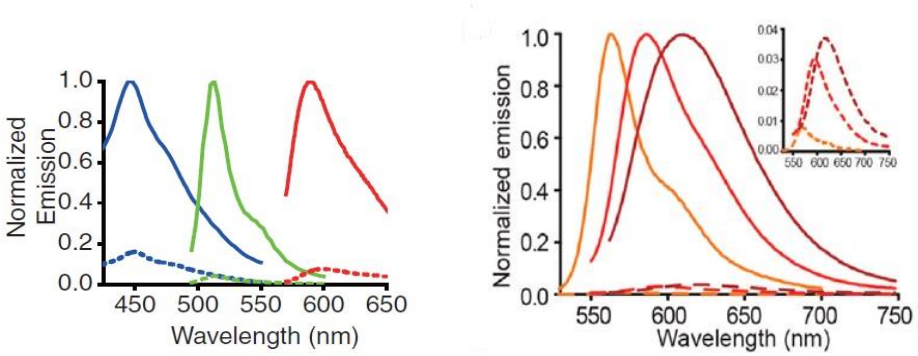

Fig. 1.8: Emission peaks of the GECOs in the free state (dashed lines) and in the calcium-bound state (solid lines). A) Blue-GECO1 (blue line), Green-GECO1 (green line), Red-GECO1 (red line). [155] B) Orange-GECO1 (orange line), Red-GECO1.2 (red line), Carmine-GECO1 (dark red line) [156].

Various versions of GECOs, with different emission and excitation spectra, different affinity for calcium and different calcium-dependent increase in fluorescence were created. Starting from the G-CaMP3 [157] through error-prone polymerase chain reaction (PCR) a library of variants was generated. Screening this library, three new sensors (Green-GECOs) were selected: G-GECO1, G-GECO1.1 and G-GECO1.2. These GECOs all share a calcium-dependent increase in the fluorescence that is approximately double of the G-CaMP3. The main difference between the three G-GECOs are the apparent dissociation constants (Kd) for Ca^{2+} which are respectively 750 nM, 620 nM and 1150 nM. The blue-GECO was obtained by introducing the GFP Y66H substitution in the G-GECO1.1 to create the histidine-derived chromophore of the blue FP. Red-shifted GECOs were generated replacing the cpEGFP of the G-GECO1.1 with the analogous version of the cp version of the mApple fluorescent protein [155]. Through error-prone PCR and additional rounds of directed evolution the Red-GECO1.2, the Orange-GECO1 and the Carmine-GECO1 were obtained in 2013 [156].

Considering the big calcium-dependent fluorescence increase, the Kd values and the availability of all these different colours in addition to the fact that they are single wavelength sensors, the GECOs could be the perfect candidate to overcome the limits of the cameleons.

In this work we propose the use of the GECOs, that have been so far tested only in animal cells, in plants. In particular, we will test the Green-GECO1.2 and the Red-GECO1.2 (Kd 1200 nM) as new tools to study nuclear calcium spiking in *M. truncatula* root hair cells during symbiotic signalling. In order to do that we will first adapt the GECOs sequence for the expression in plants though a codon optimization step, then we will build the vectors for the *Agrobacterium rhizogenes*-mediated transformation. The cloning step will be carried out using the Golden Gate technique. Finally, the response of the GECOs will be observed with wide-field and confocal microscopy methods and image analysis will be conducted.

Chapter 2

Materials and Methods

1. MATERIALS

1.1. Plant material

In this study we used two different ecotypes of wild-type *M. truncatula* seeds: ecotype Jester [158] seeds (purchased from Fertiprado, Portugal) and ecotype Jemalong A17 [159].

1.2. Bacterial strains

E. coli chemically competent cells strain DH5α (Life Technologies) were used for plasmid propagation. For the hairy root transformation *A. rhizogenes* strain 1193 (AR1193) [160] was used. The aliquots of both strains were stored in a -80 °C freezer.

1.3. Media

All the media were provided by the media kitchen of the institute. In the table 2.1 there is the complete list of the media used in this work with their compositions.

Medium	Recipe for 1 liter
Water-agar (WA)	agar (Formedium) 30 g.
Tryptone-yeast (TY)	tryptone 5.0 g, yeast extract 3.0 g, $CaCl_2 \cdot 6H_2O$ 1.325 g.
Luria-Bertani (LB)	tryptone 10 g, yeast extract 5 g and NaCl 10 g, agar (Formedium) 10 g (for solid medium).
Super-optimal broth with catabolite repression (SOC)	tryptone 20 g, yeast extract 20 g, NaCl 0.58 g, KCl 0.19 g, $MgCl_2$ 2.03 g, $MgSO_4 \cdot 7H_2O$ 2.46 g, glucose 2.6 g.
Modified Fahraeus media (Mod-FP)	$CaCl_2 \cdot 2H_20$ 0.1 g, $MgS0_4 \cdot 7H_20$ 0.12 g, KH_2PO_4 0.01 g, Na_2HPO_4 0.150 g, Ferric Citrate 5 mg, NH_4NO_3 0.5 mM, $MnCl_2 \cdot 4H_20$ 2.03 g, $CuSO_4 \cdot 5H_20$ 0.08 g, $ZnCl_2 \cdot 7H_20$ 0.22g, H_3BO_4 2.86 g, $Na_2MoO_4 \cdot 2H_20$ 0.08 g, Agar (Formedium) 8 g. NaOH to adjust the pH to 6.

Tab. 2.1: list and composition of the media used in this work

1.4. Antibiotics and chemicals

All the antibiotics and chemicals solutions were sterilized by filtration using a single use syringe and a Ministart single use filter unit of 0.20 µm and were stored at -20 °C.

antibiotic	solvent	Concentration for *E. coli* selection	Concentration for *A. rhizogenes* selection
Spectinomycin (Sigma-Aldrich)	deionized water	200 µg/ml	-
Ampicillin (Sigma-Aldrich)	deionized water	100 µg/ml	-
Kanamycin (Formedium)	deionized water	20 µg/ml	20 µg/ml
Carbenicillin (Formedium)	deionized water	-	50 µg/ml
Rifampicin (Sigma-Aldrich)	N,N-dimethylformamide (Fluka)	-	25 µg/ml
IPTG (Melford)	deionized water	100 µg/ml	-
X-Gal (Formedium)	N,N-dimethylformamide (Fluka)	40 µg/ml	-

Tab. 2.2: Complete list of antibiotics and chemicals used in this work with information about the solvents and the concentrations used.

1.5. Nod factors

Sinorizobium meliloti Nod factors used in this work were extracted by Giulia Morieri et al. [161].

1.6. Plasmids

All the backbones and the level-zero modules used for the cloning were synthesised by Life Technologies. All the new level-zero modules employed to build the level-one modules were designed using the software Vector NTI (Life Technologies).

1.7. Primers

In table 2.3 there is a complete list of the primers used in this work for the colony PCR and the sequencing. All of them were synthesised by Life Technologies.

primer	Sequence (5' → 3')	G/C %	lenght
Goldengante-3	CCCGCCAATATATCCTGTC	53	19
Goldengate-4	GCGGACGTTTTTAATGTACTG	43	21
Ben94	ATCTATGAAACCCTAATCGAG	38	21
Ben95	GAACTGATGATCTAGGACC	47	19
Ben23	TTGTGGCCGTTTACGTC	53	17
Ben26	ATCACATGGTCCTGCTG	53	17

Tab. 2.3: sequence, melting temperature (Tm), percentage of G and C (G/C%) and length of the primers used in this work

2. METHODS

2.1. Golden gate cloning

2.1.1. Principles of the cloning system and general workflow

All the vectors employed in this work for the plant transformation were built using the Golden Gate (GG) cloning technique. The GG is a modular and hierarchical cloning system that allows the directional assembly of multiple DNA fragments with high efficiency [162][163].

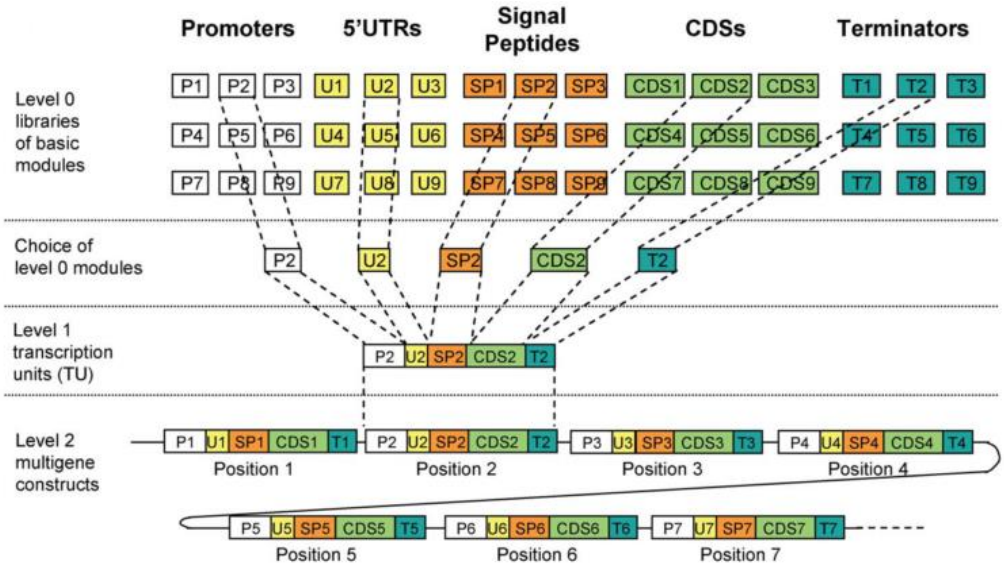

Fig. 2.1: The modular and hierarchical organization of the Golden Gate cloning system: the genetic elements required to assemble a transcription unit (pL1) are chose from a library of level-zero modules. Then, more transcription units are inserted in a pL2V to create a multigene construct [162]

As a first step, each fragment of interest is sub-cloned singularly in a specific plasmid called level-zero (pL0) backbone to form a pL0 module (pL0M). There is a level-zero backbone type for each standard element present in a gene, therefore we have a pL0-P for the promoter, a pL0-T for the terminator, a pL0-C for the coding sequence (CDS), a pL0-U for the 5' untranslated region (5' UTR) and a pL0-S for the N-terminal signal. Other pL0 backbones variants were generated to clone more than one genetic element in the same plasmid. For example in this work we used pL0-PU modules instead cloning separately promoter and 5' UTR.

Once each single genetic element required to build the gene of interest is in the appropriate pL0 backbone (and so each pL0M is created), the transcription unit (TU) can be assembled by inserting these elements together in a level-one (pL1) backbone to create a pL1 module (pL1M). The ultimate step consist of placing all the desired TUs in a level-two (pL2) backbone, to create the planned multigene construct. In this way we generate a pL2 vector (pL2V), which is the plasmid that can be used for the plant transformation. There are different types of pL1

backbones, each type allows the placement of the gene in a different position and orientation (forward or reverse) in the pL2V. Up to eleven transcription units (TU) can be combined to form a multigene level-two construct [162]. In figure 2.1 there is a schematic representation of the Golden Gate organization.

In this cloning system, in each plasmid, the DNA fragment of interest is flanked by restriction sites of type IIS restriction enzymes, while the recognition sites for the enzymes are placed in inverse orientation relative to each other to the far 5' and 3' end of the fragment. As a result, the digestion leads to the exclusion of the recognition sites from the final fragment, which will ends with particular 4 nt overhangs (fusion sites) [Fig. 2.4 B].

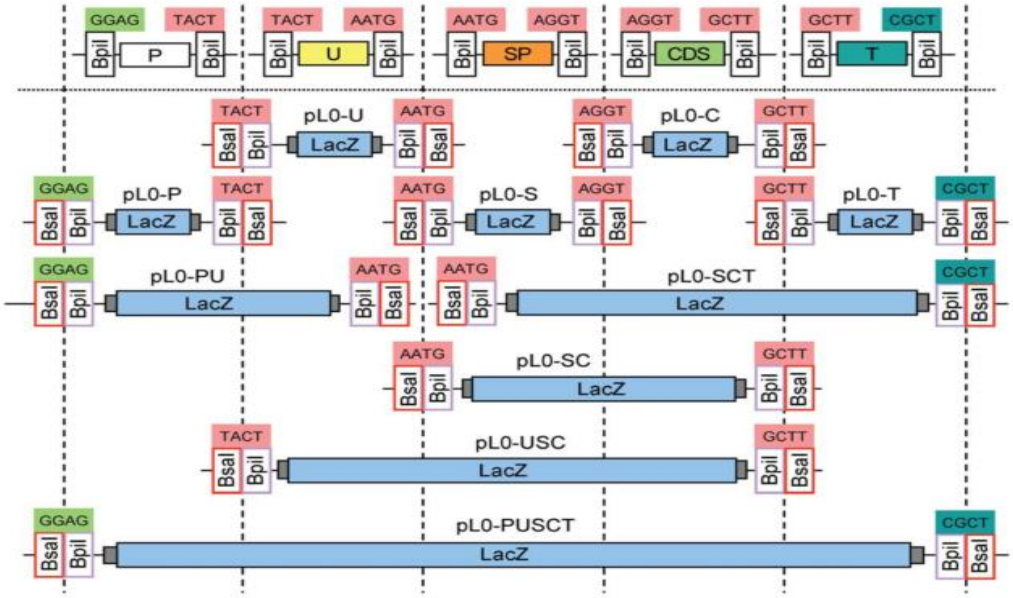

Fig. 2.2: some examples of pL0Ms with their fusion sites and their position [162].

The difference between the various types of modules of the same level lies in the sequence of the 4 nt overhangs generated by the digestion. An accurate design of the fusion sites allow the directional assembly of the fragments [Fig. 2.2].

2.1.2. Design of level-two vectors

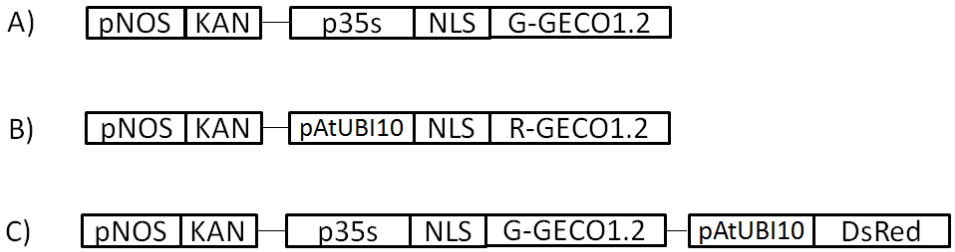

Fig. 2.3: schematic linear representation of the pL2 vectors built in this work. A) EC10791-pL2V-KAN-p35s-NLS-GreenGECO1.2 B) EC10795-pL2V-KAN-pAtUBI10-NLS-RedGECO1.2 C) EC11579-pL2V-KAN-p35s-NLS-GreenGECO1.2-DsRed

Combining different promoters, various strategies for the selection of the transformed roots and different GECOs' colours, we built three different constructs [Fig. 2.3] for the expression of the GECOs in *M. truncatula*.

As mentioned before, each pL1M type allows to place the TU in a different position (first, second, third, etc…) or orientation (forward or reverse) in the pL2V. In the pL2V2 all the gene were placed in reverse orientation, the kanamycin gene always in position one (i.e. near the T-DNA left border) and the GECO gene always in position two.

The first vector contains the kanamycin resistance for the selection of the transformed root and a GECO with an N-terminal nuclear localization signal (NLS) under the control of 35S promoter (p35S). For the Red GECO we built another version of this vector where the p35s was substituted with the *Arabidopsis thaliana* ubiquitin-10 promoter (pAtUBI10). We chose these two promoters as in literature is reported that they drive a strong and constitutive expression. In order to facilitate the selection of the transformed roots, we also built a green-GECO vector containing DsRed (*Discosoma* sp. (Sea anemone) red fluorescent protein) as a visual marker in addition to the kanamycin resistance (EC11579-pL2V-KAN-p35s-NLS-GreenGECO1.2-DsRed). Each one of these pL2Vs received an identification number as shown in figure 2.3.

2.1.3. Level-zero modules design

Almost all the pL0Ms required to build the planned vectors were already present in the laboratory with the exception of the ones containing the GECOs.

A)

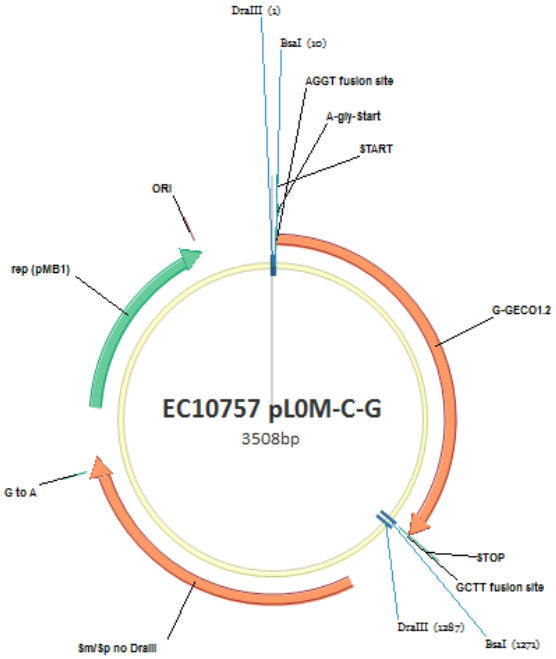

B)

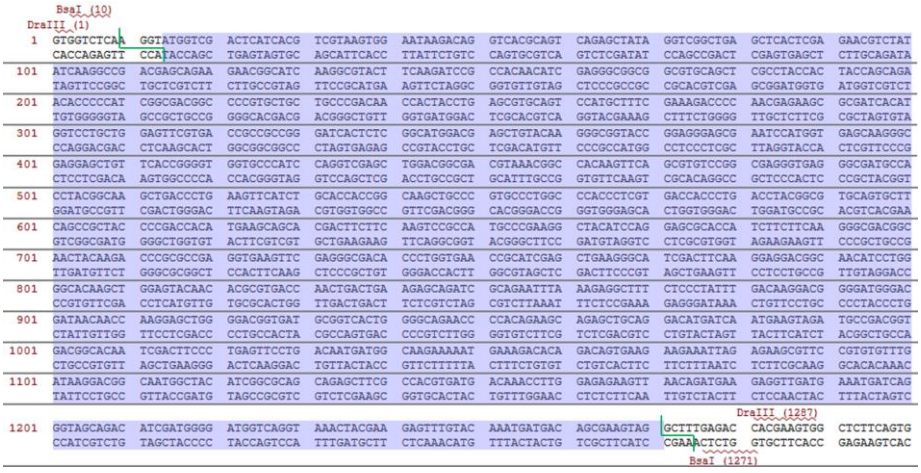

Fig. 2.4: A) EC10757-pL0-C-GreenGECO1.2 module map B) detail of the EC10757 plasmid, BsaI recognition sites (red) and cutting sites (green) flanking the CDS.

These modules were designed using the software Vector NTI (Life Technologies). Once obtained the coding sequence of interest from GenBank (G-GECO1.2

JN258415.1, R-GECO1.2 KF186685.1) the design of the pL0 modules passed through three different phases: codons optimisation, definition of the required position in the transcription unit and sequence domestication. The codon optimisation process was carried out in order to optimise the expression in plants and using the codon usage data of *A. thaliana*. Then, still *in silico*, the optimised sequences were inserted in pL0-C backbones. A pL0-C backbone is a plasmid designed to carry a CDS which has to be fused to an N-terminal signal sequence in the final transcription unit. In our case, the N-terminal signal required was the NLS, that was contained in a pL0-S module. After the digestion of a pL0-C module with the appropriate enzyme, the 4 nt overhangs at the ends of the CDS fragment are complementary to one end of the NLS fragment, on one side, and to one end of the terminator fragment, on the other side [Fig. 2.2 and 2.4].

With 'sequence domestication' we refer to the process of removing from the coding sequence, in our case, or from the sequence of interest more in general, the cutting sites of the restriction enzymes used in the GG cloning. This is necessary to prevent the enzymatic digestion of our fragment. The enzymes used in the GG cloning phases are BsaI, BpiI (BbsI), Esp3I (BsmBI) and DraIII. The first one and the second one are required to pass from the pL0Ms to the pL1Ms and from the pL1Ms to the pL2Vs respectively. To perform the sequence domestication we operated single nucleotide substitutions without changing the aminoacidic sequence.

All the pL0 backbones are based on the pUC19 backbone and so they confer spectinomycin resistance and originally present the *lacZα* for the bacterial selection [Fig. 2.5]. After this *in silico* design phase, Life Technologies synthesized the sequences and sub-cloned them in the standard level-zero modules required. So, we received from this biotechnology company plasmids like the one shown in figure 2.4, where the *lacZα* was already been cleaved and substituted with the CDS of interest.

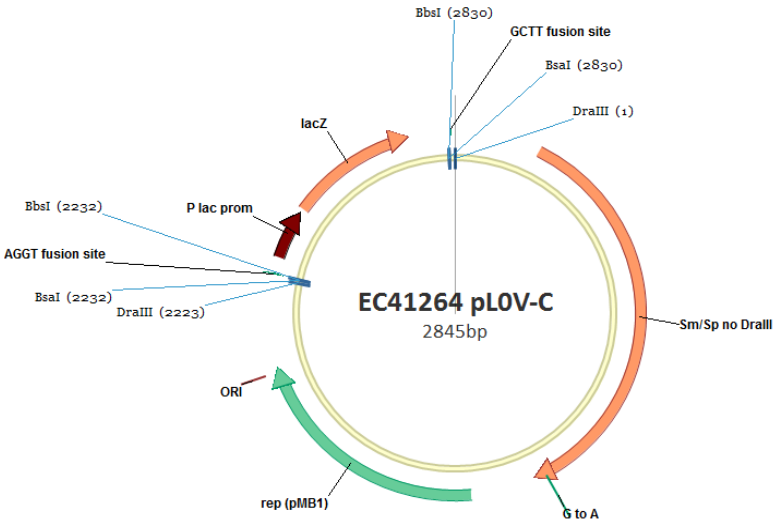

Fig. 2.5: Map of the pL0-C backbone.

2.1.4. Construction of level-one modules

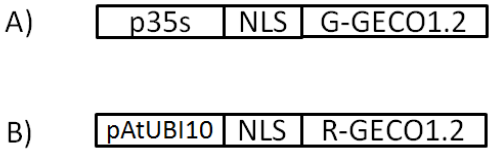

Fig 2.6: schematic linear representation of the pL1Ms built in this work. A) EC10787-pL1M-R2-p35s-NLS-GreenGECO1.2 B) EC10794-pL1M-R2-pAtUBI10-NLS-RedGECO1.2.

The cloning reaction was set up by pipetting in each tube 10 U of the restriction enzyme BsaI, 400 U of T4 DNA ligase, 1,5 µl of T4 DNA ligase buffer 10X (containing 10 mM ATP), 1.5 µl of BSA 10x, 100 ng of each required plasmid and deionized water to reach the final volume of 15 µl. The required plasmids are the pL0 modules containing the genetic elements that we need to build the TU (pL0-P, pL0-C, pL0-S and pL0-T) and the pL1 backbone of destination. Since all the pL1M containing the GECOs were designed to be placed in position two and in reverse orientation in the pL2V, the pL1 backbone required in this reactions was always the EC47811-pL1V-R2 shown in the figure 2.6.

The restriction enzymes, the BSA and the T4 DNA ligase buffer were bought from New England Biolabs and were stored at -20 ºC. The reaction mix was incubated in a thermocycler and exposed to the following variations of temperature: three minutes at 37 °C, four minutes at 16 °C, five minutes at 50 °C and five minutes at

80 °C. The first and the second step constitute the restriction-ligation cycle and were repeated 25 times. After the 25th repetition the thermocycler proceeded with the third and the fourth steps that are required for the enzyme deactivation. The complete protocol lasts around three hours and twenty minutes.

During the restriction phase, the enzyme excides the *lacZα* from the EC47811 plasmid leaving the 4 nt overhangs shown in the figure 2.7, thus a GGAG and a CGCT fusion sites are created on the backbone. At the same time and in the same way, BsaI works on the pL0 modules, so all the genetic elements are released from their L0 plasmids and they present appropriate fusion sites for a directionally assembled in the pL1M. Fusion scars of 4 nt remain between all the fragment in the assembled TUs. Only between the N-terminal signal and the coding sequence, to maintain the frame, there is a 6 nt scar encoding for a Gly-Gly linker.

In order to perform a first screen for correctly assembled level 1 modules, an aliquot of the mix resulting from each cloning reaction was used to transform *E. coli* chemically competent cells as described in paragraph 2.2. Since the pL1Ms contains the prokaryotic gene for the resistance to the ampicillin and since the assembled TU substitutes the *lacZα* in a correct pL1M, 200 µl of the bacterial liquid cultures resulting from the transformations were spread on LB Petri dishes containing ampicillin and X-Gal (see paragraph 2.3 for details on *E. coli* cultures on solid medium). Two or three white colonies for each construct were chosen to perform a further screening step through colony PCR (paragraph 2.4). Among the colonies resulted positive to the colony PCR analysis as described in the paragraph 1 of the chapter 3, one for each pL1M was selected to set up a liquid culture in order to amplify the plasmid (paragraph 2.5). The DNA extracted from these liquid cultures (see paragraph 2.6 for details) was sequenced as described in paragraph 2.9 and then employed in the next cloning phase.

A)

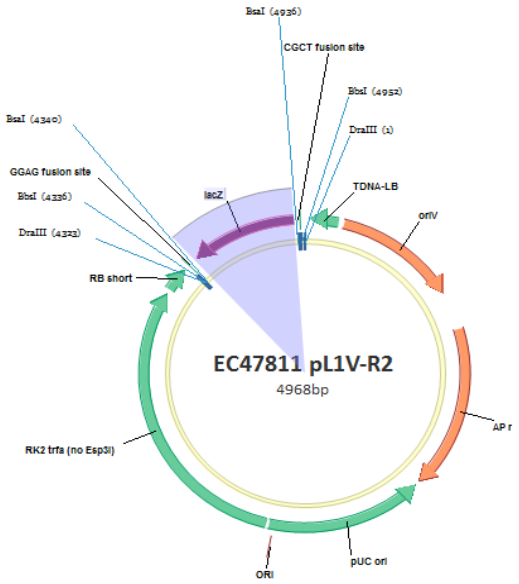

B)

DraIII (4323) BbsI (4336)

```
4301  CACTGATAGT  TTAAACCACT  TCGTGCAGAA  GACAATAGTG  GAGTGAGACC  GTCACAGCTT  GTCTGTAAGC  GGATGCCGGG  AGCAGACAAG  CCCGTCAGGG
      GTGACTATCA  AATTTGGTGA  AGCACGTCTT  CTGTTATCAC  CTCACTCTGG  CAGTGTCGAA  CAGACATTCG  CCTACGGCCC  TCGTCTGTTC  GGGCAGTCCC
                                                     BsaI (4340)
4401  CGCGTCAGCG  GGTGTTGGCG  GGTGTCGGGG  CTGGCTTAAC  TATGCGGCAT  CAGAGCAGAT  TGTACTGAGA  GTGCACCATA  TGCGGTGTGA  AATACCGCAC
      GCGCAGTCGC  CCACAACCGC  CCACAGCCCC  GACCGAATTG  ATACGCCGTA  GTCTCGTCTA  ACATGACTCT  CACGTGGTAT  ACGCCACACT  TTATGGCGTG
4501  AGATGCGTAA  GGAGAAAATA  CCGCATCAGG  CGCCATTCGC  CATTCAGGCT  GCGCAACTGT  TGGGAAGGGC  GATCGGTGCG  GGCCTCTTCG  CTATTACGCC
      TCTACGCATT  CCTCTTTTAT  GGCGTAGTCC  GCGGTAAGCG  GTAAGTCCGA  CGCGTTGACA  ACCCTTCCCG  CTAGCCACGC  CCGGAGAAGC  GATAATGCGG
4601  AGCTGGCGAA  AGGGGGATGT  GCTGCAAGGC  GATTAAGTTG  GGTAACGCCA  GGGTTTTCCC  AGTCACGACG  TTGTAAAACG  ACGGCCAGTG  AATTCGAGCT
      TCGACCGCTT  TCCCCCTACA  CGACGTTCCG  CTAATTCAAC  CCATTGCGGT  CCCAAAAGGG  TCAGTGCTGC  AACATTTTGC  TGCCGGTCAC  TTAAGCTCGA
4701  CGGTACCCGG  GGATCCTCTA  GAGTCGACCT  GCAGGCATGC  AAGCTTGGCG  TAATCATGGT  CATAGCTGTT  TCCTGTGTGA  AATTGTTATC  CGCTCACAAT
      GCCATGGGCC  CCTAGGAGAT  CTCAGCTGGA  CGTCCGTACG  TTCGAACCGC  ATTAGTACCA  GTATCGACAA  AGGACACACT  TTAACAATAG  GCGAGTGTTA
4801  TCCACACAAC  ATACGAGCCG  GAAGCATAAA  GTGTAAAGCC  TGGGGTGCCT  AATGAGTGAG  CTAACTCACA  TTAATTGCGT  TGCGCTCACT  GCCCGCTTTC
      AGGTGTGTTG  TATGCTCGGC  CTTCGTATTT  CACATTTCGG  ACCCCACGGA  TTACTCACTC  GATTGAGTGT  AATTAACGCA  ACGCGAGTGA  CGGGCGAAAG
                  BsaI (4936)                                                                 DraIII (1)
4901  CAGTCGGCAA  ACCTGTCGTG  CCAGCTGCGG  TCTCACGCTA  AGCTTGAATT  CTTGCTTGTC  TTCACAGA
      GTCAGCCGTT  TGGACAGCAC  GGTCGACGCC  AGAGTGCGAT  TCGAACTTAA  GAACGAACAG  AAGTGTCT
                                                                 BbsI (4952)
```

Fig. 2.7: A) map of the 47811-pL1V-R2 B) detail of the 47811-pL1V-R2, the blue highlighted part in the sequence corresponds to the blue highlighted part in the map. The recognition sites of the restriction enzymes are shown in red. The restriction sites of the BsaI enzyme are pointed out in green.

2.1.5. Construction of level-two modules

The 15025-pL2V-KAN plasmid, which already presents the eukaryotic kanamycin resistance gene in position one [fig 2.8], was used as destination vector to build all the level two modules of this work.

The cloning mastermix was set up as described before with a single difference: here we used 0.5 U of BsaI and 0.5 U of BpiI instead of only 1 U of BsaI. The plasmids required to build the pL2Vs EC10791 and EC10795 were the level-two

destination vector (EC15025-pL2V-KAN), the pL1M-R2 containing the desired GECO's transcription unit (respectively pL1M EC10787 and EC10794) and a pL1M containing an end linker (EC41744-pL1M-ELE-2). This end linker is a 24 nt sequence fragment designed to be an adapter and connect the gene in position two with the GGGA fusion site of the backbone.

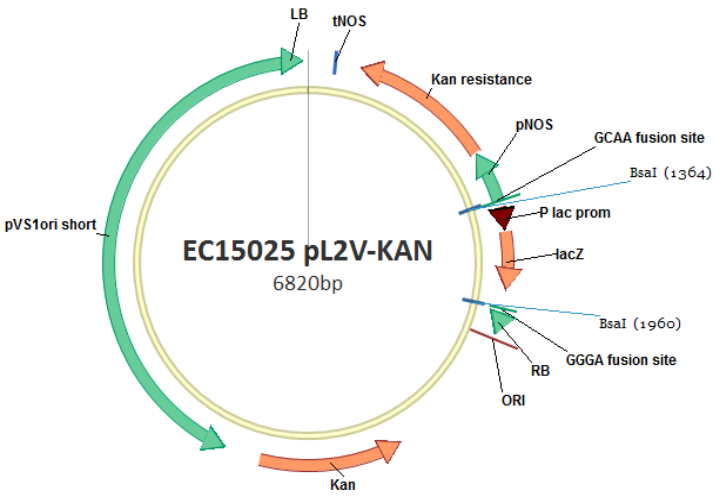

Fig. 2.8: EC15025-pL2V-KAN map

To build the EC11579-pL2V (which contain the DsREd as a visual marker for the selection of the transformed roots), we added the EC15034-pL1M-R3-pAtUBI10-DsRED to the reaction mix and we substitute the EC41744-pL1M-ELE-2 with another end linker (EC41766-pL1M-ELE-3, which is specific to connect the gene in position three with the GGGA backbone's fusion site).

The reaction mixes were finally incubated in a termocycler and exposed to the same temperature variations described before. In order to verify the correctness of these pL2Vs we carried out the white/blue colony screening, the colony PCR analysis and the sequencing (for details see respectively paragraphs 2.3, 2.4 and 2.9). For reasons that we will clarify later, the pL2V EC11579 underwent to a further step of verification carried out through enzymatic digestion (paragraph 2.7) before the sequencing phase.

2.2. *E. coli* transformation

Each module or vector built was transformed in *E. coli* both to perform a selection and to propagate the plasmid. To carry out the transformation, 100 ng of DNA (or 1 µl of the products of golden gate reaction) were added to 20 µl of *E. coli* chemically competent DH5α cells. Afterwards the cells were incubated on wet ice for twenty minutes and then they were heat shocked: the tubes were transferred in a water bath at 42 °C for thirty seconds and immediately back on wet ice. Subsequently, 500 µl of SOC medium were added to each tube and the cultures were incubated in a shaker at 37 °C for forty minutes. After the incubation, 200 µl of each cultures were plated on LB plates containing the appropriate antibiotic and chemicals. Finally, the plates were placed in an incubator at 37 °C and left there overnight.

2.3. *E. coli* cultures on solid medium

For *E. coli* cultures on solid medium Petri dishes with LB-agar were used. The purpose of these cultures was to select the transformed bacteria containing a probably correct plasmid. The required antibiotics and chemicals were added to the melted LB agar and then the medium was poured into sterile round Petri dishes and left to solidify under the laminar flow cup. IPTG (100 µg/ml) and X-GAL (40 µg/ml) were required for the white/blue colony screening of any plasmid, while different antibiotics were used to select different plasmids. For the selection of bacteria containing a pL0M we used spectinomycin (200 µg/ml), while ampicillin (100 µg/ml) was used in case of pL1Ms and kanamycin (20 µg/ml) was used for pL2Vs. The colonies on LB-agar plates appeared after one night of incubation at 37 °C. A white colony indicates that the bacteria contain the gene for the resistance to the antibiotic present on the plasmid backbone and they do not contain the *lacZα*, so they may have the plasmid with the fragment of interest in place of the *lacZα*.

2.4. Colony PCR

The colony PCR was performed on the chosen white *E. coli* colonies to verify the presence of the fragment of interest in the plasmid. The unitary reaction was

composed by 1 µl of each primer from a stock solution of 10 µM, 7.5 µl of Gotaq green mastermix 2X (purchased from Promega and stored at -20 °C) and 5.5 µl of sterile water. In this final volume of 15 µl, a colony was put using a sterile tip. After touching the chosen colony with the tip, before put the bacteria in the mix, the bacteria were streaked on a new plate in order to create a *replica* of the colony that was going to be screened. Then the mix was incubated in a termocycler and underwent to the following protocol: ten minutes at 95 °C, thirty repetitions of the cycle denaturation-annealing-elongation (30 seconds at 94 °C, 40 seconds at the chosen annealing temperature, one minute for each Kb of the fragment at 72 °C) and finally five minutes at 72 °C. The annealing temperature chosen varied depending on the characteristics of the couples of primers.

To perform the colony PCR on the pL1Ms we used a couple of primers named GoldenGate-3 (GG3) and GoldenGate-4 (GG4) [Tab. 2.3] that are matching respectively on the T-DNA RB and on the T-DNA LB. Since the melting temperatures (Tm) were 51 °C for the primer GG3 and 50 °C for the primer GG4, for this couple of primers we chose an annealing temperature (Ta) of 45 °C.

The colony PCR on *E.coli* for the constructs EC10791 and EC10795 was carried out using the primers GG3 and GG4 and the same Ta used in the previous reaction (45 °C). While to verify the presence of the GECO TU in the construct EC11579, we used the primers Ben94 and Ben95 (see table 2.3 for details) that are matching on the pAtUBI10. Even if the Tm of Ben94 and Ben95 is 49 °C, we chose a Ta of 52 °C as we saw from previous experiences that this was the best annealing temperature for these primers.

As explained in the following paragraphs, in order to perform the plant transformation we inserted the pL2Vs in *A. rhizogenes*. A colony PCR was carried out on the *A. rhizogenes* colonies before set up the liquid cultures required for the plant transformation to verify if the strains were really carrying the multigene construct of interest. In these PCRs we used the primers GG3 and GG4 on the construct EC10791 and EC10795 (Ta 45 °C) and the primers GG3 and Ben94 on the construct EC11579 (Ta 52 °C).

2.5. *E. coli* liquid cultures

One *E. coli* liquid culture for each construct was set up from the replica of a colony resulted positive to the PCR analysis in order to propagate the plasmids. Particular attention was paid to not let the duplicated colonies overgrow in order to minimize the genetic variability of the liquid cultures, so, the inoculation took place usually no more than 7-8 hours after the colonies were streaked. To perform this step, under sterile conditions, we touched the replica of the chosen colony with a tip and then we pipetted in to 10 ml of LB broth. Following the same concentration rules applied for the cultures on solid medium (paragraph 2.3), antibiotics were added to the liquid cultures to maintain the selection and to prevent the loss of the plasmids.

2.6. Plasmid extraction

The DNA was extracted from the *E. coli* liquid cultures after incubation in a shaker at 37 °C overnight. The extraction was accomplished using the QIAprep spin Miniprep kit (Qiagen) and following the protocol supplied with the kit. The DNA concentrations were measured by loading 1.5 µl of the obtained solution on the Nanodrop 2000 spectrophotometer (Thermo scientific). The sample was considered pure enough when the ratio of the absorbance at 260 nm and 280 nm was ~1.8. Afterwards the solutions were diluted with deionized sterile water to a final concentration of 100 ng/µl of DNA and stored at -20 °C.

2.7. Enzymatic digestion

The enzymatic digestion was performed on the EC11579 pL2V as an additional test after the colony PCR and before sequence the construct. The reaction was set up by pipetting in a PCR tube 1 µg of DNA, 1 U of the restriction enzyme HindIII (New England Biolabs), 2.5 µl of the CutSmart buffer (New England Biolabs) and deionized water to reach the final volume of 25 µl. Then the mix was incubated overnight at the temperature required by the enzymes, and after that 5 µl of Gel Loading Dye Blue 6X (New England Biolabs) were added to the mix to stop the reaction. The pattern of bands resulting from the electrophoresis was compared

with the *in silico* prediction performed with the software Vector NTI (Life Technologies).

2.8. Agarose gel electrophoresis

Agarose gel electrophoresis were carried on in order to check the products of the colony PCRs and the results of the enzymatic digestions. The electrophoresis gel used in this study was a 1% agarose gel. The agarose powder (purchased from Melford and stored at room temperature) was dissolved in TAE 1X. TAE stock solution 50X, was diluted with deionised water. Once melted in a microwave, the solution was stored in a water bath at 60 °C for no more than one week. Electrophoresis were performed in horizontal agarose gels, immersed in TAE 1X, at 80 to 110 V. Once the runs were completed, the gels were transferred in a 0.5 µg/ml solution of ethidium bromide and let stain for at least 15 minutes. The DNA was detected by fluorescence of the DNA-ethidium bromide complex exposed to ultraviolet (UV) light. To carry out this step and to acquire the images, we used the GeneFlash Gel Documentation (gel doc) system (Syngene).
As ladder we always used the 2-Log DNA Ladder (New England Biolabs).

2.9. DNA sequencing

Since we were already sure about the correctness of the sequence of each single DNA fragment, a partial DNA sequencing was carried out just to check if these single DNA fragments were correctly assembled in the TUs and if the TUs were correctly assembled into the multigene constructs. This partial sequencing of the pL1Ms and pL2Vs built was carried on with the Sanger method and the first step of the process was performed in our lab. The reaction mix was set up by pipetting in a PCR tube 1.6 µl of one of the primers, 1.5 µl of the sequencing buffer (Life technologies), 1 µl of BigDye V3.1 (Life technologies), 4.9 µl of deionised water and 100 ng of DNA. Then the tubes were incubated in a thermocycler and underwent to an initial denaturation step (96 °C for 1 minute) followed by 25 repetitions of the denaturation-annealing-elongation cycle (1 minute at 96 °C, 5 seconds at 50 °C, 4 minutes at 60 °C). Subsequently the products were conserved at 4 °C. Each plasmid

was partially sequenced in both directions by setting up two different reactions, one for each primer. The BigDye V3.1 contains a TaqDNA polymerases, standard dNTPs and ddNTPs labelled with fluorescent dyes of four different colours (one for each base). When the TaqDNA polymerase incorporates a ddNTPs in the growing strand, the elongation is terminated as there is no 3' hydroxyl group. Thus, the product of our reaction was a mixture of fragments starting with the primer and terminating at various levels with a labelled ddNTP. Eurofins Genomics carried out the analysis of these products detecting the ddNTPs fluorescent signals after capillary electrophoresis. What we received back as result of the sequencing was a chromatograph, generated by the detected signals, that was corresponding to a sequence of bases. Using the program Contig Express (Life Technologies) we analysed these data, and, once obtained positive results we proceeded with the transformation of *A. rhizogenes*. The primers GG3 and GG4 were used to sequence all the vectors built in this work. Due to the reasons explained in the paragraph 1.2 of the chapter 3, for the construct EC11579 two additional sequencing reaction using the primers Ben23 and Ben26 were set up (see table 2.3 for details on the primers).

2.10. *A. rhizogenes* transformation

In order to obtain roots expressing our constructs, we decided to use *A. rhizogenes* as vector for the plant transformation. Therefore, as a first step, we transformed *A. rhizogenes* electrocompetent cells with the plasmids of interest.

2.10.1. Preparation of *A. rhizogenes* electrocompetent cells

50 ml Of LB broth containing antibiotics (rifampicin and carbenicillin, see table 2.2 for the concentrations) were inoculated with a single *A. rhizogenes* colony and incubated in a shaker at 28 °C overnight. Afterwards, an aliquot of this pre-culture was added to 400 ml of pre-warmed LB broth containing the same antibiotics. This final culture was incubated at 28 °C in a shaker until reaching an OD_{600} between 0.4 and 0.7. We performed the measurement with a spectrophotometer (BioPhotometer, Eppendorf), and, once the cells reached

the desired $OD_{600,}$ we cooled the whole culture by placing the buckets on wet ice for 15 minutes. To stop the cell growth, all the following steps were carried out on ice and in a 4 °C cold room or in pre-cooled centrifuges at 6 °C. After the cooling step, the entire culture was spun with 4000 rpm for 10 min. Then, the supernatant was discarded and the cells were resuspended in cooled deionised water by gently shaking the buckets. The cells were spun and resuspended in this way two more times, but, at after the third centrifuge, we resuspended them in 10 ml of 10% glycerol. Subsequently the broth was transferred into 50 ml falcons and it was spun again for 10 min with 4000 rpm. Once discarded the supernatant, the pellet was resuspended in 1 ml of 10 % glycerol. Finally we prepared aliquots of 20 µl each and we dipped the tubes in liquid nitrogen before store them in a -80 °C freezer.

2.10.2. Electroporation

A. rhizogenes cells were transformed by electroporation using the Gene pulser I electroporation system (Bio-rad). To perform the transformation we added 125 ng of DNA to 20 µl of *A. rhizogenes* competent cells. The parameters chosen for the electroporation process were resistance (R) 200 Ω, capacity (C) 25 µF and voltage 1.25 V. Geneflow electroporation single use cuvettes 2mm gap were used and the aliquots were maintained on ice until they were moved to the cuvettes. The time constant of the circuit was checked and maintained around 4.7 s. Immediately after the electroporation, the cells were resuspended in 500 µl of SOC medium and incubated in a shaker at 28 °C for 1-2 hours. Afterwards, 200 µl of this liquid culture were spread on LB-agar Petri dishes containing the appropriate antibiotics (see table 2.2 for the concentrations).

2.11. *A. rhizogenes* cultures

Cultures in LB-agar Petri dishes containing the appropriate antibiotics were set up to select the transformed cells. Antibiotics were used to create a selective growth medium. Kanamycin (20 µg/ml) was added as the pL2Vs contain the prokaryotic kanamycin resistance gene, rifampicin (25 µg/ml) and carbenicillin (50 µg/ml) were

employed as the AR1193 strain is resistant to these antibiotics. Colonies appeared on the plates after three days of incubation at 28 °C.

Once obtained the colonies on solid medium, colony PCRs were carried out to be sure that the chosen colonies were holding our plasmids and that the plasmids were containing the fragment of interest (see paragraph 2.4 for details of the colony PCRs protocol). Among the colonies resulted positive to the PCR analysis, a single one for each construct was chosen to set up a liquid culture in 5 ml of LB broth. To maintain the selection, we added to the growth medium the same antibiotics listed above at the same concentration. The inoculation was carried out under laminar flow cup by touching a single colony with a sterile tips and then pipetting in to the growth medium. Then, the cultures were incubated in a shaker at 28 °C for about 2-3 days.

2.12. Glycerol stocks

In order to conserve the bacterial strains containing the plasmids of interest, a glycerol stock of each *E. coli* and *A. rhizogenes* culture was made by adding 0.8 ml of a 40 % glycerol solution to 0.8 ml of the fresh bacterial liquid culture under sterile conditions. The stocks were stored in the -80 °C freezer.

2.13. Hairy root transformation

2.13.1. Seed sterilization and germination

In order to avoid contaminations the seeds were sterilized before the transformation.

Jemalong seeds were scarified with sandpaper to facilitate the imbibition and then were added, under sterile condition, to a 10% hypochlorite solution. To perform this sterilization step we used an amount of hypochlorite solution sufficient to cover all the seeds. After three minutes of incubation with occasional mixing, the bleach was removed by repeated washing with deionised sterile water. Once the bleach was completely removed, the seeds were left to imbibe in deionised sterile water at room temperature for at least three hours.

After this time, the seeds were transferred, under sterile conditions, in water-agar squared plates.

The plates were sealed with micropore tape (3M), covered with aluminium foil and placed upside down at 4 °C for at least three days to synchronize the germination. Jester seeds do not need scarification, so, for this ecotype, we started directly with the sterilisation step.

The pL2Vs EC10791, EC10795 and EC11579 were employed for the plant transformation. With the aim of transform 100 seedlings for each construct we prepared 300 Jemalong seeds and 150 Jester seeds.

2.13.2. Plant transformation

Two days before the transformation liquid cultures of the required *A. rhizogenes* strain were set up on LB broth containing kanamycin, rifampicin and carbenicillin at the usual concentrations [Tab. 2.2]. One day before the transformation, the seeds plates were transferred at room temperature, still left upside down and covered with aluminium foil. After 24 hours, approximately the 80% of the seedlings had a straight root long about 1-2 cm.

The day of the transformation, 2 ml of the *A. rhizogenes* liquid cultures were spun down in a micro-centrifuge at full speed for 30 seconds. Then the pellets were resuspended in 200 µl of TY broth. Under sterile conditions, sterile water was poured into the seedling plate. Afterward, six seedlings were transferred in big drop of sterile water previously prepared in a Petri dish, to keep them hydrated. A seedling at time was transferred from the water drop into another Petri dish where about 3 mm for the root tip was cut off. Then the sectioned seedling radicle was dipped into a drop of the resuspended *A. rhizogenes* culture [Fig 2.8 A]. Afterwards the seedling was finally placed onto modified Fahraeus media (Mod FP) square plate [Fig. 2.8 B].

A) B)

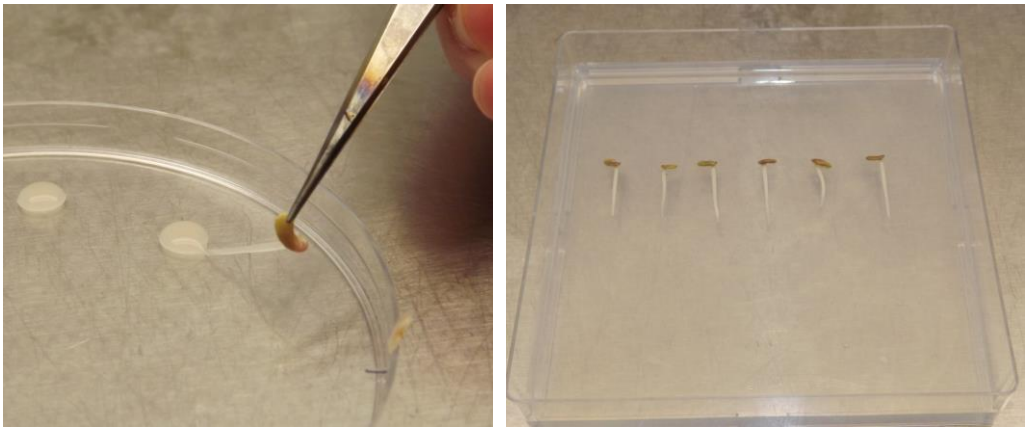

Fig. 2.8: A) inoculation of the sectioned seedling . B) *M. truncatula* seedlings placed in a 90 mm square plate on Mod-FP growth medium.

Jemalong seedlings were transformed with the EC10795 pL2V (100 seedlings) and with the EC10791 pL2V (100 seedlings). 100 Jester seedlings were used for the transformation of the construct EC11579.

The plates were labelled, sealed with micropore tape (3M) and placed upright in the growth chamber.

2.13.3. Plant growth

The growth chamber had temperature of 22 ± 1 °C, a photoperiod of 16h and a white light (each shelf had two OSRAM bulb L 70W/21-840 and one OSRAM bulb L 58W/77). After three days in the growth chamber, the plants transformed with the constructs EC10791 and EC10795 were transferred into plates containing kanamycin. Mod FP-kanamycin plates where made by adding an aliquot of the antibiotic stock solution to the melted Mod-FP medium to reach a final kanamycin concentration of 25 µg/ml.

One week after the transformation, the plates were covered with a foil of blue paper as the light in the growth room could be too bright. Three weeks after the transformation we started the screening. Although also the construct EC11579 contains the eukaryotic gene for the kanamycin resistance, we decided to leave the EC11579 plants on plates without kanamycin as the presence of the antibiotic slows down the growth and it is and additional stress for the plants.

2.14. Calcium imaging

2.14.1. Preliminary screening

For the construct EC11579 a preliminary screening was carried out in order to identify the transformed roots to be used in the following steps of imaging. The DsRed fluorescence was detected with a Leica MZFLIII fluorescence stereomicroscope while the plants were exposed to a 546/12 nm wavelength light.

For the constructs EC10791 and EC10795 we selected the roots that were looking more healthy despite of the kanamycin presence in the growth medium.

2.14.2. Roots preparation for the imaging process

Healthy and young roots were cut under sterile conditions and were placed on a large cover glass (48 mm x 64 mm, thickness #1.5, Agar scientific). A small chamber was made around the root using high vacuum grease (Dow Corning GMBH, USA). The chamber was filled with a solution of Nod factors 10^{-9} or 10^{-8} M, an amount of solution sufficient to cover the whole root was used. The chamber was then covered with a small and slim coverglass (22 mm x 50 mm, thickness #1, VWR International). This second cover glass was pushed down in order to seal the chamber and squash the solution drop. Sometimes several roots were cut at the same time, placed in a sealed water-agar plate and used during the day.

2.14.3. Imaging

Fluorescence was imaged using two different systems: Zeiss LSM780 and Nikon Eclipse FN1 upright microscope with x-light confocal unit (CAIRN).

The LSM780 has been used only for the imaging of the EC11579 construct. With this microscope, we used the Zeiss objective EC Plan-Neofluar 10x/0.3 Ph1 M27 and a pinhole dimension of 76 µm or 90 µm. The specimen was excited with the 488 nm spectral line from the argon laser at 4%-22% power. The emitted

fluorescence was monitored using 493-598 nm range filters. The electronic magnification was set between 6.1x and 45.8x. Images were collected with intervals of 3.13-0.31 s and exposure time of 100 to 500 ms.

The Eclipse FN1 was coupled with the Rolera thunder FAST 1394 mono illuminated EMCCD camera system (Qimaging). A Lumencor LED light engine was used to excite the specimen, the excitation wavelength were 470/24 nm for the green GECO and 575/25 nm for the red GECO. As objectives we used CFI Plan fluor 10xW NA 0.30 WD 3.5 mm and CFI Apo 40x NA 0.80 WD 3.5 mm. The emission filters set was composed of a 505-550 nm filter for the green channel and a 650 nm filter for the red channel. The images were acquired every 5 s with an exposure time of 500 ms or without any interval and an exposure time of 100 ms.

2.14.4. Image analysis

Average pixels intensity values of outlined regions were measured using the software Image J (National Institute of Healt; http://rsb.info.nih.gov/ij/). Subsequently the values were exported into Microsoft Excel and plotted against time.

Chapter 3

Results

1. CLONING

In the first part of this work, through the Golden Gate cloning system, we built the vectors for the expression of the GECOs in *M. truncatula*. The correctness of each pL1M and pL2V was assessed with colony PCR and partial sequencing. The results of the colony PCRs were considered positive when we obtained bands of the sizes predicted through the *in silico* analysis. The sequencing results consisted of the sequence and the chromatograph of the sequence: the latter gave us an indication on the quality of the extracted DNA and on the reliability of the results, while comparing the ~1 kb sequence obtained with the *in silico* map we obtained information on the correctness of the assembled fragment.

1.1. Correctness of the level-one modules built

As explained before, to perform the colony PCR on the pL1Ms we used the primers couple GG3-GG4 and we chose a Ta of 45 °C.

The gel electrophoresis in figure 3.1 A shows the ~2.1 kilobases (Kb) bands obtained from the colony PCR on the colonies transformed with the construct EC10787. While in figure 3.1 B we can see the ~3.2 Kb bands obtained from the colony PCR on the EC10794 colonies. The dimensions of the bands were estimated by comparison with the bands of the 2-Log DNA ladder (New England Biolabs) and

they were matching with the *in silico* predictions. Since these results revealed that the fragments assembled in the pL1Ms contained in the screened colonies had the correct sizes, we proceeded with the next step: starting from the *replica* of one of the positive colonies, we set up a liquid culture for each construct.

Afterwards, a good quantity of the plasmids was extracted from the bacteria grown in the liquid cultures and an aliquot of the DNA solution was used to perform the partial sequencing.

For the pL1Ms, the sequencing reactions were set up with the primers GG3 and GG4. The fragment of about 1 kb sequenced starting from the GG3 primer was overlapping the promoter and the beginning of the GECO CDS, while using the GG4 primer we obtained a fragment corresponding to the terminator and the last part of the GECO CDS [Fig. 3.2 A]. Comparing the sequence of the fragments with the map and the *in silico* sequence of the construct, allowed us to see that the GECO, the terminator and the promoter actually were in the assembled TU and they were in the correct position. The chromatographs obtained from the sequencing reactions of the construct EC10787 showed clear peaks and low background indicating a good quality of the extracted DNA and a successfully performed reaction.

A

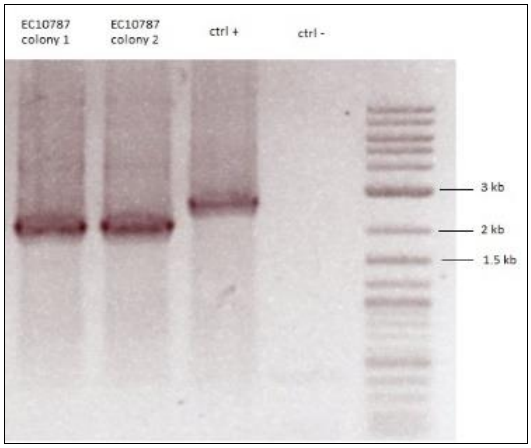

B

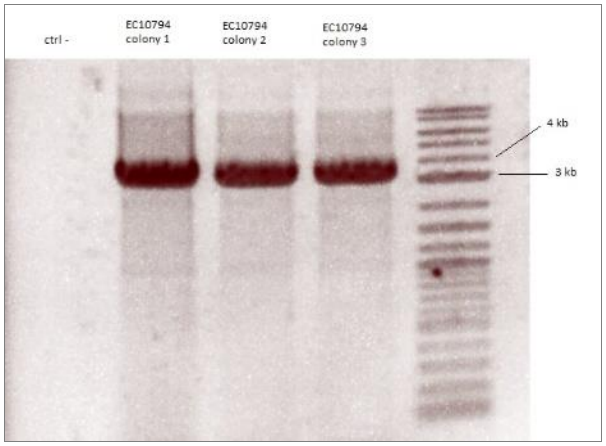

Fig 3.1: A) Gel Electrophoresis of the colony PCR on EC10787 colonies, both the selected colonies resulted positive. As positive control (ctrl +) for the PCR conditions we used the EC15034 DNA. This reaction generated a band of 2.7 kb as expected and allowed us to verify that the PCR condition were appropriate for the chosen primers. B) Electrophoresis gel showing the fragments of 3.2 kb amplified through the colony PCR on EC10794 colonies, all of them resulted positive. As negative control (ctrl -), in both gels, we used 15 µl of the PCR mastermix.

Since the construct EC10794 contains the pAtUBI10, which is 1086 base pairs longer than the p35s, starting the sequencing from the T-DNA RB (i.e. with the GG3 primer) gave us information only on the promoter. The presence and the position of the GECO in the TU has been verified anyway through the sequencing reaction starting from the GG4 primer. Also for this construct we got a good quality chromatograph.

Considering all the information obtained from the sequencing together with the results of the colony PCRs, we could say that our pL1Ms were properly assembled and so we could use them in the next cloning step.

A)

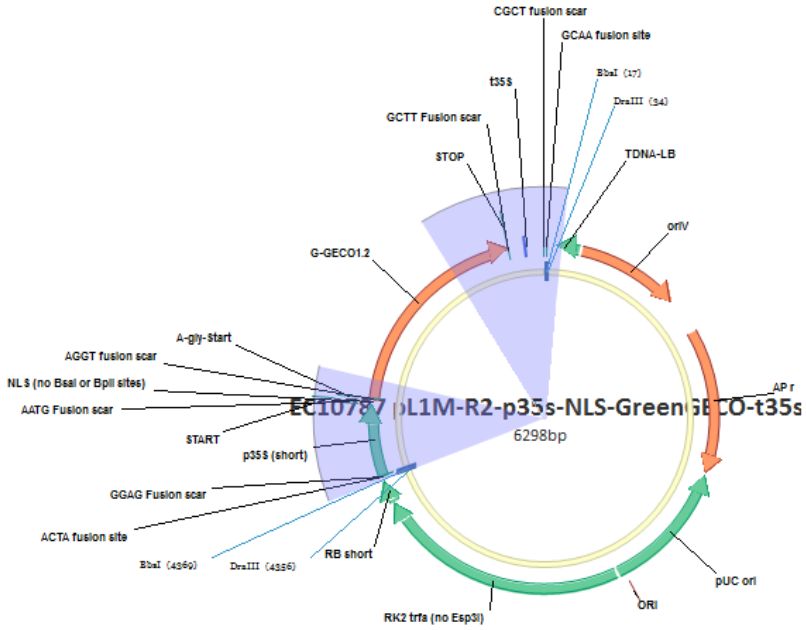

B)

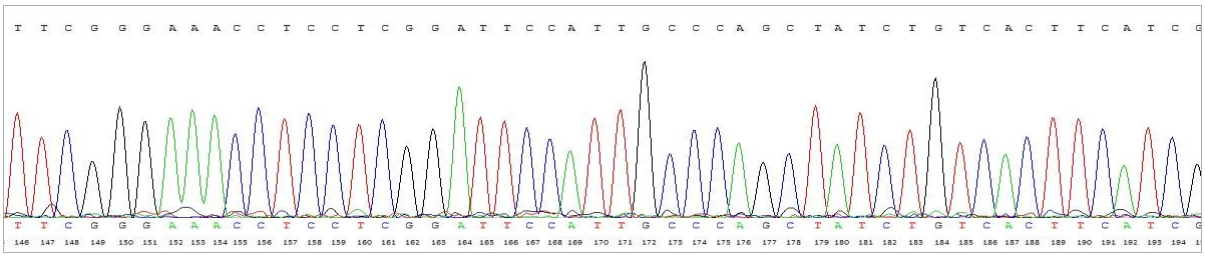

Fig 3.2: A) Map of the construct EC10787, the blue-highlighted parts are the regions corresponding to the sequenced fragments B) a part of the chromatograph resulting from the sequencing of the EC10787

1.2. Correctness of the level-two vectors built

A) B)

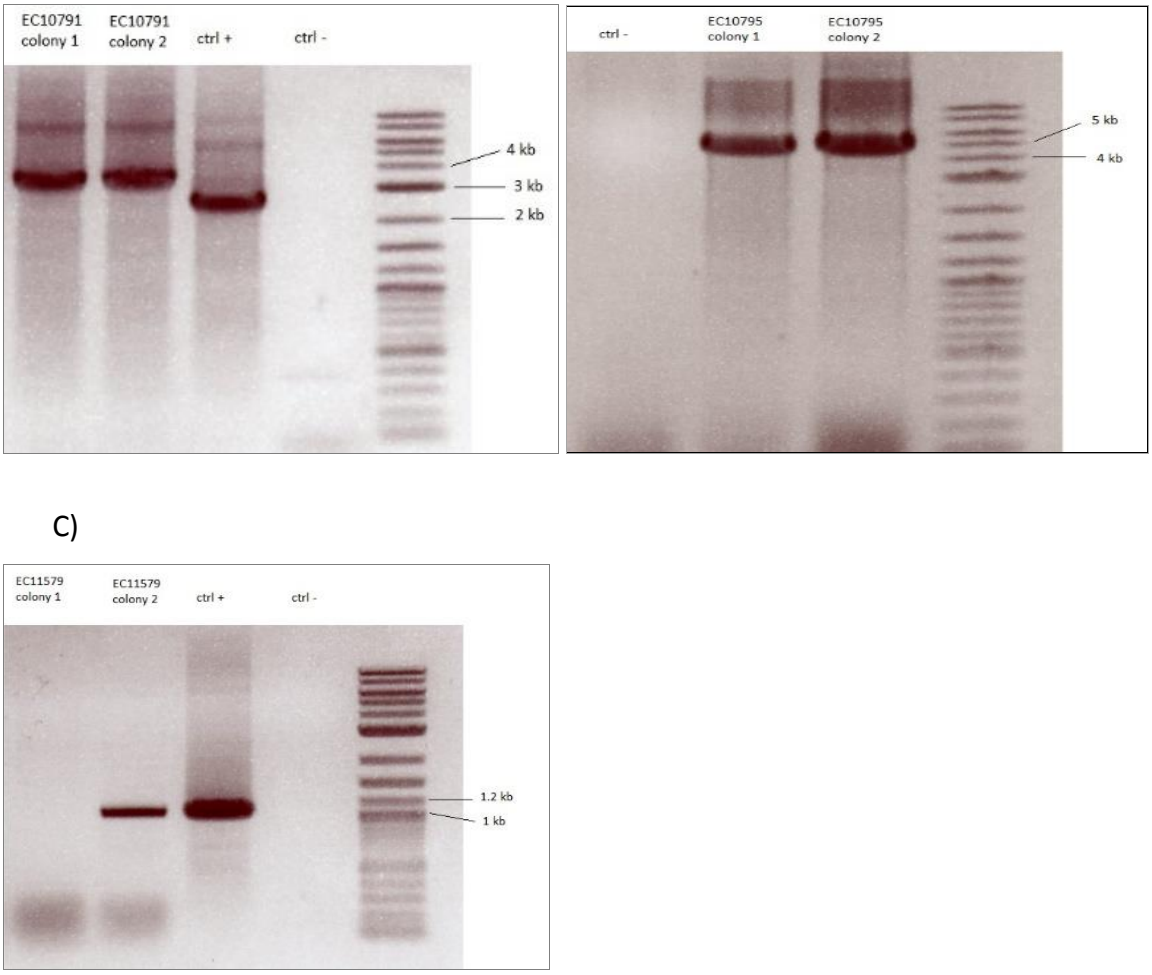

C)

Fig 3.3: Gel Electrophoresis showing the bands obtained through colony PCR on the pL2Vs colonies. As positive control (ctrl +) of the PCR conditions we used the EC15034 DNA, as negative control (ctrl -) we used 15 µl of the PCR mastermix. A) Positive result of the colony PCR on the EC10791 colonies, we obtained the expected 3.4 kb bands. B) Positive result of the colony PCR on Ec10795 colonies, we obtained 4.7 kb bands as expected. C) Results of the colony PCR on EC11579 colonies: the colony number 1 resulted negative while we obtained the expected 1.1 kb band from the colony number 2.

As mentioned in the previous chapter, the colony PCR on *E.coli* for the constructs EC10791 and EC10795 was carried out using the primers GG3 and GG4 and a Ta of 45 °C . While to verify the construct EC11579, we used the primers Ben94 and Ben95 and a Ta of 52 °C. The figure 3.3 A shows the gel with the ~3.4 kb bands obtained from the PCR on the EC10791 colonies. The bands of about 4.7 kb amplified through PCR on the EC10795 colonies are shown in the figure 3.3 B, while

in the figure 3.3 C we can see the ~1.1 kb band amplified using the couple Ben94-Ben95 during the colony PCR on the EC11579 colonies. The dimensions of the bands were estimated by comparison with the bands of the 2-Log DNA ladder (New England Biolabs) and they were matching with the *in silico* predictions.

We chose to not use the primers GG3 and GG4 on the EC11579 construct as the insert present between T-DNA RB and LB in this vector is ~6 kb; moreover, try to amplify such a big fragment, the probability of false negative results would have increased. But, since the colony PCR with the primers Ben94 and Ben95 gave us only the evidence of the pAtUBI10 presence, to get more information we also performed an enzymatic digestion of the EC11579 plasmid with the enzyme HindIII.

A) B)

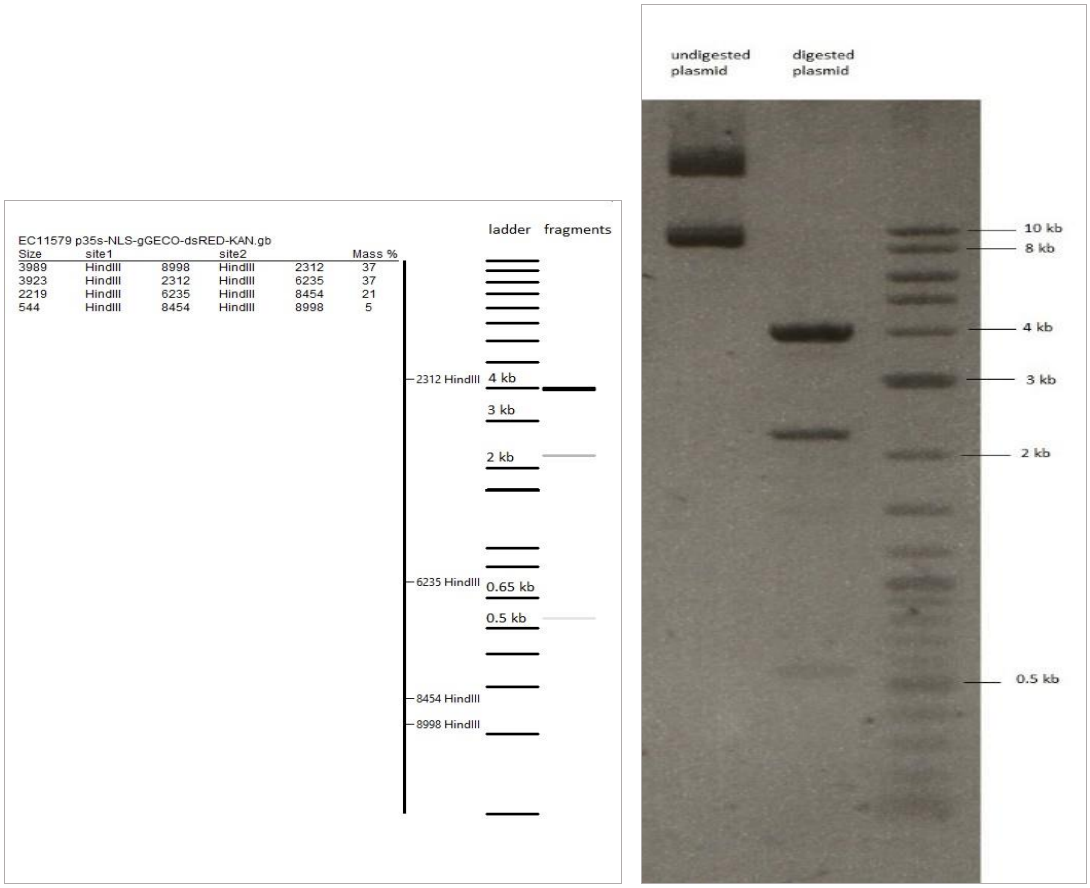

Fig. 3.4: A) *In silico* prediction of the electrophoresis gel expected running the products of the EC11579 digestion with the enzyme HindIII. B) Obtained result: as expected we can see the weak band just before the 0.5 kb ladder band, a band of about 2.2 kb and a strong double band of ~3.9 kb. In the first line (undigested plasmid) we can see two bands: the faster one is generate by the supercoiled plasmid, while the slower one is due to the presence of an open-circular form of the plasmid.

The results of this additional test are shown in the figure 3.4. As the band profile obtained in the electrophoresis gel [Fig. 3.4 B] was the same of the one expected from the *in silico* prediction [Fig. 3.4 A] we concluded that also this construct was probably assembled correctly and so we proceeded with the last verification step: the sequencing.To perform the partial sequencing we used DNA extracted from *E. coli* cells grown in liquid cultures, these were previously set up starting from the replica of a single colony resulted positive to the PCR analysis.

The sequencing reaction on the pL2Vs was performed again with the primers GG3 and GG4. Since the EC11579 contains the dsRed gene in position three, to obtain sure information on the presence of our calcium sensor, for this construct we set up two additional sequencing reactions with the primers Ben23 and Ben26, which are matching on the green GECO. As shown in figure 3.5 the sequences obtained from the sequencing of the EC11579 overlapped the dsRed promoter (pAtUBI10), the p35s, the GECO CDS and the kanamycin resistance gene.

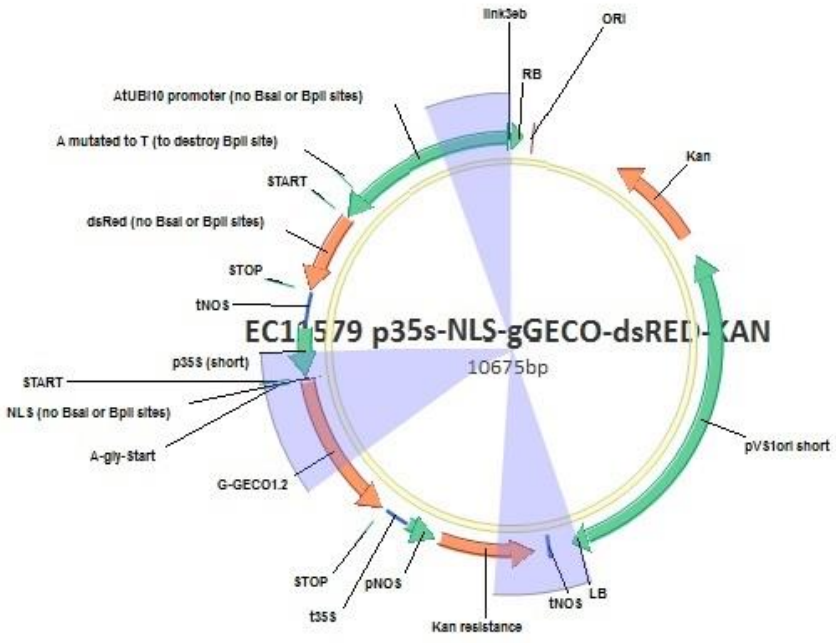

Fig. 3.5: EC11579 map, the blue-highlighted parts correspond to the sequenced fragments

Given the positive results of the sequencing and of the colony PCRs, the information so far obtained allowed us to say that our pL2Vs were correctly assembled, so we could transform them in AR1193 electrocompetent cells.

Before set up the plant transformation, a colony PCR was performed on *A. rhizogenes* colonies to prove that they were really carrying the plasmid containing the multigene construct.

A) B)

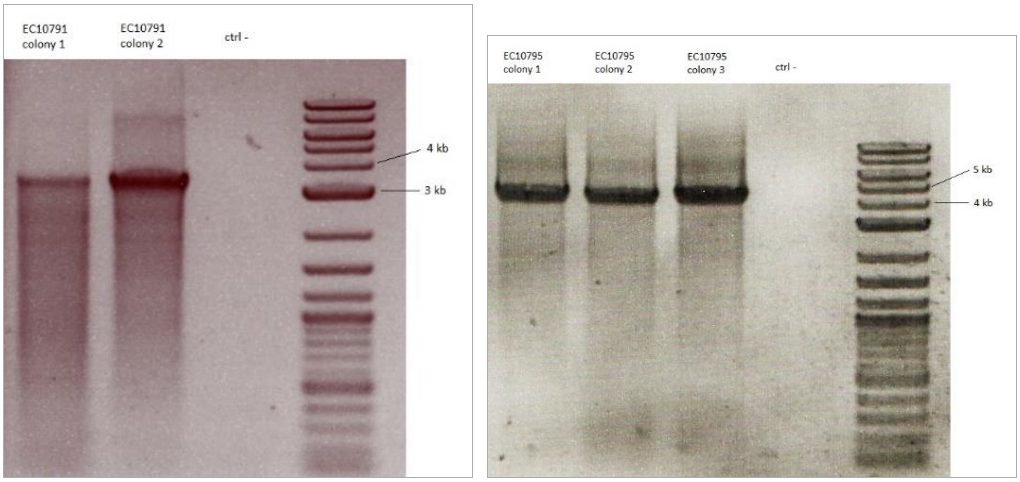

C)

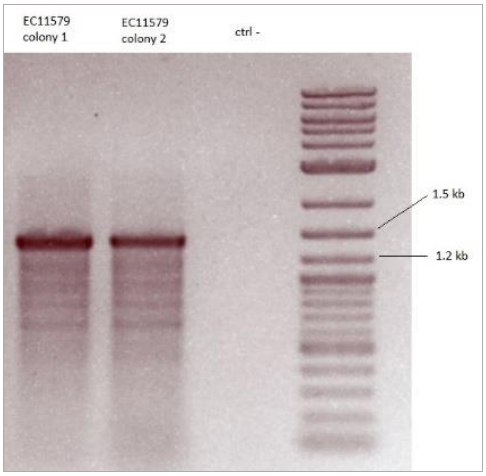

Fig. 3.6: Gel Electrophoresis showing the fragments amplified through colony PCRs on *A. rhizogenes* colonies. A) bands of about 3.4 kb amplified on the construct EC10791 B) bands of ~4.7 kb amplified on EC10795 C) ~1.4 kb band amplified on EC11579.

Using the couple of primers GG3-GG4 and a Ta of 45 °C, as expected from the *in silico* prediction, we amplified a band of ~3.4 kb on the construct EC10791 and a

band of ~4.7 kb on the construct 10795. For the PCR on the EC11579 colonies we used the primers GG3 and Ben94 (a Ta of 52 °C was used basing the choice on previous experiences). The electrophoresis gels in the figure 3.6 show the positive results of these colony PCRs on *A. rhizogenes*. The dimensions of the bands were estimated by comparison with the bands of the 2-Log DNA ladder (New England Biolabs) and they were matching with the *in silico* predictions. Considering the results of the colony PCRs on *A. rhizogenes,* we proceeded using the obtained positive colonies to set up the liquid cultures required for the plant transformation.

2. TRANSFORMATION AND IMAGING

In the second part of the work we proceeded with the transformation of *M. Truncatula* seedlings and then, after three weeks, with a preliminary screening followed by the imaging work.

The aim of the preliminary screening was to individuate the transformed roots in order to facilitate and accelerate the execution of the imaging step. The EC11579-plants were screened with the Leica MZFLIII fluorescence stereomicroscope and around the 16% of them showed at least one red fluorescent root when exposed to a 546/12 nm wavelength. In the case of the constructs EC10791 and EC10795 the preliminary screening resulted a bit more difficult because the kanamycin did not stop completely the growth of the non-transformed roots, so, to overcome the problem, we decided to choose the more healthy roots and the ones that were emerging exactly from the original cutting site.

2.1. Green-GECO1.2 reveals Nod factors-induced nuclear calcium spiking

2.1.1. Construct EC10791

Using the Nikon Eclipse FN1 upright microscope, we checked the roots selected during the preliminary screening: in about the 10% of the EC10791-plants we found roots showing a green GECO basal signal in the cell nuclei. Some of these roots resulted chimeric as they showed the green signal only in the cortex cells and not in the epidermal cells, while some other roots resulted unresponsive to

the Nod factor treatment (i.e. we could detect a green signal in the nuclei but no increase from the basal level was showed after the treatment). We observed a clear calcium spiking induced by a solution of Nod factors 10^{-9} M in 16 root hair cells belonging to three different plant.

The frame-by-frame imaging sequence in figure 3.7 A was recorded in a not confocal mode with 5 s of interval between the acquisition and shows the changes in the intensity of the GECO signal during the calcium spiking. Starting from the basal level of signal shown in the first frame, we reach the peak of the spike in 5 s (second frame) and then a slower descending phase starts. The data on the average signal intensity in the nuclear region, obtained analysing the images with the software image J (National Institute of Healt; http://rsb.info.nih.gov/ij/), were plotted against the time in order to obtain graphs like the one shown in figure 3.7 B.

A

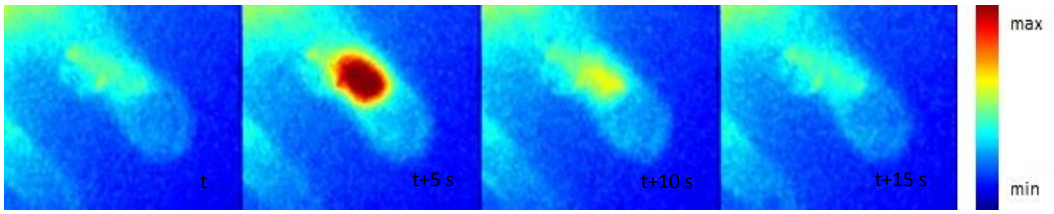

B

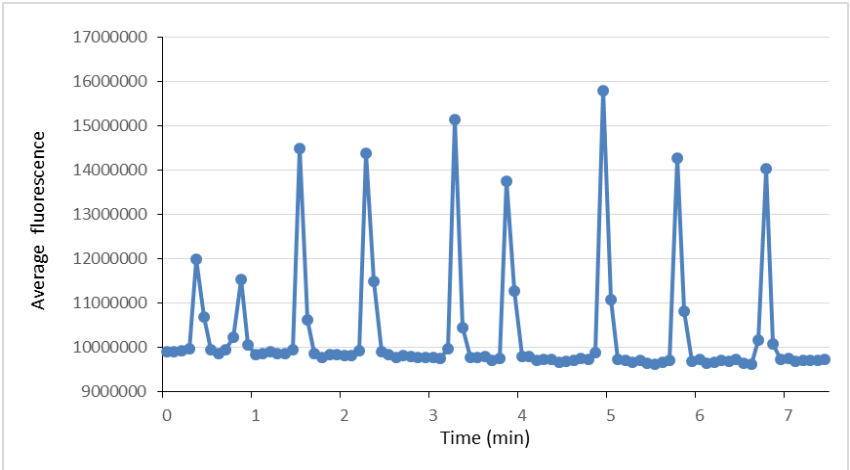

Fig. 3.7: A) frame-by-frame imaging sequence acquired with the Nikon Eclipse FN1 upright microscope (exposure 500 ms, interval 5 s, not confocal mode). The signal in the nuclear region of this root hair cells increases (in 5 s) and decreases (in 10 s) revealing the calcium spiking in response to the Nod factors treatment. B) Average intensity of the signal in the nuclear region of the same root hair cell plotted against the time.

In the experience just presented above we observed that almost all the spikes had a rising phase of 5 s and a descending phase of 10 s, but that is a not a general rule, as we can see in the graphs shown in the figure 3.8. The data of the graph A were collected from a different root of the same plant used before, while the graph B shows the calcium spiking recorded in a trichoblast of a different plant. We can notice that the rising phase of the spikes lasts 5 or 10 seconds while the descending phase can be also 20-25 s long.

A)

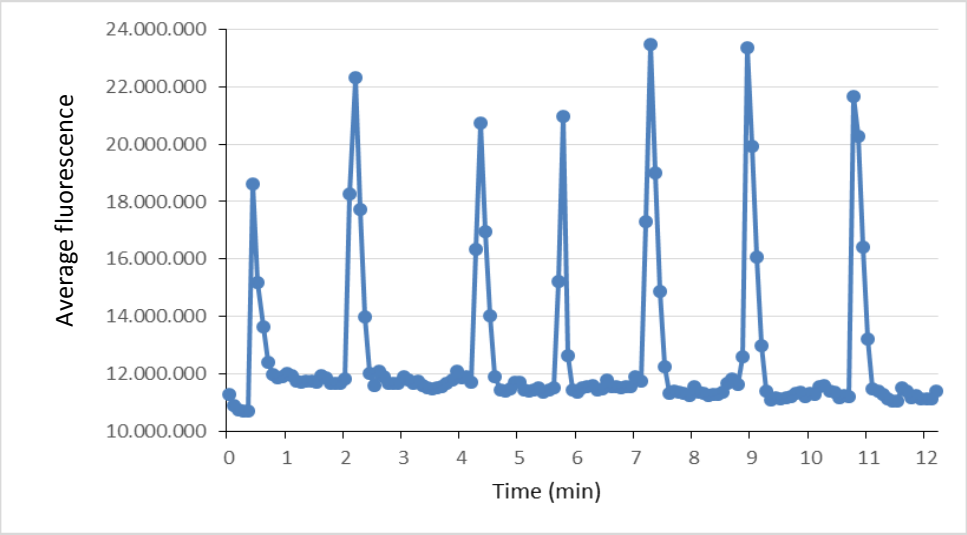

B)

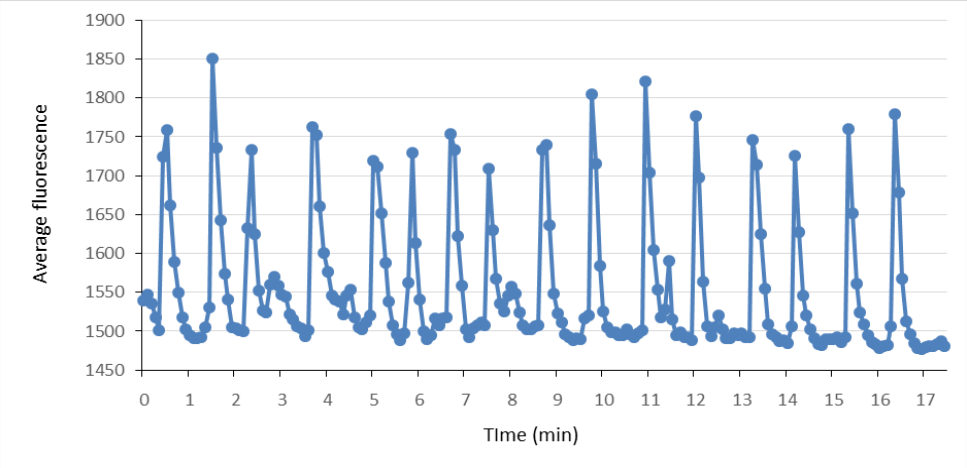

Fig 3.8: Data collected with Nikon Eclipse FN1 upright microscope (exposure 500 ms, interval 5 s, not confocal mode). The graphs show calcium spiking in trichoblasts of roots of two different EC10791-plants after Nod factors treatment.

Afterwards other data were collected using the confocal unit [Fig. 3.9 and 3.10]. The images shown in the figure 3.9 were acquired again with an exposure of 500 ms and intervals of 5 s. As we can see in the frame-by-frame imaging sequence [Fig. 3.9 A] the green GECO signal is strong enough to be clearly detected with this imaging technique and also, in the first frame, we can appreciate the basal level of the signal in the nucleus.

A)

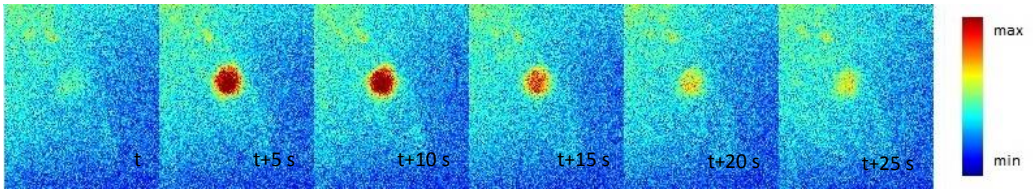

B)

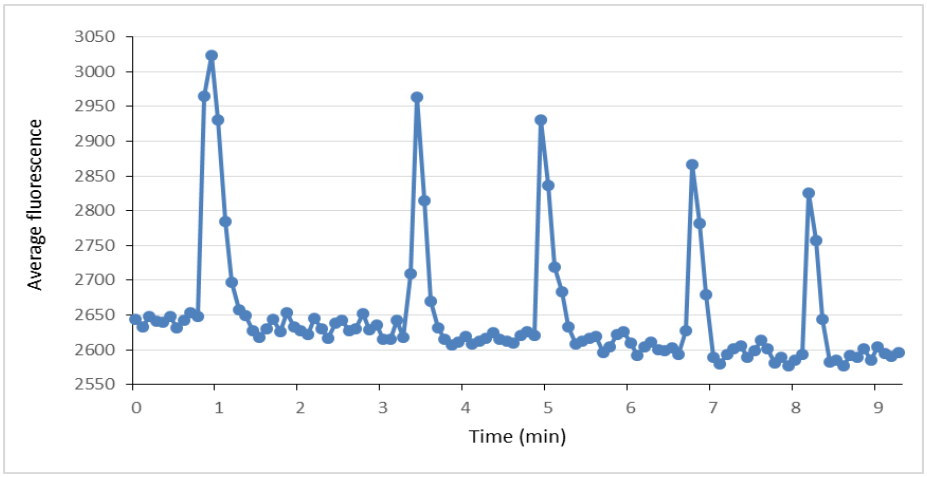

Fig. 3.9: A) frame-by-frame imaging sequence acquired with the Nikon Eclipse FN1 upright microscope (exposure 500 ms, interval 5 s, confocal mode). B) Average intensity of the signal in the nuclear region of the same root hair cell plotted against the time

The data shown in the figure 3.10 were recorded with 100 ms of exposure and no interval between the acquisitions, this allowed us to detect more detailed information on the changes of the fluorescence level in the time and so we obtained a more accurate shape of the spikes [fig 3.10 B].

A)

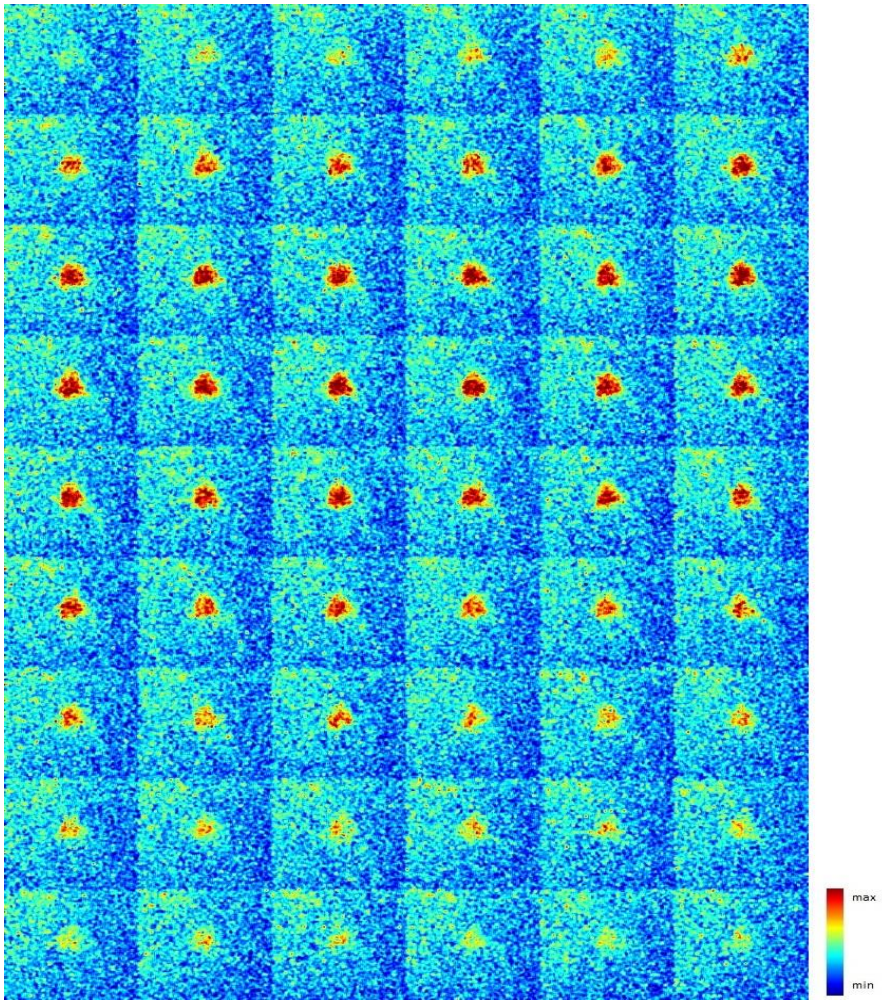

B)

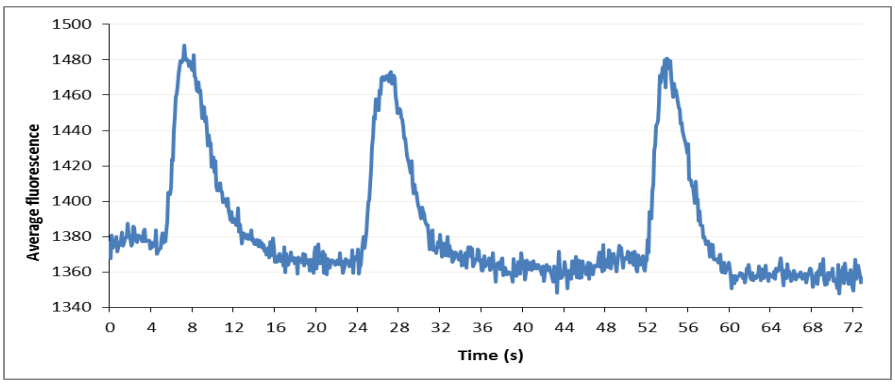

Fig. 3.10: A) frame-by-frame imaging sequence acquired with the Nikon Eclipse FN1 upright microscope (exposure 100 ms, interval 0 s, confocal mode). B) Average intensity of the signal in the nuclear region of the same root hair cell plotted against the time. A more accurate shape of the spike emerges from this analysis.

2.1.2. Construct EC11579

A)

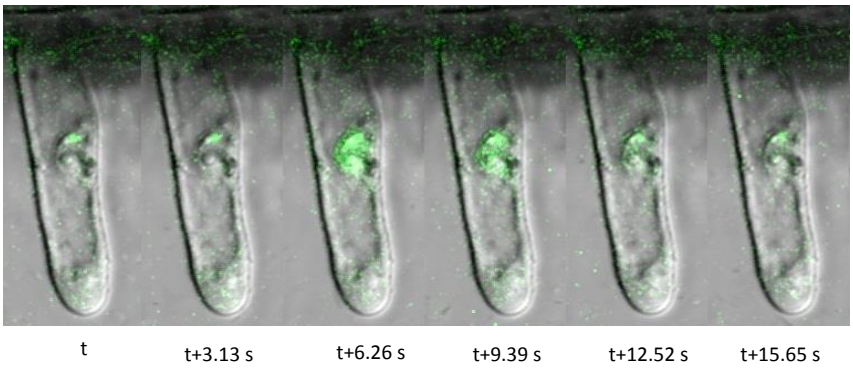

B)

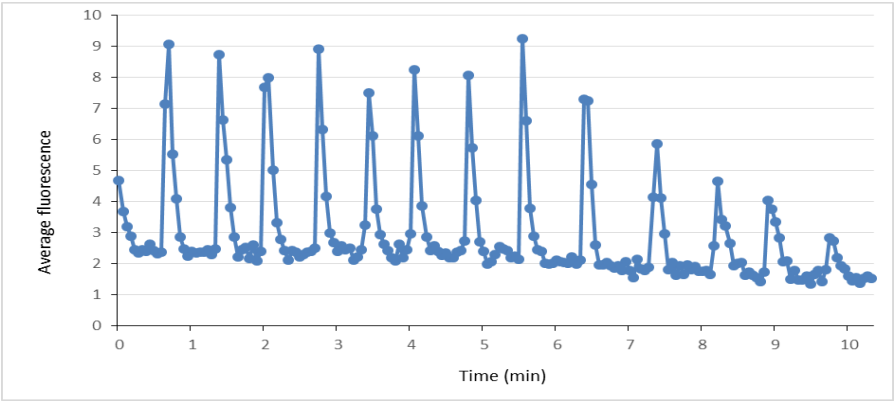

Fig. 3.11: A) frame-by-frame imaging sequence acquired with the Zeiss LSM780 B) Average intensity of the signal in the nuclear region of the same root hair cell plotted against the time.

Among the roots selected during the preliminary screening, some resulted completely negative (they were not showing any green GECO signal), some other resulted chimeric (we could see the dsRed fluorescence and the green GECO fluorescence only in deep cell layers and not in the epidermal cells), finally, some roots showed a basal green fluorescent signal in the trichoblasts nuclei but these cells were not responding to the Nod factors. A single plant of this line gave us real positive results: a low basal level of green fluorescence was observed in the cells nuclei and then, once a solution of Nod factors 10^{-9} M was added, we could see calcium spiking in the trichoblasts. With the Zeiss LSM780 we collected data on the spiking of six different cells. In the figure 3.11 A is shown one of these root trichoblasts responding to the usual Nod factor treatment, these images

were obtained by merging the data collected through the green channel and the data collected through the bright field channel. In the graph shown in the figure 3.11 B the fluorescence oscillation recorded in this cell are plotted against the time. In this case, the interval between the acquisitions was 3.13 s.

2.2. Red-GECO1.2 reveals Nod factors-induced nuclear calcium spiking

A)

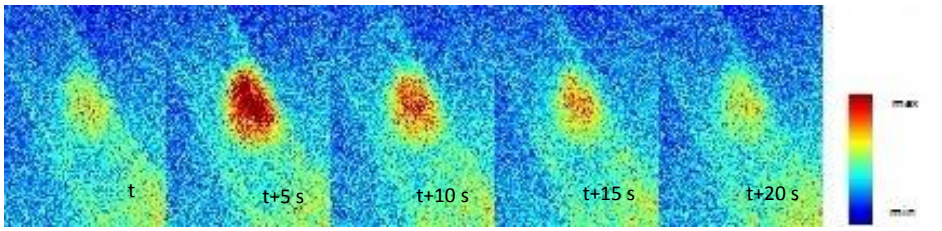

B)

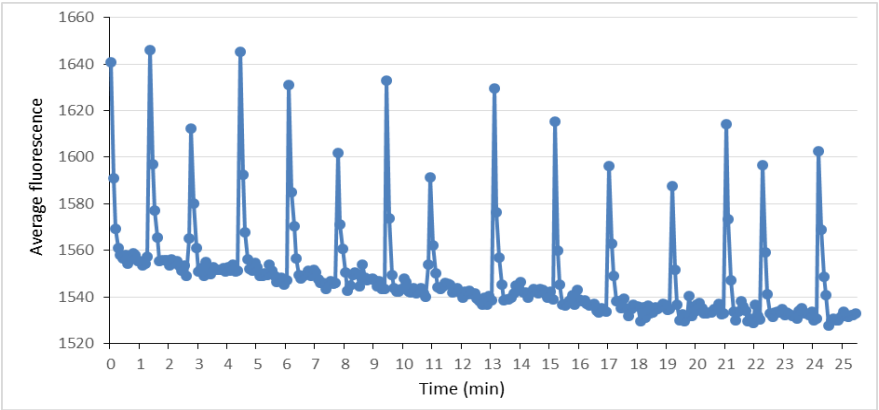

Fig. 3.12: A) frame-by-frame imaging sequence acquired with the Nikon Eclipse FN1 upright microscope (exposure 500 ms, interval 5 s, not confocal mode). B) Average intensity of the signal in the nuclear region of the same root hair cell plotted against the time.

We found roots positive for the red GECO signal in the 7% of the EC10795-plants, but in some cases the trichoblasts did not show any basal signal or they showed a basal level of fluorescence in the nuclei but they did not respond to the Nod factors treatment. We recorded calcium spiking induced by Nod factors 10^{-8} M in the nuclei of six trichoblasts belonging to a single plant. An example of these data, recorded with the Nikon Eclipse FN1 upright microscope in not confocal mode, is shown in the figure 3.12 A and B. Similarly to the green GECO, also for the red GECO we observed a dramatic and easily detectable increase in the signal.

Chapter 4

Discussion

The universality of calcium as a second messenger and its role in such a variety of different signalling processes require the existence of molecular machineries involved in coding and decoding the calcium signature message. Pumps, transportes and channels codify a message in the calcium signatures by shaping them; calcium-binding proteins decode the message by responding to the oscillation of calcium and transduce it by interacting with downstream factors.

The complexity and versatility of this system make the study in this field intriguing and exciting as well as demanding in terms of calcium reporters. Since the early 1960s when murexide, azo dyes and chlortetracycline were used, giant steps have been taken in developing more accurate, sensitive and suitable calcium reporters.

In 1997 the first GFP-based calcium sensor, the camaleon, was created. Cameleons have been used widely in plants to study calcium levels and oscillation in many cellular types and during different processes [146]. Currently the most used protein-based calcium sensor in plant science is the YC3.6, which is an evolution of that first cameleon developed in the 1990s. Although the cameleons showed many good qualities, they also present some problems. For example beside the fact that they are big molecules and it may affect their targeting efficiency, they remain two wavelength indicators FRET-based and that limits the imaging possibilities. In fact, this sensors are so limited in the colour variants and they do not leave the possibility to be combined with other fluorescent reporters. Moreover, although directed mutations increased the FRET

efficiency, and so the signal to noise ratio, of the YC3.6 compared to the first version, a certain basal noise remains.

To overcome these limitations, we propose the use of a new group of single-wavelength calcium sensors, the GECOs. In particular we tried to define whether the GECOs, developed for animal cells and not yet tested in plants in this contest, were suitable for studying symbiotic nuclear calcium spiking in *M. trucantula* root hair cells. The main advantages of the GECOs are that they exist in different colours, they are single-wavelength sensors and that in the meanwhile they also are very sensible. Moreover, the fact that they exist in a pre-docked state made them quick reporters [154] and so good candidates to be employed in studying a fast phenomenon such as nuclear calcium spiking. Although the theoretical prerequisites are good and the GECOs already showed good response in tests carried out in animal cells, this first step of testing them in the contest of the particular signalling process of interest is important. In fact the suitability of a sensor in studying a determined process strictly depends on the dynamic range and on the kinetic (of the process and of the sensor) but also on the targeting requirement and on the possibly interaction with other cellular components. For example, the original cameleons suffered from interference by endogenous CaM and has been observed that some circularly permuted fluorescent protein did not express well in some compartments [164].

The GECOs exists in many different versions that differ for the excitation and emission wavelength and for the Kd. As a first step in exploring the utility of these sensors, in this work we chose to test the Green-GECO1.2 and the Red-GECO1.2.

1. CLONING

The results of the PCR analysis, of the sequencing and of the enzymatic digestion all together allow us to say that two plasmids containing the Green-GECO and one plasmid containing the Red-GECO were efficiently built using the Golden Gate cloning technique.

Each construct contained the eukaryotic kanamycin resistance gene in order to permit the selection of the transformed roots. As we chose the *A. rhizogenes*-mediated

transformation, to lower the risk of having roots resistant to kanamycin but not containing the GECO, we placed the kanamycin gene in position one, i.e. near the T-DNA left border, and the GECO gene always in position two. In fact, because of the mechanism carried out by *Agrobacterium* in transferring the T-DNA, we have a higher probability of deletions at the left end of the fragment. Hence, if the GECO gene was in position one the higher probability of deletion near the left border would have led to a higher probability to have roots containing the kanamycin gene but not the GECO gene. This would have made the process of looking for transformed roots longer and difficult, also because in the beginning we did not know if the signal given by the GECOs in response of the basal level of calcium in the nuclei was enough to be easily detected.

As already mentioned, we have chosen to build a third construct containing a visual marker in addition to the kanamycin resistance and we made this choice in order to facilitate even more the individuation of the transformed roots. In fact, we knew from previous experiences that the kanamycin selection would not have been really strict, and so we would have seen growing also roots that were not transformed. In addition to that, we also knew that the presence of kanamycin would have reduced the growth speed and would have been an additional stress for the plants. Obviously, since this selection strategy requires the use of a second wavelength, this would somehow annul one of the advantages of using a single-wavelength calcium sensor. For example if we have to use at the same time the G-GECO and another fluorescent sensor which is red, the presence of the DsRed would interfere with the experiment. This is the reason why we did not insert a visual marker also in the first two vectors, since there is the chance that other experiment could employ the vectors build in this work.

The choice to use the p35S and the pAtUBI10 was led by the fact that has been demonstrated in several works that these promoters drive a strong and ubiquitous expression.

2. IMAGING

As already mentioned, the imaging process included both wide-field microscopy and confocal microscopy observations. The confocal microscopy experiences were carried out with two different systems: Zeiss LSM780 (which present an argon laser as source of

light) and Nikon Eclipse FN1 upright microscope with x-light confocal unit (CAIRN) (which present a LED as source of light).

Roots transformed with EC11579, EC10795 and EC10791, observed with wide-field microscopy before the Nod factors treatment, showed a low but detectable basal level of signal in the nucleus of most cells. While no obvious nuclear localised signal was detectable with the Leica MZFLIII fluorescence stereomicroscope in absence of treatment.

Once applied the Nod factors as described in the previous chapters, clear and strong calcium spikes were observed in root hair cells. The increases in the GECOs signal were strong enough to be detected also with the confocal mode. In some cases we observed a decreasing tendency in the peaks and in the basal signal level during the time (see for example figures 3.9, 3.11 and 3.12). Theoretically, this could be ascribed to a loss of focus or a photobleaching-effect. Since the examples in figure 3.9 and 3.12 are the only examples of this decreasing tendency observed while recoding in wide-field mode and using the LED as source of light, we are oriented to think that this effect in this case is due to loss of focus. This bring us to point out an advantage of the cameleons on the GECOs: since with the cameleons the calcium level is evaluated in terms of ratio between the CFP and YFP emission intensity, these reporters do not suffer of the loss of focus problem (or of variation in the expression level problem) as the ratio do not change if the signals coming from the CFP and the YFP change together.

A different consideration has to be done on the data recorded with the Zeiss LSM780. In the figure 3.11 after about 6 minutes both the basal level of signal and the peak-height started decreasing, in this case we could affirm that this is probably due mainly to a photobleaching-effect. In fact, we noticed this decreasing tendency in all the experience recorded with this microscope and it was getting stronger and faster with the increase of the laser power or with the reduction of the interval time between the acquisitions. Anyway, in some cases a low laser power was enough to detect the green-GECO signal and allowed us to record the spiking for long enough before causing photobleaching. The selection of plants with a high level of expression of the GECOs could allow us to use a low laser power and so overcome the photobleaching problem on the short recording time.

The EC10791 roots were also successfully imaged with the Nikon Eclipse FN1 upright microscope in confocal mode and resulted suitable for fast scan imaging [Fig 3.10]. This would be particularly useful in case we would like to monitor some process with a better spatial-temporal precision.

3. CONCLUSIONS AND OUTLOOK

We can conclude that the GECOs, in particular the red-GECO1.2 and the green-GECO1.2, are suitable new tools for qualitative studies of nuclear calcium oscillations in *M. trucantula* root hair cells that happen during the establishment of symbiosis. A little bit of care has to be taken during the imaging process and in handling the data as the GECOs are non-ratiometric indicators and so the intensity value recorded could be influenced by different level of expression or loss of focus.

Nevertheless this result, comprehensive of the suitability of the GECOs for confocal microscopy and fast scan analysis, open to the opportunity of high definition multicolour calcium imaging in single root hair cells.

Using the GECOs in the study of symbiotic nuclear calcium spiking would give the possibility to clarify some points that are at present still obscure or not completely demonstrated. For example, a nuclear localized GECO could be used in combination with an ER-localised calcium sensor to finally demonstrate if the nuclear envelope is really the nuclear calcium store. A good candidate to be used as an ER-localised calcium sensor in combination with the nuclear-localised red-GECO could be the CatchER. CatchER is a single EGFP-based calcium sensor with an high Kd (about 0.18 mM) and a fast kinetic of ion binding that make it appropriate for the use in the ER [165][166]. Moreover, a nuclear localised red-GECO could be used in combination with a fluorescent voltage sensor inserted in the inner nuclear membrane of the nuclear envelope. In this way, we would be able to monitor the voltage changes of this membrane in relation to the calcium spiking in the nucleus and so perhaps give a further validation of the model presented in the paragraph 3.4. About one year ago, an ultrafast GFP-based voltage sensor, ASAP1 (accelerated sensor of action potential), have been developed [167]. This sensor could be addressed to the nuclear envelope membrane using the nuclear localisation signals of DMI1 or the N-terminal domain of

the protein SUN1. In fact this protein resulted to be located only in the inner nuclear membrane of the nuclear envelope and its N-terminal domain resulted involved in the targeting [167][168].

Both the CatchER and ASAP1 have never been tested in plants, as well as the targeting of a protein to the inner nuclear membrane of the nuclear envelope using the N-terminal domain of SUN1. Hence, the first steps toward these new projects would be test these sensors in plants, as we did in this work with the GECOs.

Acknowledgements

I would like to thank Giles Oldroyd, who gave me the chance to get in touch with the wonderful scientific and human environment of his laboratory. Thanks to all the people in the lab for being always enthusiastic, passionate and ready to help. Above all, a special thanks goes to Ben for his daily moral and scientific support. Thank you Ben for being such a kind person and a great teacher.

Finally, a special thanks goes also to rugby, that saved me in at least three different ways.

Ringraziamenti

Grazie alla mia relatrice per avermi dato la possibilità di intraprendere questa esperienza concedendomi fiducia e sostegno, ma soprattutto grazie per l'esempio di passione, impegno ed onestà.

Grazie a Chiara, Maria Chiara, Martina e Martina che nonostante tutto sono sempre qui e non sembrano volersene andare.

Grazie ai Rottami perché sono state un tornado di sorrisi, emozioni, sorprese e scoperte in questi nostri tre anni.

Grazie a Chiara e Vito per la loro follia, la spontaneità e l'affetto.

Grazie a Valeria per il coraggio che ha messo in gioco per affrontare un pezzo di mondo insieme, e per molto altro.

Grazie a zia Urbana perché c'è sempre e perché mi ha sorpreso.

Grazie ai miei genitori ai quali non dimostro mai abbastanza il mio amore. Da grande vorrei essere come voi.

Grazie a Elena e a Gianluca che si illudono di star diventando gradi e che non sanno che per me saranno sempre piccolini.

Grazie a Giacomo perché è il mio punto fermo e non c'è stato un instante in cui non lo abbia sentito al mio fianco. Tra tutte, sei la parte di me più importante.

Bibliography

[1] M. J. Berridge, P. Lipp, and M. D. Bootman, “The versatility and universality of calcium signalling.,” *Nat. Rev. Mol. Cell Biol.*, vol. 1, no. 1, pp. 11–21, 2000.

[2] S. Miyazaki, H. Shirakawa, K. Nakada, and Y. Honda, “Essential role of the inositol 1,4,5-trisphosphate receptor/Ca2+ release channel in Ca2+ waves and Ca2+ oscillations at fertilization of mammalian eggs.,” *Developmental biology*, vol. 158, no. 1. pp. 62–78, 1993.

[3] S. Kume, a Muto, H. Okano, and K. Mikoshiba, “Developmental expression of the inositol 1,4,5-trisphosphate receptor and localization of inositol 1,4,5-trisphosphate during early embryogenesis in *Xenopus laevis*.,” *Mech. Dev.*, vol. 66, no. 1–2, pp. 157–168, 1997.

[4] S. Kume, a Muto, T. Inoue, K. Suga, H. Okano, and K. Mikoshiba, “Role of inositol 1,4,5-trisphosphate receptor in ventral signaling in *Xenopus* embryos.,” *Science*, vol. 278, no. 5345, pp. 1940–1943, 1997.

[5] E. Reinhard, H. Yokoe, K. R. Niebling, N. L. Allbritton, M. a Kuhn, and T. Meyer, “Localized calcium signals in early zebrafish development.,” *Developmental biology*, vol. 170, no. 1. pp. 50–61, 1995.

[6] R. Créton, J. a Kreiling, and L. F. Jaffe, “Presence and roles of calcium gradients along the dorsal-ventral axis in *Drosophila* embryos.,” *Dev. Biol.*, vol. 217, no. 2, pp. 375–385, 2000.

[7] X. Gu and N. C. Spitzer, “Breaking the code: regulation of neuronal differentiation by spontaneous calcium transients,” *Dev. Neurosci.*, vol. 19, pp. 33–41, 1997.

[8] T. M. Gomez and N. C. Spitzer, “In vivo regulation of axon extension and pathfinding by growth-cone calcium transients,” *Nature*, vol. 397, no. May, pp. 350–355, 1999.

[9] A. Kondratskyi, K. Kondratska, R. Skryma, and N. Prevarskaya, “Ion channels in the regulation of apoptosis,” *Biochim. Biophys. Acta - Biomembr.*, 2014.

[10] M. M. Atkinson, L. D. Keppler, E. W. Orlandi, C. J. Baker, and C. F. Mischke, “Involvement of plasma membrane calcium influx in bacterial induction of the k/h and hypersensitive responses in tobacco.,” *Plant Physiol.*, vol. 92, no. 1, pp. 215–221, Jan. 1990.

[11] a Levine, R. I. Pennell, M. E. Alvarez, R. Palmer, and C. Lamb, “Calcium-mediated apoptosis in a plant hypersensitive disease resistance response.,” *Curr. Biol.*, vol. 6, no. 4, pp. 427–437, 1996.

[12] W. Ma and G. a. Berkowitz, “The grateful dead: Calcium and cell death in plant innate immunity,” *Cell. Microbiol.*, vol. 9, no. 11, pp. 2571–2585, 2007.

[13] V. E. Franklin-Tong, T. L. Holdaway-Clarke, K. R. Straatman, J. G. Kunkel, and P. K. Hepler, “Involvement of extracellular calcium influx in the self-incompatibility response of *Papaver rhoeas*,” *Plant J.*, vol. 29, no. 3, pp. 333–345, 2002.

[14] P. J. White and M. R. Broadley, “Calcium in plants,” *Ann. Bot.*, vol. 92, no. 4, pp. 487–511, 2003.

[15] M. R. McAinsh and J. K. Pittman, “Shaping the calcium signature,” *New Phytol.*, vol. 181, pp. 275–292, 2009.

[16] P. Marschner, *Mineral Nutrition of Higher Plants*, Third. Elsevier Inc., 2012.

[17] P. J. White, “Calcium channels in higher plants,” *Biochim. Biophys. Acta - Biomembr.*, vol. 1465, no. 1–2, pp. 171–189, 2000.

[18] S. Stael, B. Wurzinger, A. Mair, N. Mehlmer, U. C. Vothknecht, and M. Teige, “Plant organellar calcium signalling: An emerging field,” *J. Exp. Bot.*, vol. 63, no. 4, pp. 1525–1542, 2012.

[19] B. B. Buchanan and R. L. Jones, *Biochemistry and Molecular Biology of Plants*. I.K. International Publishing House Pvt. Limited, 2007.

[20] K. Yuasa and M. Maeshima, “Organ specificity of a vacuolar Ca2+-binding protein RVCaB in radish and its expression under Ca2+-deficient conditions.,” *Plant Mol. Biol.*, vol. 47, no. 5, pp. 633–640, Nov. 2001.

[21] R. Dutta and K. R. Robinson, “Identification and characterization of stretch-activated ion channels in pollen protoplasts.,” *Plant Physiol.*, vol. 135, no. 3, pp. 1398–1406, Jul. 2004.

[22] P. Maser, S. Thomine, J. I. Schroeder, J. M. Ward, K. Hirschi, H. Sze, I. N. Talke, A. Amtmann, F. J. Maathuis, D. Sanders, J. F. Harper, J. Tchieu, M. Gribskov, M. W. Persans, D. E. Salt, S. A. Kim, and M. L. Guerinot, “Phylogenetic relationships within cation transporter families of *Arabidopsis*.,” *Plant Physiol.*, vol. 126, no. 4, pp. 1646–1667, Aug. 2001.

[23] B. Lacombe, D. Becker, R. Hedrich, R. DeSalle, M. Hollmann, J. M. Kwak, J. I. Schroeder, N. Le Novere, H. G. Nam, E. P. Spalding, M. Tester, F. J. Turano, J. Chiu, and G. Coruzzi, “The identity of plant glutamate receptors.,” *Science (New York, N.Y.)*, vol. 292, no. 5521. United States, pp. 1486–1487, May-2001.

[24] C. Balagué, B. Lin, C. Alcon, G. Flottes, S. Malmstrom, C. Kohler, G. Neuhaus, G. Pelletier, F. Gaymard, and D. Roby, “HLM1, an essential signaling component in the hypersensitive response, is a member of the cyclic nucleotide-gated channel ion channel family.,” *Plant Cell*, vol. 15, no. 2, pp. 365–379, Feb. 2003.

[25] S. Frietsch, Y.-F. Wang, C. Sladek, L. R. Poulsen, S. M. Romanowsky, J. I. Schroeder, and J. F. Harper, “A cyclic nucleotide-gated channel is essential for polarized tip growth of pollen.,” *Proc. Natl. Acad. Sci. U. S. A.*, vol. 104, no. 36, pp. 14531–14536, Sep. 2007.

[26] F. Chang, A. Yan, L.-N. Zhao, W.-H. Wu, and Z. Yang, “A Putative Calcium-Permeable Cyclic Nucleotide-Gated Channel, CNGC18, Regulates Polarized Pollen Tube Growth,” *J. Integr. Plant Biol.*, vol. 49, no. 8, pp. 1261–1270, 2007.

[27] J. Li, S. Zhu, X. Song, Y. Shen, H. Chen, J. Yu, K. Yi, Y. Liu, V. J. Karplus, P. Wu, and X. W. Deng, “A rice glutamate receptor-like gene is critical for the division and survival of individual cells in the root apical meristem.,” *Plant Cell*, vol. 18, no. 2, pp. 340–349, Feb. 2006.

[28] S. Kang, H. B. Kim, H. Lee, J. Y. Choi, S. Heu, C. J. Oh, S. Il Kwon, and C. S. An, "Overexpression in Arabidopsis of a plasma membrane-targeting glutamate receptor from small radish increases glutamate-mediated Ca2+ influx and delays fungal infection.," *Mol. Cells*, vol. 21, no. 3, pp. 418–427, Jun. 2006.

[29] I. I. Pottosin and G. Schönknecht, "Vacuolar calcium channels," *J. Exp. Bot.*, vol. 58, no. 7, pp. 1559–1569, 2007.

[30] S. R. Muir and D. Sanders, "Inositol 1,4,5-trisphosphate-sensitive Ca2+ release across nonvacuolar membranes in cauliflower.," *Plant Physiol.*, vol. 114, no. 4, pp. 1511–1521, Aug. 1997.

[31] L. Navazio, P. Mariani, and D. Sanders, "Mobilization of Ca2+ by cyclic ADP-ribose from the endoplasmic reticulum of cauliflower florets.," *Plant Physiol.*, vol. 125, no. 4, pp. 2129–2138, Apr. 2001.

[32] F. Lemtiri-Chlieh, E. A. C. MacRobbie, A. A. R. Webb, N. F. Manison, C. Brownlee, J. N. Skepper, J. Chen, G. D. Prestwich, and C. A. Brearley, "Inositol hexakisphosphate mobilizes an endomembrane store of calcium in guard cells.," *Proc. Natl. Acad. Sci. U. S. A.*, vol. 100, no. 17, pp. 10091–10095, Aug. 2003.

[33] L. Navazio, M. A. Bewell, A. Siddiqua, G. D. Dickinson, A. Galione, and D. Sanders, "Calcium release from the endoplasmic reticulum of higher plants elicited by the NADP metabolite nicotinic acid adenine dinucleotide phosphate.," *Proc. Natl. Acad. Sci. U. S. A.*, vol. 97, no. 15, pp. 8693–8698, Jul. 2000.

[34] B. Klusener, G. Boheim, and E. W. Weiler, "Modulation of the ER Ca2+ channel BCC1 from tendrils of *Bryonia dioica* by divalent cations, protons and H2O2.," *FEBS Lett.*, vol. 407, no. 2, pp. 230–234, Apr. 1997.

[35] Klusener and Weiler, "A calcium-selective channel from root-Tip endomembranes of garden cress," *Plant Physiol.*, vol. 119, no. 4, pp. 1399–1406, Apr. 1999.

[36] B. Hong, A. Ichida, Y. Wang, J. S. Gens, B. G. Pickard, and J. F. Harper, "Identification of a calmodulin-regulated Ca2+-ATPase in the endoplasmic reticulum.," *Plant Physiol.*, vol. 119, no. 4, pp. 1165–1176, Apr. 1999.

[37] F. Liang, K. W. Cunningham, J. F. Harper, and H. Sze, "ECA1 complements yeast mutants defective in Ca2+ pumps and encodes an endoplasmic reticulum-type Ca2+-ATPase in *Arabidopsis thaliana*.," *Proc. Natl. Acad. Sci. U. S. A.*, vol. 94, no. 16, pp. 8579–8584, Aug. 1997.

[38] M. C. Bonza, P. Morandini, L. Luoni, M. Geisler, M. G. Palmgren, and M. I. De Michelis, "At-ACA8 encodes a plasma membrane-localized calcium-ATPase of *Arabidopsis* with a calmodulin-binding domain at the N terminus.," *Plant Physiol.*, vol. 123, no. 4, pp. 1495–1506, Aug. 2000.

[39] S. M. Lee, H. S. Kim, H. J. Han, B. C. Moon, C. Y. Kim, J. F. Harper, and W. S. Chung, "Identification of a calmodulin-regulated autoinhibited Ca2+-ATPase (ACA11) that is localized to vacuole membranes in *Arabidopsis*.," *FEBS Lett.*, vol. 581, no. 21, pp. 3943–3949, Aug. 2007.

[40] L. Baekgaard, A. T. Fuglsang, and M. G. Palmgren, “Regulation of plant plasma membrane H+- and Ca2+-ATPases by terminal domains.,” *J. Bioenerg. Biomembr.*, vol. 37, no. 6, pp. 369–374, Dec. 2005.

[41] C. C. Subbaiah and M. M. Sachs, “Maize cap1 encodes a novel SERCA-type calcium-ATPase with a calmodulin-binding domain.,” *J. Biol. Chem.*, vol. 275, no. 28, pp. 21678–21687, Jul. 2000.

[42] H. Sze, F. Liang, I. Hwang, A. C. Curran, and J. F. Harper, “Diversity and regulation of plant Ca2+ pumps: insights from expression in yeast.,” *Annu. Rev. Plant Physiol. Plant Mol. Biol.*, vol. 51, pp. 433–462, 2000.

[43] L. E. Wimmers, N. N. Ewing, and A. B. Bennett, “Higher plant Ca(2+)-ATPase: primary structure and regulation of mRNA abundance by salt.,” *Proc. Natl. Acad. Sci. U. S. A.*, vol. 89, no. 19, pp. 9205–9209, Oct. 1992.

[44] F. J. M. Maathuis, V. Filatov, P. Herzyk, G. C. Krijger, K. B. Axelsen, S. Chen, B. J. Green, Y. Li, K. L. Madagan, R. Sanchez-Fernandez, B. G. Forde, M. G. Palmgren, P. A. Rea, L. E. Williams, D. Sanders, and A. Amtmann, “Transcriptome analysis of root transporters reveals participation of multiple gene families in the response to cation stress.,” *Plant J.*, vol. 35, no. 6, pp. 675–692, Sep. 2003.

[45] T. Shigaki and K. D. Hirschi, “Diverse functions and molecular properties emerging for CAX cation/H+ exchangers in plants.,” *Plant Biol. (Stuttg).*, vol. 8, no. 4, pp. 419–429, Jul. 2006.

[46] M. Kasai and S. Muto, “Ca2+ pump and Ca2+/H+ antiporter in plasma membrane vesicles isolated by aqueous two-phase partitioning from corn leaves.,” *J. Membr. Biol.*, vol. 114, no. 2, pp. 133–142, Mar. 1990.

[47] H. Ueoka-Nakanishi, T. Tsuchiya, M. Sasaki, Y. Nakanishi, K. W. Cunningham, and M. Maeshima, “Functional expression of mung bean Ca2+/H+ antiporter in yeast and its intracellular localization in the hypocotyl and tobacco cells.,” *Eur. J. Biochem.*, vol. 267, no. 10, pp. 3090–3098, May 2000.

[48] T. Kamiya, T. Akahori, M. Ashikari, and M. Maeshima, “Expression of the vacuolar Ca2+/H+ exchanger, OsCAX1a, in rice: cell and age specificity of expression, and enhancement by Ca2+.,” *Plant Cell Physiol.*, vol. 47, no. 1, pp. 96–106, Jan. 2006.

[49] K. D. Hirschi, R. G. Zhen, K. W. Cunningham, P. A. Rea, and G. R. Fink, “CAX1, an H+/Ca2+ antiporter from Arabidopsis.,” *Proc. Natl. Acad. Sci. U. S. A.*, vol. 93, no. 16, pp. 8782–8786, Aug. 1996.

[50] J. Sai and C. H. Johnson, “Dark-stimulated calcium ion fluxes in the chloroplast stroma and cytosol.,” *Plant Cell*, vol. 14, no. 6, pp. 1279–1291, Jun. 2002.

[51] Ettinger, Clear, Fanning, and Peck, “Identification of a Ca2+/H+ antiport in the plant chloroplast thylakoid membrane,” *Plant Physiol.*, vol. 119, no. 4, pp. 1379–1386, Apr. 1999.

[52] I. I. Pottosin and G. Schonknecht, “Ion channel permeable for divalent and monovalent cations in native spinach thylakoid membranes.,” *J. Membr. Biol.*, vol. 152, no. 3, pp. 223–233, Aug. 1996.

[53] D. Wang, Y. Xu, Q. Li, X. Hao, K. Cui, F. Sun, and Y. Zhu, “Transgenic expression of a putative calcium transporter affects the time of *Arabidopsis* flowering.,” *Plant J.*, vol. 33, no. 2, pp. 285–292, Jan. 2003.

[54] J. Li, D.-Y. Wang, Q. Li, Y.-J. Xu, K.-M. Cui, and Y.-X. Zhu, “PPF1 inhibits programmed cell death in apical meristems of both G2 pea and transgenic *Arabidopsis* plants possibly by delaying cytosolic Ca2+ elevation.,” *Cell Calcium*, vol. 35, no. 1, pp. 71–77, Jan. 2004.

[55] H. Nomura, T. Komori, M. Kobori, Y. Nakahira, and T. Shiina, “Evidence for chloroplast control of external Ca2+-induced cytosolic Ca2+ transients and stomatal closure.,” *Plant J.*, vol. 53, no. 6, pp. 988–998, Mar. 2008.

[56] D. C. Logan and M. R. Knight, “Mitochondrial and Cytosolic Calcium Dynamics Are Differentially Regulated in Plants1,” vol. 133, no. 1, pp. 21–24, 2011.

[57] C. Mazars, S. Bourque, A. Mithöfer, A. Pugin, and R. Ranjeva, “Calcium homeostasis in plant cell nuclei.,” *New Phytol.*, vol. 181, no. 2008, pp. 261–274, 2009.

[58] N. Pauly, M. R. Knight, P. Thuleau, A. Graziana, S. Muto, R. Ranjeva, and C. Mazars, “The nucleus together with the cytosol generates patterns of specific cellular calcium signatures in tobacco suspension culture cells.,” *Cell Calcium*, vol. 30, no. 6, pp. 413–421, Dec. 2001.

[59] D. Lecourieux, R. Ranjeva, and A. Pugin, “Calcium in plant defence-signalling pathways.,” *New Phytol.*, vol. 171, no. 2, pp. 249–269, 2006.

[60] A. Walter, C. Mazars, M. Maitrejean, J. Hopke, R. Ranjeva, W. Boland, and A. Mithofer, “Structural requirements of jasmonates and synthetic analogues as inducers of Ca2+ signals in the nucleus and the cytosol of plant cells.,” *Angew. Chem. Int. Ed. Engl.*, vol. 46, no. 25, pp. 4783–4785, 2007.

[61] T. C. Xiong, A. Jauneau, R. Ranjeva, and C. Mazars, “Isolated plant nuclei as mechanical and thermal sensors involved in calcium signalling.,” *Plant J.*, vol. 40, no. 1, pp. 12–21, Oct. 2004.

[62] D. Worrall, C. K.-Y. Ng, and A. M. Hetherington, “Sphingolipids, new players in plant signaling.,” *Trends Plant Sci.*, vol. 8, no. 7, pp. 317–320, Jul. 2003.

[63] T. C. Xiong, S. Coursol, S. Grat, R. Ranjeva, and C. Mazars, “Sphingolipid metabolites selectively elicit increases in nuclear calcium concentration in cell suspension cultures and in isolated nuclei of tobacco.,” *Cell Calcium*, vol. 43, no. 1, pp. 29–37, Jan. 2008.

[64] E. Peiter, J. Sun, A. B. Heckmann, M. Venkateshwaran, B. K. Riely, M. S. Otegui, A. Edwards, G. Freshour, M. G. Hahn, D. R. Cook, D. Sanders, G. E. D. Oldroyd, J. A. Downie, and J.-M. Ane, “The *Medicago truncatula* DMI1 protein modulates cytosolic calcium signaling.,” *Plant Physiol.*, vol. 145, no. 1, pp. 192–203, Sep. 2007.

[65] A. H. van Der Luit, C. Olivari, A. Haley, M. R. Knight, and A. J. Trewavas, “Distinct calcium signaling pathways regulate calmodulin gene expression in tobacco.,” *Plant Physiol.*, vol. 121, no. 3, pp. 705–714, Nov. 1999.

[66] C. Lachaud, D. Da Silva, V. Cotelle, P. Thuleau, T. C. Xiong, A. Jauneau, C. Briere, A. Graziana, Y. Bellec, J.-D. Faure, R. Ranjeva, and C. Mazars, “Nuclear calcium controls the apoptotic-like cell

death induced by d-erythro-sphinganine in tobacco cells.," *Cell Calcium*, vol. 47, no. 1, pp. 92–100, Jan. 2010.

[67] D. W. Ehrhardt, R. Wais, and S. R. Long, "Calcium spiking in plant root hairs responding to rhizobium modulation signals," *Cell*, vol. 85, no. 5, pp. 673–681, 1996.

[68] H. Miwa, J. Sun, G. E. D. Oldroyd, and J. Allan Downie, "Analysis of calcium spiking using a cameleon calcium sensor reveals that nodulation gene expression is regulated by calcium spike number and the developmental status of the cell," *Plant J.*, vol. 48, pp. 883–894, 2006.

[69] M. Chabaud, A. Genre, B. J. Sieberer, A. Faccio, J. Fournier, M. Novero, D. G. Barker, and P. Bonfante, "Arbuscular mycorrhizal hyphopodia and germinated spore exudates trigger Ca2+ spiking in the legume and nonlegume root epidermis," *New Phytol.*, vol. 189, no. 1, pp. 347–355, 2011.

[70] C. Grygorczyk and R. Grygorczyk, "A Ca2+- and voltage-dependent cation channel in the nuclear envelope of red beet.," *Biochim. Biophys. Acta*, vol. 1375, no. 1–2, pp. 117–130, Oct. 1998.

[71] L. Downie, J. Priddle, C. Hawes, and D. E. Evans, "A calcium pump at the higher plant nuclear envelope?," *FEBS Lett.*, vol. 429, no. 1, pp. 44–48, Jun. 1998.

[72] T. D. Bunney, P. J. Shaw, P. A. Watkins, J. P. Taylor, A. F. Beven, B. Wells, G. M. Calder, and B. K. Drobak, "ATP-dependent regulation of nuclear Ca(2+) levels in plant cells.," *FEBS Lett.*, vol. 476, no. 3, pp. 145–149, Jul. 2000.

[73] J. Kudla, O. Batistic, and K. Hashimoto, "Calcium signals: the lead currency of plant information processing.," *Plant Cell*, vol. 22, no. 3, pp. 541–563, Mar. 2010.

[74] I. S. Day and A. S. N. Reddy, "Elucidation of calcium-signaling components and networks," in *Coding and Decoding of Calcium Signals in Plants*, 2011, pp. 147–175.

[75] L. Du, G. S. Ali, K. A. Simons, J. Hou, T. Yang, A. S. N. Reddy, and B. W. Poovaiah, "Ca(2+)/calmodulin regulates salicylic-acid-mediated plant immunity.," *Nature*, vol. 457, no. 7233, pp. 1154–1158, Feb. 2009.

[76] C. J. Doherty, H. A. Van Buskirk, S. J. Myers, and M. F. Thomashow, "Roles for *Arabidopsis* CAMTA transcription factors in cold-regulated gene expression and freezing tolerance.," *Plant Cell*, vol. 21, no. 3, pp. 972–984, Mar. 2009.

[77] O. Batistic and J. Kudla, "Integration and channeling of calcium signaling through the CBL calcium sensor/CIPK protein kinase network.," *Planta*, vol. 219, no. 6, pp. 915–924, Oct. 2004.

[78] J. F. Harper, G. Breton, and A. Harmon, "Decoding Ca(2+) signals through plant protein kinases.," *Annu. Rev. Plant Biol.*, vol. 55, pp. 263–288, 2004.

[79] V. Albrecht, S. Weinl, D. Blazevic, C. D'Angelo, O. Batistic, U. Kolukisaoglu, R. Bock, B. Schulz, K. Harter, and J. Kudla, "The calcium sensor CBL1 integrates plant responses to abiotic stresses.," *Plant J.*, vol. 36, no. 4, pp. 457–470, Nov. 2003.

[80] Y. H. Cheong, K.-N. Kim, G. K. Pandey, R. Gupta, J. J. Grant, and S. Luan, “CBL1, a calcium sensor that differentially regulates salt, drought, and cold responses in *Arabidopsis*.,” *Plant Cell*, vol. 15, no. 8, pp. 1833–1845, Aug. 2003.

[81] T. Kurusu, J. Hamada, H. Nokajima, Y. Kitagawa, M. Kiyoduka, A. Takahashi, S. Hanamata, R. Ohno, T. Hayashi, K. Okada, J. Koga, H. Hirochika, H. Yamane, and K. Kuchitsu, “Regulation of microbe-associated molecular pattern-induced hypersensitive cell death, phytoalexin production, and defense gene expression by calcineurin B-like protein-interacting protein kinases, OsCIPK14/15, in rice cultured cells.,” *Plant Physiol.*, vol. 153, no. 2, pp. 678–692, Jun. 2010.

[82] I. C. Mori, Y. Murata, Y. Yang, S. Munemasa, Y.-F. Wang, S. Andreoli, H. Tiriac, J. M. Alonso, J. F. Harper, J. R. Ecker, J. M. Kwak, and J. I. Schroeder, “CDPKs CPK6 and CPK3 function in ABA regulation of guard cell S-type anion- and Ca(2+)-permeable channels and stomatal closure.,” *PLoS Biol.*, vol. 4, no. 10, p. e327, Oct. 2006.

[83] M. Kobayashi, I. Ohura, K. Kawakita, N. Yokota, M. Fujiwara, K. Shimamoto, N. Doke, and H. Yoshioka, “Calcium-dependent protein kinases regulate the production of reactive oxygen species by potato NADPH oxidase.,” *Plant Cell*, vol. 19, no. 3, pp. 1065–1080, Mar. 2007.

[84] R. M. Mitra, C. A. Gleason, A. Edwards, J. Hadfield, J. A. Downie, G. E. D. Oldroyd, and S. R. Long, “A Ca2+/calmodulin-dependent protein kinase required for symbiotic nodule development: Gene identification by transcript-based cloning.,” *Proc. Natl. Acad. Sci. U. S. A.*, vol. 101, no. 13, pp. 4701–4705, Mar. 2004.

[85] S. M. Swensen, “The evolution of actinorhizal symbioses: evidence for multiple origins of the symbiotic association,” *Am. J. Bot.*, vol. 83, no. 11, pp. 1503–1512, 1996.

[86] G. Gualtieri and T. Bisseling, “The evolution of nodulation.,” *Plant Mol. Biol.*, vol. 42, no. 1, pp. 181–194, Jan. 2000.

[87] B. Lafay, E. Bullier, and J. J. Burdon, “Bradyrhizobia isolated from root nodules of Parasponia (Ulmaceae) do not constitute a separate coherent lineage.,” *Int. J. Syst. Evol. Microbiol.*, vol. 56, no. Pt 5, pp. 1013–1018, May 2006.

[88] P. Lerouge, P. Roche, C. Faucher, F. Maillet, G. Truchet, J. C. Prome, and J. Denarie, “Symbiotic host-specificity of Rhizobium meliloti is determined by a sulphated and acylated glucosamine oligosaccharide signal.,” *Nature*, vol. 344, no. 6268, pp. 781–784, Apr. 1990.

[89] F. Maillet, V. Poinsot, O. Andre, V. Puech-Pages, A. Haouy, M. Gueunier, L. Cromer, D. Giraudet, D. Formey, A. Niebel, E. A. Martinez, H. Driguez, G. Becard, and J. Denarie, “Fungal lipochitooligosaccharide symbiotic signals in arbuscular mycorrhiza.,” *Nature*, vol. 469, no. 7328, pp. 58–63, Jan. 2011.

[90] W. Capoen, G. Oldroyd, S. Goormachtig, and M. Holsters, “*Sesbania rostrata*: a case study of natural variation in legume nodulation.,” *New Phytol.*, vol. 186, no. 2, pp. 340–345, Apr. 2010.

[91] M. Charpentier and G. Oldroyd, “How close are we to nitrogen-fixing cereals?,” *Curr. Opin. Plant Biol.*, vol. 13, no. 5, pp. 556–564, Oct. 2010.

[92] B. Winkel-Shirley, “Flavonoid biosynthesis. A colorful model for genetics, biochemistry, cell biology, and biotechnology.,” *Plant Physiol.*, vol. 126, no. 2, pp. 485–493, Jun. 2001.

[93] M. C. Peck, R. F. Fisher, and S. R. Long, “Diverse flavonoids stimulate NodD1 binding to nod gene promoters in Sinorhizobium meliloti.,” *J. Bacteriol.*, vol. 188, no. 15, pp. 5417–5427, Aug. 2006.

[94] R. F. Fisher and S. R. Long, “Interactions of NodD at the nod Box: NodD binds to two distinct sites on the same face of the helix and induces a bend in the DNA.,” *J. Mol. Biol.*, vol. 233, no. 3, pp. 336–348, Oct. 1993.

[95] X.-C. Chen, J. Feng, B.-H. Hou, F.-Q. Li, Q. Li, and G.-F. Hong, “Modulating DNA bending affects NodD-mediated transcriptional control in *Rhizobium leguminosarum*.,” *Nucleic Acids Res.*, vol. 33, no. 8, pp. 2540–2548, 2005.

[96] G. Caetano-Anolles, D. K. Crist-Estes, and W. D. Bauer, “Chemotaxis of *Rhizobium meliloti* to the plant flavone luteolin requires functional nodulation genes.,” *J. Bacteriol.*, vol. 170, no. 7, pp. 3164–3169, Jul. 1988.

[97] P. E. Schmidt, W. J. Broughton, and D. Werner, “Nod Factors of *Bradyrhizobium-Japonicum* and *Rhizobium Sp Ngr234* Induce Flavonoid Accumulation in Soybean Root Exudate,” *Molecular Plant-Microbe Interactions*, vol. 7, no. 3. pp. 384–390, 1994.

[98] X. Perret, C. Staehelin, and W. J. Broughton, “Molecular basis of symbiotic promiscuity.,” *Microbiol. Mol. Biol. Rev.*, vol. 64, no. 1, pp. 180–201, 2000.

[99] J. Denarie, F. Debelle, and J. C. Prome, “Rhizobium lipo-chitooligosaccharide nodulation factors: signaling molecules mediating recognition and morphogenesis.,” *Annu. Rev. Biochem.*, vol. 65, pp. 503–535, 1996.

[100] P. Roche, F. Debelle, F. Maillet, P. Lerouge, C. Faucher, G. Truchet, J. Denarie, and J. C. Prome, “Molecular basis of symbiotic host specificity in *Rhizobium meliloti*: nodH and nodPQ genes encode the sulfation of lipo-oligosaccharide signals.,” *Cell*, vol. 67, no. 6, pp. 1131–1143, Dec. 1991.

[101] G. E. D. Oldroyd, “Speak, friend, and enter: signalling systems that promote beneficial symbiotic associations in plants.,” *Nat. Rev. Microbiol.*, vol. 11, no. 4, pp. 252–63, 2013.

[102] J. A. Downie, “The roles of extracellular proteins, polysaccharides and signals in the interactions of rhizobia with legume roots.,” *FEMS Microbiol. Rev.*, vol. 34, no. 2, pp. 150–170, Mar. 2010.

[103] N. J. Brewin, “Plant Cell Wall Remodelling in the *Rhizobium*–Legume Symbiosis,” *CRC. Crit. Rev. Plant Sci.*, vol. 23, no. 4, pp. 293–316, Jul. 2004.

[104] F. Xie, J. D. Murray, J. Kim, A. B. Heckmann, A. Edwards, G. E. D. Oldroyd, and J. A. Downie, “Legume pectate lyase required for root infection by rhizobia.,” *Proc. Natl. Acad. Sci. U. S. A.*, vol. 109, no. 2, pp. 633–638, Jan. 2012.

[105] B. J. Sieberer, M. Chabaud, J. Fournier, A. C. J. Timmers, and D. G. Barker, “A switch in Ca2+ spiking signature is concomitant with endosymbiotic microbe entry into cortical root cells of *Medicago truncatula*.,” *Plant J.*, vol. 69, no. 5, pp. 822–830, Mar. 2012.

[106] H. H. Felle, E. Kondorosi, A. Kondorosi, and M. Schultze, “Elevation of the cytosolic free [Ca2+] is indispensable for the transduction of the Nod Factor signal in alfalfa.,” *Plant Physiol.*, vol. 121, no. 1, pp. 273–280, Sep. 1999.

[107] G. E. D. Oldroyd and J. A. Downie, “Calcium, kinases and nodulation signalling in legumes.,” *Nat. Rev. Mol. Cell Biol.*, vol. 5, no. 7, pp. 566–576, 2004.

[108] N. C. a De Ruijter, M. B. Rook, T. Bisseling, and a. M. C. Emons, “Lipochito-oligosaccharides re-initiate root hair tip growth in Vicia sativa with high calcium and spectrin-like antigen at the tip,” *Plant J.*, vol. 13, no. 3, pp. 341–350, 1998.

[109] Cardenas, Feijo, Kunkel, Sanchez, Holdaway-Clarke, Hepler, and Quinto, “Rhizobium nod factors induce increases in intracellular free calcium and extracellular calcium influxes in bean root hairs,” *Plant J.*, vol. 19, no. 3, pp. 347–352, Aug. 1999.

[110] Felle, Kondorosi, Kondorosi, and Schultze, “Nod factors modulate the concentration of cytosolic free calcium differently in growing and non-growing root hairs of *Medicago sativa* L.,” *Planta*, vol. 209, no. 2, pp. 207–212, Aug. 1999.

[111] S. L. Shaw and S. R. Long, “Nod factor elicits two separable calcium responses in *Medicago truncatula* root hair cells.,” *Plant Physiol.*, vol. 131, no. 3, pp. 976–984, 2003.

[112] B. J. Sieberer, M. Chabaud, A. C. Timmers, A. Monin, J. Fournier, and D. G. Barker, “A nuclear-targeted cameleon demonstrates intranuclear Ca2+ spiking in *Medicago truncatula* root hairs in response to rhizobial nodulation factors.,” *Plant Physiol.*, vol. 151, no. November, pp. 1197–1206, 2009.

[113] E. B. Madsen, L. H. Madsen, S. Radutoiu, M. Olbryt, M. Rakwalska, K. Szczyglowski, S. Sato, T. Kaneko, S. Tabata, N. Sandal, and J. Stougaard, “A receptor kinase gene of the LysM type is involved in legume perception of rhizobial signals.,” *Nature*, vol. 425, no. 6958, pp. 637–640, Oct. 2003.

[114] G. Buist, A. Steen, J. Kok, and O. P. Kuipers, “LysM, a widely distributed protein motif for binding to (peptido)glycans.,” *Mol. Microbiol.*, vol. 68, no. 4, pp. 838–847, May 2008.

[115] S. Radutoiu, L. H. Madsen, E. B. Madsen, H. H. Felle, Y. Umehara, M. Gronlund, S. Sato, Y. Nakamura, S. Tabata, N. Sandal, and J. Stougaard, “Plant recognition of symbiotic bacteria requires two LysM receptor-like kinases.,” *Nature*, vol. 425, no. 6958, pp. 585–592, Oct. 2003.

[116] S. Radutoiu, L. H. Madsen, E. B. Madsen, A. Jurkiewicz, E. Fukai, E. M. H. Quistgaard, A. S. Albrektsen, E. K. James, S. Thirup, and J. Stougaard, “LysM domains mediate lipochitin-oligosaccharide recognition and Nfr genes extend the symbiotic host range.,” *EMBO J.*, vol. 26, no. 17, pp. 3923–3935, Sep. 2007.

[117] S. Stracke, C. Kistner, S. Yoshida, L. Mulder, S. Sato, T. Kaneko, S. Tabata, N. Sandal, J. Stougaard, K. Szczyglowski, and M. Parniske, “A plant receptor-like kinase required for both bacterial and fungal symbiosis.,” *Nature*, vol. 417, no. 6892, pp. 959–962, Jun. 2002.

[118] G. Endre, A. Kereszt, Z. Kevei, S. Mihacea, P. Kalo, and G. B. Kiss, “A receptor kinase gene regulating symbiotic nodule development.,” *Nature*, vol. 417, no. 6892, pp. 962–966, Jun. 2002.

[119] M. Antolin-Llovera, M. K. Ried, A. Binder, and M. Parniske, “Receptor kinase signaling pathways in plant-microbe interactions.,” *Annu. Rev. Phytopathol.*, vol. 50, pp. 451–473, 2012.

[120] Z. Kevei, G. Lougnon, P. Mergaert, G. V Horvath, A. Kereszt, D. Jayaraman, N. Zaman, F. Marcel, K. Regulski, G. B. Kiss, A. Kondorosi, G. Endre, E. Kondorosi, and J.-M. Ane, “3-hydroxy-3-methylglutaryl coenzyme a reductase 1 interacts with NORK and is crucial for nodulation in *Medicago truncatula*.,” *Plant Cell*, vol. 19, no. 12, pp. 3974–3989, Dec. 2007.

[121] T. Chen, H. Zhu, D. Ke, K. Cai, C. Wang, H. Gou, Z. Hong, and Z. Zhang, “A MAP kinase kinase interacts with SymRK and regulates nodule organogenesis in *Lotus japonicus*.,” *Plant Cell*, vol. 24, no. 2, pp. 823–838, Feb. 2012.

[122] M. Charpentier, R. Bredemeier, G. Wanner, N. Takeda, E. Schleiff, and M. Parniske, “*Lotus japonicus* CASTOR and POLLUX are ion channels essential for perinuclear calcium spiking in legume root endosymbiosis.,” *Plant Cell*, vol. 20, no. 12, pp. 3467–3479, Dec. 2008.

[123] W. Capoen, J. Sun, D. Wysham, M. S. Otegui, M. Venkateshwaran, S. Hirsch, H. Miwa, J. A. Downie, R. J. Morris, J.-M. Ane, and G. E. D. Oldroyd, “Nuclear membranes control symbiotic calcium signaling of legumes.,” *Proc. Natl. Acad. Sci. U. S. A.*, vol. 108, no. 34, pp. 14348–14353, Aug. 2011.

[124] B. K. Riely, G. Lougnon, J.-M. Ane, and D. R. Cook, “The symbiotic ion channel homolog DMI1 is localized in the nuclear membrane of *Medicago truncatula* roots.,” *Plant J.*, vol. 49, no. 2, pp. 208–216, Jan. 2007.

[125] M. Venkateshwaran, A. Cosme, L. Han, M. Banba, K. A. Satyshur, E. Schleiff, M. Parniske, H. Imaizumi-Anraku, and J.-M. Ane, “The recent evolution of a symbiotic ion channel in the legume family altered ion conductance and improved functionality in calcium signaling.,” *Plant Cell*, vol. 24, no. 6, pp. 2528–2545, Jun. 2012.

[126] E. Granqvist, D. Wysham, S. Hazledine, W. Kozlowski, J. Sun, M. Charpentier, T. V. Martins, P. Haleux, K. Tsaneva-Atanasova, J. A. Downie, G. E. D. Oldroyd, and R. J. Morris, “Buffering capacity explains signal variation in symbiotic calcium oscillations.,” *Plant Physiol.*, vol. 160, no. 4, pp. 2300–2310, Dec. 2012.

[127] M. Charpentier and G. E. D. Oldroyd, “Nuclear calcium signaling in plants.,” *Plant Physiol.*, vol. 163, no. 2, pp. 496–503, 2013.

[128] A. Edwards, A. B. Heckmann, F. Yousafzai, G. Duc, and J. A. Downie, “Structural implications of mutations in the pea SYM8 symbiosis gene, the DMI1 ortholog, encoding a predicted ion channel.,” *Mol. Plant. Microbe. Interact.*, vol. 20, no. 10, pp. 1183–1191, Oct. 2007.

[129] M. Charpentier, T. Vaz Martins, E. Granqvist, G. E. D. Oldroyd, and R. J. Morris, “The role of DMI1 in establishing Ca (2+) oscillations in legume symbioses.,” *Plant Signal. Behav.*, vol. 8, no. 2, p. e22894, Feb. 2013.

[130] M. Groth, N. Takeda, J. Perry, H. Uchida, S. Draxl, A. Brachmann, S. Sato, S. Tabata, M. Kawaguchi, T. L. Wang, and M. Parniske, “NENA, a *Lotus japonicus* homolog of Sec13, is required for rhizodermal infection by arbuscular mycorrhiza fungi and rhizobia but dispensable for cortical endosymbiotic development.,” *Plant Cell*, vol. 22, no. 7, pp. 2509–2526, Jul. 2010.

[131] K. Saito, M. Yoshikawa, K. Yano, H. Miwa, H. Uchida, E. Asamizu, S. Sato, S. Tabata, H. Imaizumi-Anraku, Y. Umehara, H. Kouchi, Y. Murooka, K. Szczyglowski, J. A. Downie, M. Parniske, M. Hayashi, and M. Kawaguchi, “NUCLEOPORIN85 is required for calcium spiking, fungal and bacterial symbioses, and seed production in *Lotus japonicus*.,” *Plant Cell*, vol. 19, no. 2, pp. 610–624, Feb. 2007.

[132] N. Kanamori, L. H. Madsen, S. Radutoiu, M. Frantescu, E. M. H. Quistgaard, H. Miwa, J. A. Downie, E. K. James, H. H. Felle, L. L. Haaning, T. H. Jensen, S. Sato, Y. Nakamura, S. Tabata, N. Sandal, and J. Stougaard, “A nucleoporin is required for induction of Ca2+ spiking in legume nodule development and essential for rhizobial and fungal symbiosis.,” *Proc. Natl. Acad. Sci. U. S. A.*, vol. 103, no. 2, pp. 359–364, Jan. 2006.

[133] F. Alber, S. Dokudovskaya, L. M. Veenhoff, W. Zhang, J. Kipper, D. Devos, A. Suprapto, O. Karni-Schmidt, R. Williams, B. T. Chait, A. Sali, and M. P. Rout, “The molecular architecture of the nuclear pore complex.,” *Nature*, vol. 450, no. 7170, pp. 695–701, Nov. 2007.

[134] M. C. King, C. P. Lusk, and G. Blobel, “Karyopherin-mediated import of integral inner nuclear membrane proteins.,” *Nature*, vol. 442, no. 7106, pp. 1003–1007, Aug. 2006.

[135] M. Deng and M. Hochstrasser, “Spatially regulated ubiquitin ligation by an ER/nuclear membrane ligase.,” *Nature*, vol. 443, no. 7113, pp. 827–831, Oct. 2006.

[136] L. Tirichine, H. Imaizumi-Anraku, S. Yoshida, Y. Murakami, L. H. Madsen, H. Miwa, T. Nakagawa, N. Sandal, A. S. Albrektsen, M. Kawaguchi, A. Downie, S. Sato, S. Tabata, H. Kouchi, M. Parniske, S. Kawasaki, and J. Stougaard, “Deregulation of a Ca2+/calmodulin-dependent kinase leads to spontaneous nodule development.,” *Nature*, vol. 441, no. 7097, pp. 1153–1156, Jun. 2006.

[137] C. Gleason, S. Chaudhuri, T. Yang, A. Munoz, B. W. Poovaiah, and G. E. D. Oldroyd, “Nodulation independent of rhizobia induced by a calcium-activated kinase lacking autoinhibition.,” *Nature*, vol. 441, no. 7097. England, pp. 1149–1152, Jun-2006.

[138] N. Takeda, T. Maekawa, and M. Hayashi, “Nuclear-localized and deregulated calcium- and calmodulin-dependent protein kinase activates rhizobial and mycorrhizal responses in *Lotus japonicus*.,” *Plant Cell*, vol. 24, no. 2, pp. 810–822, Feb. 2012.

[139] J. B. Miller, A. Pratap, A. Miyahara, L. Zhou, S. Bornemann, R. J. Morris, and G. E. D. Oldroyd, “Calcium/Calmodulin-dependent protein kinase is negatively and positively regulated by calcium, providing a mechanism for decoding calcium responses during symbiosis signaling.,” *Plant Cell*, vol. 25, no. 12, pp. 5053–66, 2013.

[140] E. Messinese, J.-H. Mun, L. H. Yeun, D. Jayaraman, P. Rouge, A. Barre, G. Lougnon, S. Schornack, J.-J. Bono, D. R. Cook, and J.-M. Ane, “A novel nuclear protein interacts with the symbiotic DMI3 calcium- and calmodulin-dependent protein kinase of *Medicago truncatula*.,” *Mol. Plant. Microbe. Interact.*, vol. 20, no. 8, pp. 912–921, Aug. 2007.

[141] B. Horvath, L. H. Yeun, A. Domonkos, G. Halasz, E. Gobbato, F. Ayaydin, K. Miro, S. Hirsch, J. Sun, M. Tadege, P. Ratet, K. S. Mysore, J.-M. Ane, G. E. D. Oldroyd, and P. Kalo, "*Medicago truncatula* IPD3 is a member of the common symbiotic signaling pathway required for rhizobial and mycorrhizal symbioses.," *Mol. Plant. Microbe. Interact.*, vol. 24, no. 11, pp. 1345–1358, Nov. 2011.

[142] K. Yano, S. Yoshida, J. Muller, S. Singh, M. Banba, K. Vickers, K. Markmann, C. White, B. Schuller, S. Sato, E. Asamizu, S. Tabata, Y. Murooka, J. Perry, T. L. Wang, M. Kawaguchi, H. Imaizumi-Anraku, M. Hayashi, and M. Parniske, "CYCLOPS, a mediator of symbiotic intracellular accommodation.," *Proc. Natl. Acad. Sci. U. S. A.*, vol. 105, no. 51, pp. 20540–20545, Dec. 2008.

[143] P. Smit, J. Raedts, V. Portyanko, F. Debelle, C. Gough, T. Bisseling, and R. Geurts, "NSP1 of the GRAS protein family is essential for rhizobial Nod factor-induced transcription.," *Science*, vol. 308, no. 5729, pp. 1789–1791, Jun. 2005.

[144] R. Y. Tsien, "New calcium indicators and buffers with high selectivity against magnesium and protons: design, synthesis, and properties of prototype structures.," *Biochemistry*, vol. 19, no. 11, pp. 2396–2404, 1980.

[145] R. Rudolf, M. Mongillo, R. Rizzuto, and T. Pozzan, "Looking forward to seeing calcium.," *Nat. Rev. Mol. Cell Biol.*, vol. 4, no. 7, pp. 579–586, 2003.

[146] C. N. Kanchiswamy, M. Malnoy, A. Occhipinti, and M. E. Maffei, "Calcium imaging perspectives in plants," *Int. J. Mol. Sci.*, vol. 15, no. 3, pp. 3842–3859, 2014.

[147] A. Miyawaki, J. Llopis, R. Heim, J. M. McCaffery, J. A. Adams, M. Ikura, and R. Y. Tsien, "Fluorescent indicators for Ca2+ based on green fluorescent proteins and calmodulin.," *Nature*, vol. 388, no. 6645, pp. 882–887, Aug. 1997.

[148] G. S. Baird, D. A. Zacharias, and R. Y. Tsien, "Circular permutation and receptor insertion within green fluorescent proteins.," *Proc. Natl. Acad. Sci. U. S. A.*, vol. 96, no. 20, pp. 11241–11246, Sep. 1999.

[149] T. Nagai, a Sawano, E. S. Park, and a Miyawaki, "Circularly permuted green fluorescent proteins engineered to sense Ca2+.," *Proc. Natl. Acad. Sci. U. S. A.*, vol. 98, no. 6, pp. 3197–3202, 2001.

[150] V. A. Romoser, P. M. Hinkle, and A. Persechini, "Detection in living cells of Ca2+-dependent changes in the fluorescence emission of an indicator composed of two green fluorescent protein variants linked by a calmodulin-binding sequence. A new class of fluorescent indicators.," *J. Biol. Chem.*, vol. 272, no. 20, pp. 13270–13274, May 1997.

[151] L. Technoligies, Ed., "Indicators for Ca2+, Mg2+, Zn2+ and other metal ions," in *The molecular probes handbook - a guide to fruorescent probes and labeling technologies*, 11th ed., 2010.

[152] T. Nagai, S. Yamada, T. Tominaga, M. Ichikawa, and A. Miyawaki, "Expanded dynamic range of fluorescent indicators for Ca(2+) by circularly permuted yellow fluorescent proteins.," *Proc. Natl. Acad. Sci. U. S. A.*, vol. 101, no. 29, pp. 10554–10559, 2004.

[153] J. Nakai, M. Ohkura, and K. Imoto, “A high signal-to-noise Ca(2+) probe composed of a single green fluorescent protein.,” *Nat. Biotechnol.*, vol. 19, pp. 137–141, 2001.

[154] Q. Wang, B. Shui, M. I. Kotlikoff, and H. Sondermann, “Structural basis for Calcium Sensing by GCaMP2,” *Structure*, vol. 16, no. 12, pp. 1817–1827, 2008.

[155] Y. Zhao, S. Araki, J. Wu, T. Teramoto, Y.-F. Chang, M. Nakano, a. S. Abdelfattah, M. Fujiwara, T. Ishihara, T. Nagai, and R. E. Campbell, “An Expanded Palette of Genetically Encoded Ca2+ Indicators,” *Science (80-.).*, vol. 333, no. 2011, pp. 1888–1891, 2011.

[156] J. Wu, L. Liu, T. Matsuda, Y. Zhao, A. Rebane, M. Drobizhev, Y. F. Chang, S. Araki, Y. Arai, K. March, T. E. Hughes, K. Sagou, T. Miyata, T. Nagai, W. H. Li, and R. E. Campbell, “Improved orange and red Ca2+ indicators and photophysical considerations for optogenetic applications,” *ACS Chem. Neurosci.*, vol. 4, pp. 963–972, 2013.

[157] L. Tian, S. A. Hires, T. Mao, D. Huber, M. E. Chiappe, S. H. Chalasani, L. Petreanu, J. Akerboom, S. A. McKinney, E. R. Schreiter, C. I. Bargmann, V. Jayaraman, K. Svoboda, and L. L. Looger, “Imaging neural activity in worms, flies and mice with improved GCaMP calcium indicators.,” *Nat. Methods*, vol. 6, no. 12, pp. 875–881, Dec. 2009.

[158] S. Guo, L. G. Kamphuis, L. Gao, O. R. Edwards, and K. B. Singh, “Two independent resistance genes in the *Medicago truncatula* cultivar jester confer resistance to two different aphid species of the genus Acyrthosiphon.,” *Plant Signal. Behav.*, vol. 4, no. 4, pp. 328–331, 2009.

[159] D. G. Barker, S. Bianchi, F. Blondon, G. Duc, S. Essad, P. Flament, G. Génier, P. Guy, X. Muel, J. Dénarié, and T. Huguet, “*Medicago truncatula*, a Model Plant for Studying the Molecular Genetics of the *Rhizobium*- Legume Symbiosis,” *Plant Molecualr Biol. Report.*, vol. 8, no. 1, pp. 40–49, 1990.

[160] J. Stougaard, D. Abildsten, and K. a Marcker, “System for Transformation of Plants,” *Mol. Gen. Genet.*, vol. 207, pp. 251–255, 1987.

[161] G. Morieri, E. a. Martinez, A. Jarynowski, H. Driguez, R. Morris, G. E. D. Oldroyd, and J. A. Downie, “Host-specific Nod-factors associated with Medicago truncatula nodule infection differentially induce calcium influx and calcium spiking in root hairs,” *New Phytol.*, vol. 200, pp. 656–662, 2013.

[162] E. Weber, C. Engler, R. Gruetzner, S. Werner, and S. Marillonnet, “A modular cloning system for standardized assembly of multigene constructs,” *PLoS One*, vol. 6, no. 2, 2011.

[163] C. Engler, R. Gruetzner, R. Kandzia, and S. Marillonnet, “Golden gate shuffling: A one-pot DNA shuffling method based on type ils restriction enzymes,” *PLoS One*, vol. 4, no. 5, 2009.

[164] A. E. Palmer and R. Y. Tsien, “Measuring calcium signaling using genetically targetable fluorescent indicators.,” *Nat. Protoc.*, vol. 1, no. 3, pp. 1057–1065, 2006.

[165] S. Tang, H.-C. Wong, Z.-M. Wang, Y. Huang, J. Zou, Y. Zhuo, a. Pennati, G. Gadda, O. Delbono, and J. J. Yang, “Design and application of a class of sensors to monitor Ca2+ dynamics in high Ca2+ concentration cellular compartments,” *Proc. Natl. Acad. Sci.*, vol. 108, no. 39, pp. 16265–16270, 2011.

[166] Y. Zhang, F. Reddish, S. Tang, Y. Zhuo, Y. F. Wang, J. J. Yang, and I. T. Weber, “Structural basis for a hand-like site in the calcium sensor CatchER with fast kinetics,” *Acta Crystallogr. Sect. D Biol. Crystallogr.*, vol. 69, pp. 2309–2319, 2013.

[167] F. St-Pierre, J. D. Marshall, Y. Yang, Y. Gong, M. J. Schnitzer, and M. Z. Lin, “High-fidelity optical reporting of neuronal electrical activity with an ultrafast fluorescent voltage sensor.,” *Nat. Neurosci.*, vol. 17, no. April, pp. 884–9, 2014.

[168] X. Zhou and I. Meier, “How plants LINC the SUN to KASH.,” *Nucleus*, vol. 4, no. 3, pp. 206–15.

[169] K. Graumann, H. W. Bass, and G. Parry, “SUNrises on the International Plant Nucleus Consortium,” *Nucleus*, vol. 4, no. 1, pp. 3–7.